DELIVERY OF OSELTAMIVIR PHOSPHATE AND GEMCITABINE FROM IMPLANTABLE POLY (D,L-LACTIC-CO-GLYCOLIC ACID) CYLINDERS FOR THE TREATMENT OF PANCREATIC CANCER

by

Stephanie Nadine Allison

A thesis submitted to the Department of Chemical Engineering

In conformity with the requirements for

the degree of Master of Applied Science

Queen's University

Kingston, Ontario, Canada

(August, 2015)

Abstract

The aim of the study was to develop implantable poly (D,L-lactic-co-glycolic acid) (PLGA) cylinders capable of releasing oseltamivir phosphate (OP) and gemcitabine (GEM) over 30 days and to establish proof of principle for the sustained delivery of OP and GEM for the treatment of pancreatic cancer.

Resistance to the current standard of care, gemcitabine (GEM), is common in pancreatic cancer. Recent studies have indicated mammalian neuraminidase 1 (Neu1) as a potential therapeutic target due to its role in receptor tyrosine kinase activation. Oseltamivir phosphate (OP) inhibits Neu1 and has shown promise as a therapeutic agent for the treatment of pancreatic cancer. In vitro experiments have indicated combined treatment with OP and GEM may be more effective than either drug alone.

Localized treatment with OP and GEM will allow a higher drug concentration at the tumor site while reducing systemic toxicity. OP and GEM were encapsulated in implantable poly (D,L-lactic-co-glycolic acid) (PLGA) single layered and double layered cylinders, which were capable of releasing OP and GEM over 30 days. Single layered cylinders were approximately 9 mm in length and 4 mm in diameter, while double layered cylinders were 10 mm by 5 mm. Double layered cylinders containing OP and GEM in distinct layers, termed OP^{in}/GEM^{out} and GEM^{in}/OP^{out}, displayed the most linear release of OP and GEM and were selected for cell viability testing. OP and GEM released from OP^{in}/GEM^{out} and GEM^{in}/OP^{out} cylinders effectively reduced cell viability of pancreatic cancer cell line PANC1 and GEM-resistant PANC1 (PANC1 GEMR) in experiments lasting 3, 6, 10, and 15 days. PLGA had no effect on cell viability. Future

work should include in vivo studies with OP^{in}/GEM^{out} and GEM^{in}/OP^{out} cylinders in a murine model of pancreatic cancer.

Acknowledgements

My dissertation would not have been possible without the support and guidance of Dr. Ron Neufeld and Dr. Myron Szewczuk. Thank you for always being happy to answer my frequent questions and for teaching me how to effectively share my work with others.

I would like to thank my labmates Vitaliy Kapishon, Kurt Wood, and Fiona Haxho for their support, assistance, and afternoons at the Grad Club throughout the last 2 years. Thank you to Leah O'Shea and Olivia Geen who taught me the ropes of the Szewczuk lab and more than I'll ever need to know about One Direction.

Thank you Amanda Brissenden and Michelle Louie for your great work this year. You were a joy to supervise! Amanda Brissenden performed SEM and completed release experiments of single layered cylinders containing OP as seen in Figures 17A, 19C, and section 5.2.3.2, while Michelle performed the scratch wound assays included in sections 5.3.1.2 and 5.3.2.1.

I couldn't have done it without my boyfriend Andrew, who was always happy to listen to me ramble when I was excited about my project and support me when things were not going well, even if he had no idea what I was talking about. Thanks to all of our friends who welcomed me into the fold when I moved to Kingston and to the new friends I made in Chemical Engineering!

Last but not least, I would like to thank my family. Thank you to my mom, dad, and Sonia for your support. Thank you Trish and Don for giving me a home away from home, and to my grandparents for your homemade meals and carrot cake!

Table of Contents

List of Figures

List of Tables

Chapter 1

Introduction

Cancer is characterized by uncontrolled cell proliferation and can result in a high mortality rate because of the ability of cancer cells to metastasize [1]. The cellular mechanisms leading to cancer are complex, making cancer difficult to treat. More than 100 types of cancer have been identified [2]. Pancreatic cancer is one of the most lethal forms of cancer, with a 5-year survival rate of 9%. Pancreatic cancer is difficult to treat because patients are not often diagnosed until after metastasis has occurred. Currently, pancreatic cancer is treated using gemcitabine (GEM), a nucleoside analogue. However, pancreatic cancer is aggressive and resistance to GEM is common [3].

Resistance to chemotherapy has been observed during prolonged treatment of several types of cancer, included pancreatic [4], breast [5], ovarian [6], and colorectal cancers [7]. In recent years, chemoresistance has been linked to epithelial-mesenchymal transition (EMT), a process that is essential during embryogenesis but leads to metastasis in cancer cells [8].

Receptor tyrosine kinases (RTKs) are a family of mammalian receptors commonly overexpressed in many forms of cancer. A novel signaling paradigm has indicated mammalian neuraminidase 1 (Neu1) plays a central role in RTK activation [9]. Oseltamivir phosphate (OP) is an anti-influenza drug capable of inhibiting Neu1, and in vitro experiments using pancreatic cancer cell line PANC1 and GEM-resistant PANC1 (PANC1 GEMR) have demonstrated that OP reduces PANC1 and PANC1 GEMR cell viability and reverses certain cellular characteristics associated with chemoresistance and

EMT [10]. In vivo experiments demonstrated treatment with OP inhibited tumor growth in a murine model of pancreatic cancer [11].

Another obstacle in the treatment of pancreatic cancer is dose-limiting toxicity. Pancreatic cancer patients are typically treated with one high dose of GEM per week by intravenous infusion [12]. Therapeutics can be released from a delivery vehicle at the tumor site for an extended period of time, ranging from days up to several months, leading to higher therapeutic concentrations at the tumor site and lower systemic concentrations. Biocompatible, biodegradable polymers such as poly (D,L-lactic-co-glycolic acid) (PLGA) are being investigated for long-term delivery of anti-cancer therapeutics [13] and several PLGA-based drug delivery systems are already on the market [14–20].

Preliminary experimentation with PLGA cylinders in our lab demonstrated potential for extended term release of OP. Implantation of PLGA cylinders containing 20 mg OP resulted in decreased neovascularization, metastasis, and inhibition of tumor growth in PANC1 tumor-bearing mice. However, tumor growth began to increase 35 days after cylinder implantation, when all OP had been released [21]. Recently, in vitro experiments have indicated combined therapy with OP and GEM may be more effective than either drug alone. This present research will focus on the development of a PLGA cylinder capable of releasing OP and GEM for 30 days, and the effect of OP and GEM released from the cylinder on PANC1 and PANC1 GEMR cell viability and cell surface expression of E-cadherin and N-cadherin over 15 days.

Chapter 2

Literature Review

2.1 Pancreatic Cancer

Pancreatic cancer is the fourth leading cause of cancer death, despite being only the tenth most commonly diagnosed cancer. The pancreas is a gland located in the abdomen, between the stomach and the small intestine. The primary function of the pancreas is to produce digestive enzymes and buffers, which are transported to the small intestine through the pancreatic duct. Most pancreatic tumors originate in epithelial cells that line the pancreatic duct. This type of cancer is called pancreatic cancer or an adenocarcinoma. Approximately 5% of pancreatic tumors originate in the islet cells of the pancreas, and are referred to as islet cell cancer or neuroendocrine cancer [22]. This report will focus solely on pancreatic adenocarcinoma.

Pancreatic cancer is one of the most lethal forms of cancer, with a five-year survival rate of 9%. In 2012, 4600 Canadians were diagnosed with pancreatic cancer, while 4300 Canadians died from the disease. The mortality rate of pancreatic cancer nearly equals the incidence rate and there has been no significant change in the mortality rate between 1986 and 2015 [23]. The high mortality rate of pancreatic cancer is largely due to the late appearance of symptoms, and therefore late detection. In 52% of diagnoses, the cancer is detected after metastasis has occurred, and the five-year survival rate is 2% [24]. Only 17% of patients underwent surgical therapy in 2009-2010 [23], leaving the majority to undergo chemotherapy. The current standard of care for unresectable pancreatic cancer is gemcitabine hydrochloride (GEM) [25]. While GEM has been shown to be more effective

than other chemotherapy drugs, such as matrix metalloproteinase (MMP) inhibitor BAY 12-9566 [26] and fluorouracil (5-FU) [27], GEM is not a cure for pancreatic cancer.

2.1.1 GEM for the Treatment of Pancreatic Cancer

GEM is the current standard of care for patients with unresectable, locally advanced or metastatic pancreatic cancer, and is also used in the treatment of breast, ovarian, and non-small cell lung cancers [28]. GEM (2',2'-difluoro 2'-deoxycytidine) is a hydrophilic nucleoside analogue [27] and has a molecular weight of 263 g/mol. GEM requires cellular uptake and transport into the nucleus before it can be converted to its active metabolites GEM diphosphate (dFdCDP) and GEM triphosphate (dFdCTP) by nucleoside kinases [29]. dFdCDP inhibits ribonucleotide reductase, which is involved in the generation of deoxynucleoside triphosphates for DNA synthesis. This inhibition causes a decrease in deoxynucleotide concentrations [30,31]. dFdCTP competes with deoxycytidine triphosphate (dCTP) for incorporation into DNA during DNA synthesis [25]. The addition of GEM triphosphate into the growing DNA strand ultimately results in cell death via apoptosis [3].

For the treatment of pancreatic cancer, GEM is typically administered at a dose of 1000 mg/m^2 over 30 min by intravenous infusion once per week for seven weeks, followed by a week with no treatment. Following the first 8 weeks of treatment, GEM is administered on a 28 day cycle, with 30 min treatments on days 1, 8, and 15. The half-life of GEM is shorter in men than in women, and increases with age. For typical patients receiving an infusion of less than 70 min, GEM half-life is shortest in young men (42 minutes for 29 year old males) and longest in elderly women (94 minutes in 79 year old

women). During long infusions, which can range from 70-285 min, the half-life and volume of distribution both increase significantly [12].

Despite being the current standard of care, resistance to GEM is a major obstacle during treatment of pancreatic cancer. GEM has a partial response rate of 5%, a median progression-free period of 3.5 months, and a median survival period of 6.6 months [26]. The variability in response to GEM is thought to be at least in part due to differences in enzyme concentrations between patients. GEM must reach the nucleus and be metabolized prior to action, and is therefore dependent on several transporters and enzymes. The residence time of GEM and GEM metabolites in the nucleus is strongly correlated to its efficacy, and is dependent on various enzymes and transporters [3,32]. Due to the variability and resistance to GEM, the joint use of GEM and other antineoplastic agents is becoming more common [3].

2.1.2 Epithelial-Mesenchymal Transition and Chemoresistance in Pancreatic Cancer

During periods of prolonged treatment, many forms of cancer (including colorectal, pancreatic, and breast cancer) stop responding to chemotherapy and become resistant, and high rates of recurrence are also common [33–35]**.** In recent years, chemoresistance has become closely linked with epithelial-mesenchymal transition (EMT) [4,36], an essential process in embryological development. During EMT, cell-cell adhesion and polarity are lost and the cytoskeleton is reorganized, leading to a more migratory phenotype. While essential during development, tumor cells that undergo EMT

show increased ability to migrate out of the tumor, metastasize to other parts of the body, and invade new tissues [37,38,8,39].

Cells undergoing EMT have decreased expression of epithelial markers such as E-cadherin, occludin, cytokeratins, and desmoplakin, while showing increased expression of the mesenchymal markers N-cadherin, vimentin, and fibronectin [39–42]. Transcription factors Slug, Snail, Twist, and Zeb-1 are repressors of E-cadherin, and upregulation has also been linked to chemoresistance and EMT [43–46].

Chemoresistance and EMT have been well documented and studied in pancreatic cancer. Surgically resected specimens of pancreatic cancer have shown increased expression of Snail, Slug, and N-cadherin when compared to healthy pancreatic tissue[44,47]. Pancreatic cancer cells lines resistant to GEM have shown high levels of Zeb-1 and low levels of E-cadherin, while pancreatic cancer cells which are sensitive to GEM show lower levels of Zeb-1 and increased E-cadherin [43,48]. It is interesting to note that cancer cells resistant to GEM were also resistant to 5-FU and cisplatin, while GEM-sensitive cells were also sensitive to 5-FU and cisplatin [43].

The link between EMT and chemoresistance has only been strengthened by the discovery that reversing EMT can restore drug sensitivity. Aruguman et al [43] were able to reverse EMT and restore GEM sensitivity using siRNA to knock down Zeb-1 expression. As expected, E-cadherin expression increased, and formerly resistant cells became sensitive to GEM, 5-FU, and cisplatin. Abnormal microRNA expression has also been implicated in EMT due to miRNA's ability to degrade and/or inhibit the translation of mRNA [48–50]. Li et al [48] compared miRNA expression in GEM-sensitive and GEM-resistant pancreatic cancer cells and found three members of the miR-200 family were

down regulated in GEM resistant cells. Restored expression of miR-200 via miRNA transfection resulted in a more epithelial morphology, increased E-cadherin expression and decreased Zeb-1 and vimentin expression, and increased sensitivity to GEM [48]. While useful for elucidating the mechanisms involved in the development of EMT and chemoresistance, miRNA transfections are not possible in vivo and delivery of siRNA to reduce expression of specific proteins in a particular cell type is still highly experimental. For effective treatment of pancreatic cancer, an administrable drug capable of reversing EMT is required.

2.2 Receptor Tyrosine Kinases (RTK)

Several growth factors are overexpressed in pancreatic cancer, making growth factors and corresponding receptors potential targets for anti-cancer drugs. Overexpression of mammalian receptor tyrosine kinases (RTK), a family of growth factors, has been observed in several types of cancer [51]**.** The RTK family includes vascular endothelial growth factor receptor (VEGFR), epidermal growth factor receptor (EGFR), insulin-like growth factor-I receptor 1 (IGF-IR), and human epidermal growth factor receptor 2 (HER2) [52]. Since RTKs are involved in the regulation of cell proliferation, differentiation, survival, growth, and metabolism, it is not surprising that the overexpression of the above receptors has been linked to cancer progression and tumor growth [51,53].

2.3 Novel Signaling Paradigm

Recently, our lab has described a novel signaling paradigm in which a G-protein-coupled receptor (GPCR) is complexed with an RTK, mammalian neuraminidase 1 (Neu1), and matrix metalloproteinase-9 (MMP-9) at the cell surface. Upon RTK ligand binding, MMP-9 is activated, inducing Neu1 to cleave an α-2,3-sialic acid on the RTK. Cleavage of the α-2,3-sialic acid from the receptor removes steric hindrance and allows the RTK to form a dimer, which is essential for subsequent downstream signaling [9]. This paradigm has been demonstrated for several RTKs including EGFR [11], nerve growth factor TrkA receptors [54], insulin receptor [55], intracellular Toll-like receptor (TLR)-7 and -9 [9], and extracellular TLR-4 [56,57], all of which are known to play a role in cancer. By inhibiting activation of Neu1, RTK dimerization is prevented and downstream signaling cannot occur. Neu1 can be inhibited directly through Neu1 inhibition, or indirectly through GPCR or MMP-9 inhibition. Therefore, Neu1 is a viable therapeutic target for the treatment of pancreatic cancer.

2.4 Oseltamivir Phosphate for the Treatment of Pancreatic Cancer

2.4.1 Oseltamivir Phosphate

Oseltamivir phosphate (OP, Tamiflu®) is a neuraminidase inhibitor developed as an anti-influenza drug. OP is used to treat human influenza type A and B viruses, which are responsible for seasonal flu epidemics and most severe cases of influenza. The third type of influenza, type C viruses, is not believed to cause epidemics and infections typically result in mild respiratory illness [58].

OP is a hydrophilic drug with a molecular weight of 410.4 g/mol and a pKa of 7.75 [59]. OP as a prodrug is converted to the active metabolite oseltamivir carboxylate (OC) by esterase enzymes in the liver, as seen in Figure 1. OC is a sialic acid analogue and binds to neuraminidases on the surface of the virus, to prevent newly formed virus particles from leaving infected cells [59]. Jayanth et al [54] demonstrated that OP completely inhibits sialidase activity of Neu1 in rat adrenal gland cells (PC-12) and mouse fibroblast cells (NIH/3T3). By inhibiting Neu1 activity, OP can inhibit the cleavage of α-2,3-sialic acid from RTKs and prevent dimerization and receptor activation, as seen in Figure 2.

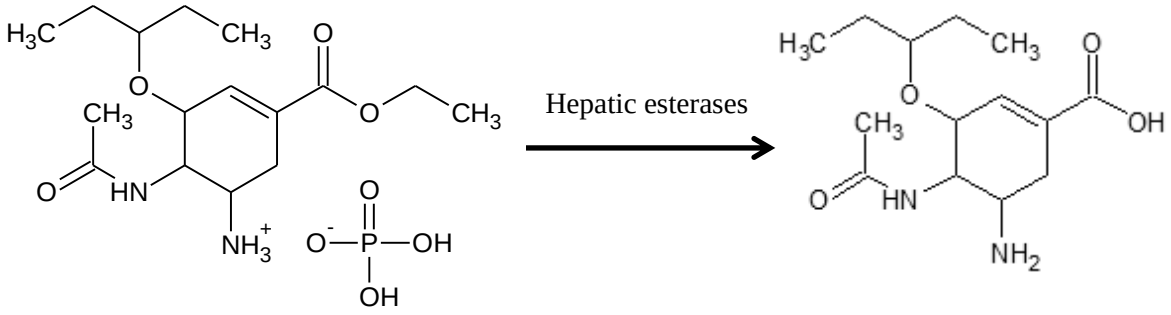

Figure 1. Oseltamivir phosphate is converted to oseltamivir carboxylate by esterase enzymes in the liver.

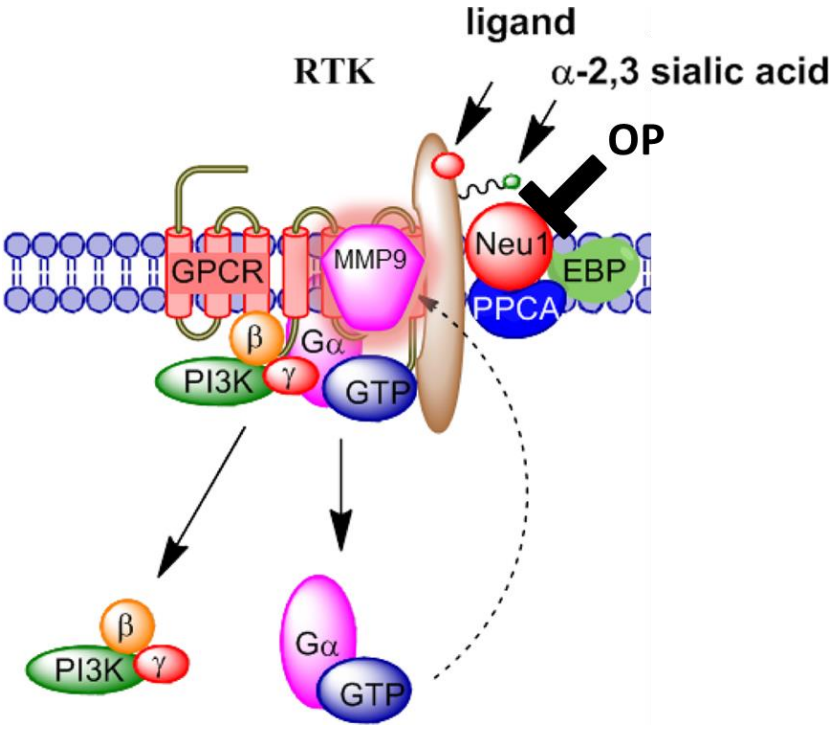

Figure 2. OP inhibits Neu1, preventing α-2,3-sialic acid from being cleaved from the RTK and thereby inhibiting dimerization and receptor activation. Modified from Abdulkhalek *et al.* 2013 Research and Reports in Biochemistry 3, 17-30 [60].

2.4.2 OP for the Treatment of Pancreatic Cancer

Gilmour et al [11] investigated the effects of neuraminidase inhibitors on EGFR activation due to the role of Neu1 as a central enzyme in RTK activation. OP, a known Neu1 inhibitor, inhibited EGF-induced EGFR activation in a dose-dependent manner. Additional experiments confirmed OP treatment did not reduce the amount of EGFR on the cell surface, but only prevented its activation.

Further studies confirmed OP inhibited EGFR activation by preventing the cleavage of α-2,3-sialic acid, thereby preventing receptor dimerization. OP, Neu1 antibody, and MMP-9 inihibitor (MMP9i) were all able to reduce Neu1 activity to

background levels. OP was also shown to dose-dependently reduce cell viability in PANC1 and MiaPaca-2 pancreatic cancer cell lines [11].

A reversal of EMT was observed during treatment of PANC1 GEM resistant (PANC1 GEMR) cells with 500 µg/mL OP for 48 hours. PANC1 GEMR cells had less pseudopodia and a more organized and columnar shape when compared to untreated PANC1 GEMR, giving the cells an appearance more similar to PANC1 cells. PANC1 and PANC1 GEMR both showed a significant increase in E-cadherin and a significant decrease in N-cadherin following treatment with 600 µg/mL OP for 24 hours [10].

OP has been shown through in vivo experiments to have potential as an anti-cancer drug. RAG-2 χCγ double mutant mice on a BALB/c genetic background were implanted with either MiaPaca-2-eGFP [11] or PANC1 [10] cells in the right back flank. RAG-2 χCγ are deficient in mature T-cells, B-cells, natural killer cells, and cytokine signaling. The immunodeficiency of the mice results in improved engraftment of the human cells, and allows for metastasis, which is more representative of a human model than other murine cancer models [11]. O'Shea et al [10] treated mice with 30 mg/kg GEM, 2 mg/kg OP, or 30 mg/kg GEM + 5 mg/kg OP, beginning 22-23 days post-implantation of PANC1 cells. Following necropsy, tumor sections from all treated and untreated mice were immunostained for E- and N-cadherin. Mice treated with OP or GEM+OP showed greater E-cadherin expression than the untreated cohort. Mice treated with GEM alone showed no increase in E-cadherin expression compared to the untreated mice. N-cadherin levels were similar for both untreated and treated cohorts, although mice treated with OP+GEM did show a slight decrease in N-cadherin. Despite the increase in E-cadherin, mice treated with OP or OP+GEM still showed metastasis to the liver and lungs [10].

Gilmour et al [11] treated tumor-bearing mice daily with OP at 100 mg/kg beginning 42 days after MiaPaca-2 implantation. Mice were terminated 47 days post implantation. Mice treated with OP showed no significant increase in tumor volume following onset of treatment, while the tumor volume of the untreated mice doubled. Mice treated with OP showed statistically significant lower tumor size and weight when compared to the untreated cohort. The treated group also had less blood vessel formation near the tumor, indicating that OP treatment inhibited neovascularization. Untreated mice showed significant metastasis of MiaPaca-2-eGFP cells to the lung and liver, while OP-treated mice had a much lower degree of metastatic spread and a lower number of metastatic clusters in the lung and liver. The decrease in metastasis in the OP-treated cohort could be due to less neovascularization at the tumor site or the reversal of EMT by OP [11].

2.4.3 Combination Treatment of OP and GEM

Cell viability assays performed on PANC1 and PANC1 resistant to cisplatin (PANC1 CisR), GEM (PANC1 GEMR), or cisplatin and GEM (PANC1 CisR/GEMR) indicated that chemoresistant cells may be more sensitive to OP than chemosensitive cells[10]. These results suggest that OP may be sensitizing chemoresistant cells to chemotherapeutic drugs that were previously ineffective, thereby increasing the efficacy of the chemotherapeutic drugs. It may then be possible to reverse some or all of the effects of chemoresistance by treating cells with OP. This is consistent with other reports, where the reversal of EMT coincided with the restoration of drug sensitivity [43,48]. These results also suggest combinatorial treatment with both OP and chemotherapeutic drugs may be more effective than treatment with either drug alone.

2.5 Sustained and Local Drug Delivery

The primary methods of pancreatic cancer treatment are currently surgery, radiation, and chemotherapy. Surgery and radiation are both localized forms of treatment, while chemotherapy is typically systemic [61].

Implantable drug delivery systems are designed to improve treatment by providing sustained release of the drug as near to the tumor as possible. Jain [62] stated that for effective cancer treatment with drug therapy, the drug must reach target cells at high enough concentrations to be effective while inflicting minimal toxicity to healthy cells, and that the drug must be effective in the tumor microenvironment. Prior to reaching the tumor, a drug administered intravenously must be distributed through vascular space, transported across microvessel walls, then diffuse through the interstitial space within the tumor [62]. For a drug injected directly into the tumor or in the immediate vicinity of the tumor, only diffusion through the interstitial space within the tumor is required, greatly improving the chances of the drug reaching the tumor with a sufficient concentration to have a significant therapeutic effect [63].

Localized therapy also reduces the side effects associated with systemic chemotherapy. Chemotherapeutic drugs inhibit cell division, often targeting DNA synthesis. These drugs do not specifically target cancer cells and will affect any cell undergoing cell division, including healthy cells. Therefore, most cancer drugs exhibit dose-limiting toxicity when administered systemically [64]. Through localized delivery, the number of healthy cells affected is dramatically reduced, resulting in a significant decrease in side effects while increasing treatment efficacy.

Sustained release enables improved treatment because the duration of treatment within the therapeutic window is increased. The therapeutic window is an important concept in pharmacology, and includes the concentration of drug above that which a therapeutic effect is produced (minimum effective concentration) and the concentration below which toxicity occurs (minimum toxic concentration), as shown in Figure 3. Many chemotherapeutics have a short half-life, which is why they are administered by intravenous infusion. However, since treatment is typically weekly, patients are given the maximum tolerated dose (MTD), which brings the concentration above the therapeutic window and into the toxic region. Sustained, localized release allows for longer duration and reduced toxicity, enabling more efficacious treatment [65].

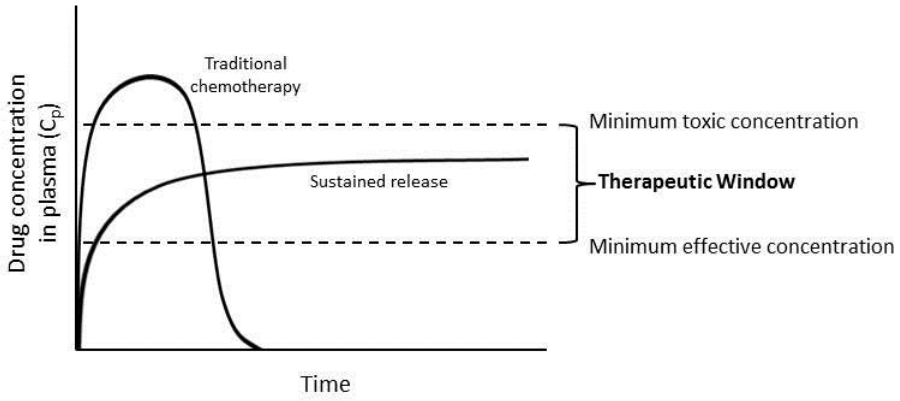

Figure 3. The therapeutic window includes the concentration of drug above which a therapeutic effect is produced (minimum effective concentration) and the concentration below which toxicity occurs (minimum toxic concentration). Sustained release allows the drug concentration to remain within the therapeutic window for a longer period of time.

2.6 Polymers for Biomedical Applications

Biodegradable polymers have been studied extensively over the last 30 years for use in biomedical applications, and are rapidly overtaking traditional materials such as ceramics, metals, and alloys [13]. Biodegradable polymers are currently being studied and used in temporary prostheses, drug delivery vehicles, and scaffolds for tissue engineering. Biodegradable polymers are degraded in vivo through hydrolysis or enzymatic activity to non-toxic products that can be further metabolized or excreted [13]. To perform well in a biomedical application, the polymer must also be biocompatible. Biocompatibility was defined by Williams as the ‘‘ability of a material to perform with an appropriate host response in a specific situation’’ [66]. To be biocompatible, any polymer used as part of a drug delivery system must be non-immunogenic, non-pyrogenic, non-carcinogenic, and non-toxic.

Since the requirements for use in a biomedical application are fairly stringent, there are a number of polymers that are frequently used. Commonly used polymers include poly (D,L-lactic-co-glycolic acid), poly (ε-caprolactone), poly (ethylene glycol), chitosan, and alginate [67].

2.6.1 Poly (D,L-lactic-co-glycolic acid)

Poly (D,L-lactic-co-glycolic acid) (PLGA) is a type of poly(α-ester), a group of thermoplastic polymers that are susceptible to hydrolytic degradation of the ester linkage on the polymer backbone [13]. PLGA is a copolymer composed of lactic and glycolic acid monomers. The properties of PLGA, such as crystallinity, erosion time, and mechanical properties, are highly dependent on the ratio of lactic:glycolic acids [68,69]. Intermediate copolymers, such as 50/50 PLGA, are more susceptible to hydrolysis and are degraded

more quickly than a PLGA with a higher percentage of one monomer. Mooney et al [70] produced hollow tubes composed of 85/15 PLGA, 50/50 PLGA, poly (D,L-lactic acid), or poly (lactic acid). Tubes formed from 50/50 PLGA were completely degraded in seven weeks while tubes formed from 85/15 PLGA began losing mass at 10 weeks and were completely degraded after 35 weeks, The lactic acid polymers did not show any loss in mass for 20 weeks or longer. The erosion time of PLGA is also affected by molecular weight, with higher molecular weight polymers degrading more quickly [71].

PLGA is non-toxic, biodegradable, and biocompatible. PLGA is ultimately degraded to its monomers, lactic and glycolic acid, as seen in Figure 4. Glycolic acid can be excreted in urine, and both lactic and glycolic acid can be metabolized to water and carbon dioxide via the citric acid cycle [72]. Because PLGA degradation can be easily altered by changing the ratio of lactic:glycolic acids or the molecular weight of the polymer, PLGA has been researched extensively as a drug delivery vehicle.

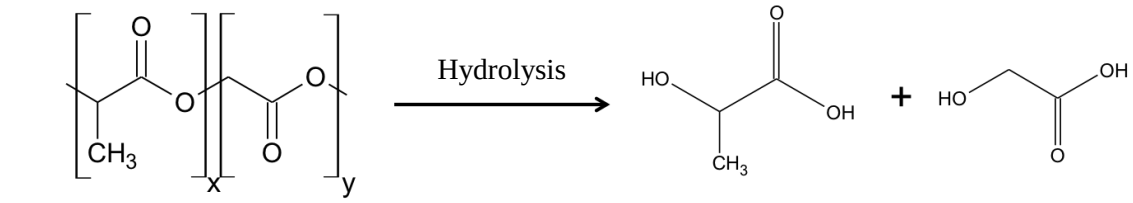

Poly (D,L-lactic-co-glycolic acid) Lactic acid Glycolic acid

Figure 4. Poly (D,L-lactic-co-glycolic acid) undergoes hydrolytic degradation to form lactic acid and glycolic acid.

2.6.1.1 PLGA for Drug Delivery

One of the major problems with chemotherapy is toxicity of the therapeutic toward healthy tissues and cells [73]. By using a vehicle such as PLGA to deliver drugs directly to the tumor site, the systemic toxic effects associated with chemotherapy should be greatly decreased. Encapsulation in PLGA can also increase the half-life of therapeutics. Several anticancer drugs including hypericin, paclitaxel, and cisplatin have shown increased anti-tumor effects when incorporated into PLGA nanoparticles in comparison to the free drugs [74].

PLGA is a commonly used vehicle for drug delivery because it is biocompatible, biodegradable, and has been studied extensively. PLGA is tunable, and molecular weight and monomer ratio can be altered to obtain the desired rate of degradation and rate of drug release. PLGA can be used to encapsulate a wide range of therapeutics in many different delivery systems. Nanoparticles, in situ forming depots, and implantable delivery systems have been developed, and some examples are shown in Table 1. Several PLGA drug delivery applications for humans have already been approved by the US Food and Drug Administration (FDA), European Medicine Agency [75] , and Health Canada [76]. Several PLGA-based long-term delivery systems approved by the FDA and currently on the market are shown in Table 2.

Table 1. Examples of PLGA-based drug delivery systems published within the last 10 years.

Delivery System	Therapeutic	Duration of Delivery	Indication	Reference
In situ forming depot	Leuprolide acetate	1, 3, 4, or 6 months	Prostate cancer	[14]
Microspheres	Oligonucleotide decoy of NF-κB	40 days	Chronic inflammation	[77]
Implantable cylinder	Oseltamivir phosphate	30 days	Pancreatic cancer	[21]
Microspheres	Doxorubicin and paclitaxel	20 days	Lung cancer	[78]
Nanoparticle	Paclitaxel	11 days	Liver cancer	[79]
Implantable wafer	1,3-bis(2-chloroethyl)-1-nitrosourea (BCNU)	7 days	Glioblastoma	[80]
Nanoparticle	Carboplatin	24h	Glioblastoma	[81]

Table 2. PLGA-based drug delivery systems approved by the FDA and currently on the market. Adapted from Schwendeman [82].

Name	Company	Delivery system	Drug	Dosing	Indication	Prescribing Information
Lupron Depot	Takeda/ Abbott	In situ forming depot	Leuprolide	1, 3, 4, or 6 months	Prostate cancer	[15]
Eligard	QLT	In situ forming depot	Leuprolide	1, 3, 4, or 6 months	Prostate cancer	[14]
Decapeptyl, Trelstar, Pamorelin	Debiopharm	In situ forming depot	Triptorelin	1, 3, or 6 months	Prostate cancer, endometriosis	[16]
Zoladex	AstraZeneca	Injectable implant	Goserelin	1 or 3 months	Prostate cancer	[17,19]
Sandostatin LAR	Novartis	In situ forming depot	Octreotide	1 month	Acromegaly, neuroendocrine tumors	[20]
Risperdal Consta	Janssen Alkermes	Microspheres	Resperidone	1 month	Schizophrenia, bipolar disorder	[83]
Bydureon	AstraZeneca	Microspheres	Exenatide	1 week	Type 2 diabetes	[18]

2.6.1.2 Delivery of OP from PLGA Cylinder

Our lab has worked to encapsulate OP in an implantable PLGA cylinder and has demonstrated that the cylinders can release OP for up to 30 days, as seen in Figure 5. Although small hydrophilic drugs are often difficult to encapsulate, this method has near 100% encapsulation efficiency [21].

PLGA cylinders containing 20 mg OP were surgically implanted near the tumor site in a RAG-$2^{-/-}$ $\chi C\gamma^{-/-}$ murine model of pancreatic cancer. Implanted OP cylinders effectively inhibited tumor growth in mice, as seen in Figure 6. A large difference in tumor size between the mice implanted with the 20 mg OP cylinders and those implanted with the blank cylinders can be observed between days 40 and 71. From days 75-85, tumor volumes from both groups are similar. Tumors were weighed after necropsy and mice treated with PLGA cylinder containing 20 mg OP had significantly lower tumor volumes than untreated mice ($p < 0.0251$) [21].

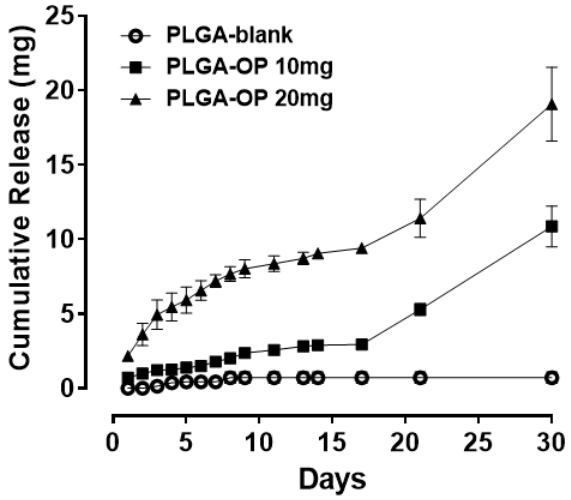

Figure 5. Release of OP from PLGA cylinders containing 0, 10, or 20 mg OP over 30 days [21].

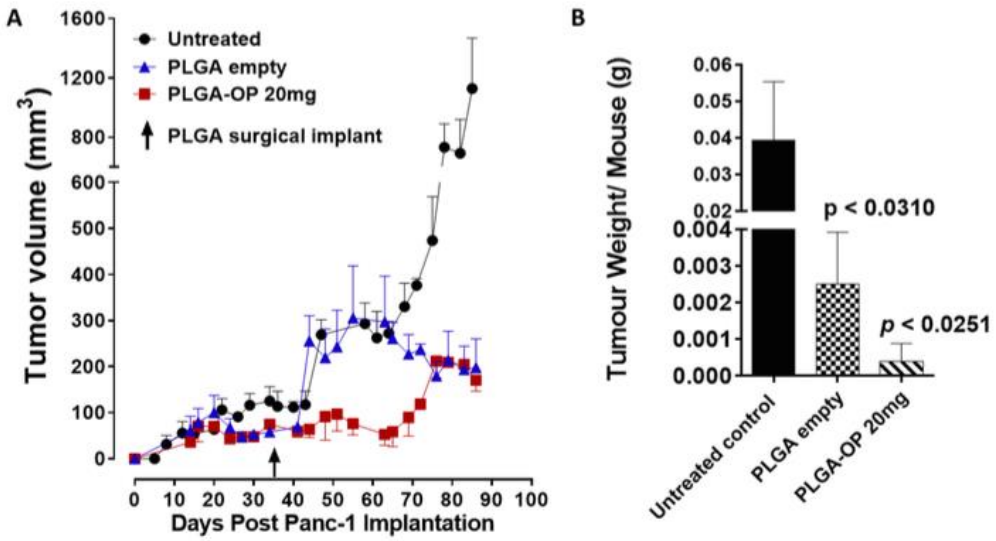

Figure 6. Tumor volume in RAG-2 χCγ double mutant mice following treatment with PLGA cylinder containing no OP, PLGA cylinder containing 20 mg OP, or untreated control mice (A). Tumor weight per mouse after necropsy following treatment with PLGA cylinder containing no OP, PLGA cylinder containing 20 mg OP, or untreated control mice (B) [21].

Post termination necropsy revealed neovascularization was greatly reduced in mice implanted with the 20 mg OP cylinder in comparison to the blank cylinder [21]. Limiting angiogenesis decreases the risk of metastasis, since the easiest method of transport for cancer cells is through the blood stream.

2.7 Summary

Pancreatic cancer has a 5-year survival rate of only 9%. Although the current standard of care, GEM, is more effective than other chemotherapy agents during the treatment of pancreatic cancer, it is not a cure. EMT and chemoresistance are major obstacles in the treatment of pancreatic cancer. A novel signaling paradigm has identified

Neu1 as a potential therapeutic target for pancreatic cancer treatment, due to its central role in RTK activation. OP is a Neu1 inhibitor, and in vitro and in vivo experiments have demonstrated OP can reduce cell viability and reverse EMT in GEM resistant pancreatic cancer cells. Although treatment with OP alone inhibited tumor growth, in vitro experiments have indicated that OP may sensitize cells to GEM and that a combined treatment of OP and GEM may be even more effective.

PLGA is a biodegradable, biocompatible polymer that has been studied extensively and is well established as a drug delivery vehicle. Our lab has developed implantable PLGA cylinders that release OP for 30 days, and inhibited neovascularization, metastasis, and tumor growth in a murine model of pancreatic cancer. Since concurrent treatment of OP and GEM may be more effective than either drug alone, the next step is to develop an implantable PLGA cylinder capable of releasing OP and GEM for 30 days.

Chapter 3

Objectives

Current difficulties in the treatment of pancreatic cancer involve dose-limiting toxicity and poor response to the current standard of care, gemcibatine (GEM). The use of a delivery vehicle allows for sustained release of therapeutics at the tumor site, reducing systemic toxicity while increasing the local concentration of the therapeutic. Biocompatible, biodegradable polymers, such as poly (D,L-lactic-co-glycolic acid) (PLGA), are being investigated as drug delivery vehicles for the treatment of cancer.

Resistance to GEM is common, however discovery of a novel signaling paradigm has indicated mammalian neuraminidase 1 (Neu1) as a new therapeutic target. In vivo and in vitro studies have indicated that concurrent treatment with Neu1 inhibitor oseltamivir phosphate (OP) and GEM may reduce viability of pancreatic cancer cells to a greater extent than GEM alone. Combined delivery of OP and GEM from a PLGA implant could result in higher drug concentration at the tumor site, greater reduction in cancer cell viability through combined use of OP and GEM, and reduced adverse effects associated with chemotherapy. To overcome current issues in the treatment of pancreatic cancer, the primary objectives of the study were to:

1. Develop a method of detecting and quantifying therapeutic levels of OP and GEM in release experiment supernatants using high performance liquid chromatography (HPLC).

2. Develop an implantable PLGA cylinder capable of releasing OP and GEM for an extended period (eg. 30 days) and tailor release of OP and GEM to projected release profile as determined previously by treatment of tumor-bearing mice with OP and/or GEM.
3. Investigate response of pancreatic cancer cell line PANC1 and GEM-resistant PANC1 (PANC1 GEMR) to OP and GEM released from PLGA cylinders in terms of cell viability and cell surface expression of E- cadherin and N-cadherin.

Chapter 4

Materials and Methods

4.1 Materials

4.1.1 Gemcitabine Hydrochloride (GEM)

Gemcitabine hydrochloride (GEM) (Sigma-Aldrich Canada Co, Oakville, ON, Canada) was dissolved in phosphate-buffered saline pH 7.4 (PBS) to form a 133.5 mM GEM stock and stored at -20˚C. This stock was diluted in 1 × Dulbecco's Modified Eagle's Medium (DMEM) (Gibco, Rockville, MD, USA) containing 10% fetal bovine serum (FBS) (HyClone, Logan, UT, USA) and 5 μg/mL Plasmocin™ (InvivoGen, San Diego, CA, USA) to produce 0.01 μM GEM, which was added to PANC1 GEMR tissue culture flasks upon each change of medium.

4.1.2 Oseltamivir Phosphate (OP)

Pure (98%) oseltamivir phosphate (OP) (Hangzhou DayangChem Co, Ltd Hangzhou City, People's Republic of China) was dissolved in PBS to form a 20 mg/mL stock. The stock solution was diluted in cell culture medium containing 1 × DMEM, 10% FBS, and 5 μg/mL Plasmocin™ to concentrations of 500–800 μg/mL.

Extracted OP was obtained by purifying oral dosage 75 mg Tamiflu® capsules. Capsules were dissolved in 25 mL distilled water and subjected to centrifugation at 1100 × g for 5 min to remove insoluble material. Supernatant was frozen at -80˚C, then lyophilized for 24-48h, resulting in OP crystals. Extracted OP crystals were stored at 4˚C. Extraction of OP from Tamiflu® capsules was performed by Jordan Ellis.

4.1.3 Poly (D,L-lactic-co-glycolic acid) (PLGA)

PLGA (50/50) was obtained from Purac Biomaterials (Gorinchem, Netherlands). The molecular weight was determined by gel permeation chromatography (Viscotek GPCmas VE 2001; Malvern Instruments Ltd, Worcestershire, UK), calibrated with poly(ethylene oxide) standards. PLGA was determined to have a molecular weight (M_W) of 16,400 (M_W/M_n =1.58).

4.1.4 Antibodies

Rabbit monoclonal E-cadherin antibody serum (Cell Signaling Technology, Inc, Danvers, MA, USA) and rabbit monoclonal N-cadherin (Cell Signaling Technology, Inc), recognize human E- and N-cadherin epitopes and were used for immunocytochemistry. E-cadherin and N-cadherin antibodies were diluted 1 in 400 and 1 in 200, respectively, in PBS pH 7.4 containing 1% bovine serum albumin. DyLight™ 594 goat anti-rabbit IgG secondary antibody (Molecular Probes, Invitrogen Detection Technologies, OR, USA) was used for immunocytochemistry at a 1:500 dilution to detect E-cadherin and N-cadherin primary antibodies.

4.1.5 Cell Lines

PANC1 (human epithelioid carcinoma, epithelial-like, ATCC® CRL-1469™) were purchased from the American Type Culture Collection (ATCC) (Manassas, VA, USA). Cells were grown at 37˚C with 5% CO_2 and cultured with 1 × DMEM containing 10% FBS and 5 μg/mL Plasmocin™. PANC1 cells resistant to GEM (PANC1 GEMR) were developed by culturing PANC1 cells in 1 × DMEM containing 10% FBS, 5 μg/mL

Plasmocin™, and gradually increasing concentrations of GEM up to 0.01 μM GEM. PANC1 GEMR cells are stable and have been cultured in medium containing 0.01 μM GEM for 3 years.

4.2 Methods

4.2.1 HPLC Analysis

A 1260 Infinity HPLC and a Poroshell 120 SB-C18 threaded column (Agilent Technologies, Santa Barbara, CA, USA) 4.6 mm × 50 mm (2.7 μm) were used. OP (Hangzhou DayangChem Co, Ltd) and GEM were dissolved in HPLC grade methanol. The mobile phase was 60% HPLC grade methanol and 40% 0.04 M ammonium acetate buffer (pH 5.2) at a flow rate of 1 mL/min. OP and GEM were detected at 230 nm. The column temperature was 25°C, the injection volume was 20 μL, and each sample was analyzed for 6 min.

4.2.2 Cylinder Production

PLGA (80 mg), 4-6 mg sorbitan monooleate (SPAN 80), and the desired drug, were mixed together in 400 μL acetone. The solution was ejected dropwise onto a Teflon sheet, then stored at 4°C overnight or at 20°C for 72h. The polymer film was removed from the Teflon sheet using a razor blade and rolled around a 16 gauge needle tip. The razor blade and needle tip were greased with glycerol to prevent the film from sticking. Once rolled, the hollow polymer cylinder was removed from the needle tip. To form a double cylinder, a second layer was rolled around the first cylinder. Control, OP, and OP

and GEM double layered cylinders were produced. Single layered cylinders were approximately 9 mm in length and 4 mm in diameter while double layered cylinders were approximately 10 mm in length and 5 mm in diameter.

4.2.3 Scanning Electron Microscopy

Samples were fixed to aluminum inserts with carbon tape and gold sputtered. Scanning electron microscopy was performed using a JEOL 840 (USA) with an accelerating voltage of 10 kV.

4.2.4 Release Kinetic Experiments

Cylinders were suspended in 0.1M sodium phosphate buffer pH 7.4 and stored at 37˚C. Supernatants were extracted periodically and replaced with fresh buffer. Supernatants were stored at -20˚C pending analysis. OP and GEM released from cylinders were reported as a percent of the total amount of drug released after 30 days.

4.2.5 Scratch Wound Assay

Scratch wound assays were performed with PANC1 and PANC1 GEMR using two different methods. Both methods yielded similar results, and results from both types of assay were combined and presented together.

4.2.5.1 Manual Scratch

Scratch wound assays were completed in 24 multiwell plates (Corning Inc, Corning, NY, USA) with the PANC1 and PANC1 GEMR. Cells were plated and cultured until

confluent (approximately 24h). A P1000 pipette tip was used to scratch one line down the length of each well.

4.2.5.2 Silicone Insert

Silicone inserts, as seen in Figure 7, were obtained from Ibidi (Martinsreid, Germany) and placed in 24 multiwell plates. 70 µL of $7x10^5$ PANC1 or PANC1 GEMR cells/mL were plated in each cutout of the insert and incubated overnight. Inserts were removed after 24h. Cell-free zone formed using insert is 500 µm wide.

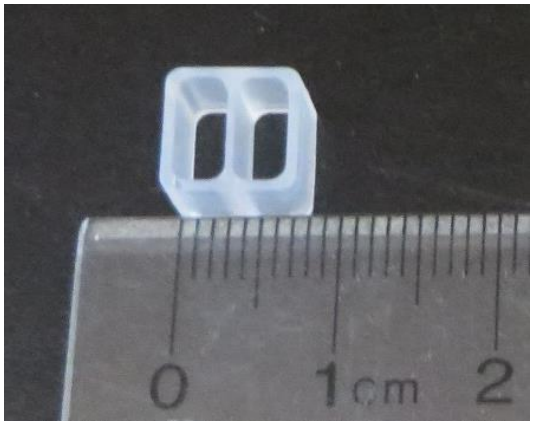

Figure 7. Silicone insert obtained from Ibidi (Martinsreid, Germany) for use in scratch wound assay.

Use of silicone inserts lead to cell-free zones that were straight and of uniform width. After cell-free zone was formed, whether manually or using insert, cells were treated with 0, 400, or 800 µg/mL OP for 48h. A line was drawn on the leading edge of migrating cells and used to measure the width of the cell-free zone at 24 or 48h. The width of the cell-free zone was measured 3 times in each well at 0, 24, and 48h.

Cell regrowth filling in the cell-free zone as a percentage of initial cell-free zone width was calculated after 24 and 48h OP treatment as shown:

$$Cell\ growth\ as\ percent\ of\ initial\ cell-free\ zone = \frac{Initial\ \ width - width\ at\ time\ t}{Initial\ width} \times 100\%$$

4.2.6 Alexa Fluor 488 Phalloidin Staining for F-actin

Cells were plated on glass coverslips in 24 multiwell plates and cultured overnight in a 37°C CO_2 incubator. Cells were then stained with Alexa Fluor 488 conjugated phalloidin diluted 1 in 40 in PBS pH 7.4 (Life Technologies Inc, Burlington, ON, Canada) by mixing 5µL phalloidin with 5µL mounting media on a glass slide and covering with a glass coverslip. Cell staining was examined using a Zeiss M2 fluorescence microscope at 400 × magnification.

4.2.7 Immunocytochemistry

Immunocytochemistry was performed to visualize and quantify E-cadherin and N-cadherin expression in PANC1 and PANC1 GEMR negative control and cylinder treated cells. Cells were plated on 12 mm glass coverslips in 24 multiwell plates and incubated overnight. Cells were washed once with PBS pH 7.4 and fixed with 4% paraformaldehyde for 30 min on ice. Cells were then blocked for at least 1h with 1% bovine serum albumin in phosphate-buffered saline. Cells were treated with E- or N-cadherin antibodies for 1h at 20°C, followed by secondary antibody DyLight™ 594 for another hour at 20°C. The background control had no primary antibody added during the

procedure described above, and was treated with secondary antibody only. Stained cells were visualized 24h after completion of the assay using a Zeiss M2 fluorescence microscope (Carl Zeiss AG, Oberkochen, Germany) at 200 and 400 × magnification. Images were taken in 3 fields of view. Quantitative analysis was done by assessing the density of cell staining of individual cells from multiple images, and corrected for background using Corel Photo Paint 8.0 software (Corel Corporation, Ottawa, ON, Canada). For calculation of mean fluorescence and standard deviation, n=8 for all time points and treatments except for 15 day GEM^{in}/OP^{out} cylinder, where n=4 for E-cadherin and n=6 for N-cadherin.

4.2.8 WST-1 Cell Viability Assay

The WST-1 assay determines cell viability based on the conversion of an insoluble tetrazolium salt to a soluble derivative. PANC1 and PANC1 GEMR cells were plated in 96 multiwell plates at a density of 5000 cells/well and incubated at 37°C overnight. The following day, cells were exposed to various treatments or left untreated as a control for 0, 24, 48, and 72h. 100 μL of WST-1 reagent (Roche Diagnostics Division of Hoffman La Roche Limitée, Laval-des-Rapides, QC, Canada) diluted 1:10 in culture medium were added to wells for 2h prior to reading of absorbance at 420 nm at each time point. Cell viability was presented as a percentage of control using GraphPad Prism software (GraphPad Software, La Jolla, CA, USA). The following formula was used to determine cell viability as a percent of control for each time point and treatment:

$$\frac{(Absorbance\ of\ cells\ in\ a\ given\ concentration\ of\ drug) - (Media\ absorbance)}{(Absorbance\ of\ cells\ alone) - (Media\ absorbance)} \times 100\%$$

4.2.9 PLGA Cylinders in Cell Culture

PANC1 and PANC1 GEMR cells were plated in 25 cm^2 cell culture flasks at approximately 112,500 and 45,000 cells per flask respectively, and incubated overnight. PANC1 GEMR were plated at a lower density due to a faster growth rate. Experiments were carried out for 3, 6, 10, or 15 days. For each time point, flasks contained a control, OP^{in}/GEM^{out}, or GEM^{in}/OP^{out} double layered cylinder, and negative control flasks did not contain a cylinder. Control cylinders did not contain any drug. OP^{in}/GEM^{out} cylinders contained 16 mg OP in the inner layer and 3 mg GEM in the outer layer, while GEM^{in}/OP^{out} cylinders contained 3 mg GEM in the inner layer and 16 mg OP in the outer layer. Media was changed every 3 days. On the final day, cells were lifted using TrypLE Express (Life Technologies Inc.) and counted twice using a hemocytometer. Trypan Blue was added to cells prior to counting to ensure only viable cells were counted. Cell viability was measured as cell count, percentage of the control.

4.2.10 Dissolution of PLGA Cylinders Containing OP and GEM

Several cylinders that had been placed in cell culture for 3 to 15 days were dissolved to determine the amount of OP and GEM remaining in the cylinders. Selected cylinders were dissolved in 10 mL acetone, centrifuged for 10 min at 3500 rpm, and supernatant was discarded. The drug pellet was resuspended in 3 mL distilled water prior to being freeze dried and lyophilized overnight. The powdered drug was dissolved in HPLC grade water and OP and GEM were quantified using HPLC. Only cylinders used to treat PANC1 cells were selected, to avoid the addition of any GEM to the samples, due to GEM present in media used for PANC1 GEMR cell culture.

4.2.11 Statistical Analysis

Statistical analysis was carried out using GraphPad Prism 5. One-way ANOVA and unpaired t-test were performed.

Chapter 5

Results and Discussion

The primary goal of the thesis research was to develop an implantable cylinder capable of releasing oseltamivir phosphate (OP) alone or in combination with gemcitabine (GEM) for an extended period (eg. 30 days). The release profiles of OP/GEM and the stability of the respective drugs in terms of the ability to elicit a tumor cell response in vitro will be one of the methods used to characterize the cylinders. The results and discussion have been divided into three main sections:

- Drug detection, quantification, and stability
- Cylinder production and controlled release of OP and GEM
- In vitro effects of drugs released from cylinders on pancreatic cancer cell viability and protein expression

5.1 Drug Detection, Quantification, and Stability

5.1.1 Detection and Quantification of OP and GEM

High performance liquid chromatography was used to detect and quantify the amount of OP and GEM released from the cylinders. A method was developed where both OP and GEM could be detected in the same sample using the same mobile phase. Several methods were attempted based on the work of previous students and methodologies developed for the detection of either OP or GEM described in the literature, until one method was selected. The selected method used a Poroshell 120 SB-C18 threaded column and a mobile phase of 60% methanol and 40% 0.04M ammonium acetate buffer pH 5.2, with UV detection at 230 nm. GEM had a retention time of

approximately 1.1 min while OP had a retention time of approximately 3.0 min as shown in Figure 8. Calibration curves illustrated in Figure 9 for OP and GEM were developed to quantify the concentration of drug in solution.

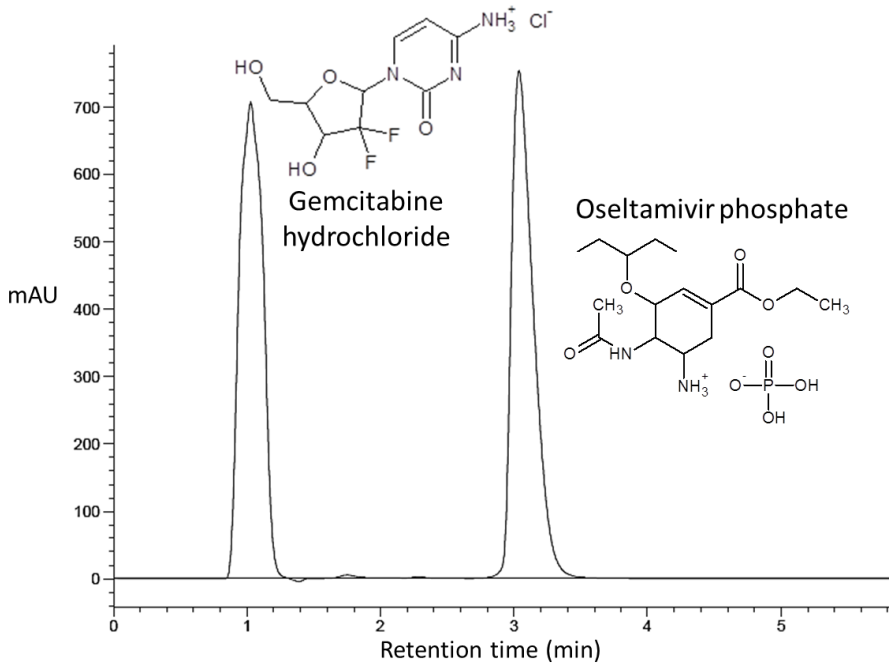

Figure 8. Detection of GEM and OP using HPLC. GEM and OP have retention times of 1.1 and 3.0 min respectively.

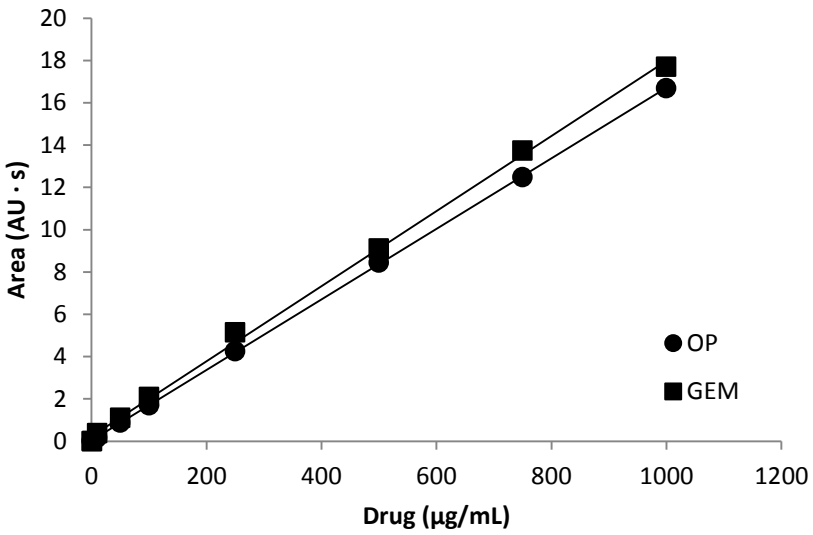

Figure 9. Calibration curve for OP and GEM using HPLC.

5.1.2 Drug Stability

Although OP and GEM are both FDA and Health Canada approved drugs, they have not been investigated for long-term stability due to the usual route of administration. OP is administered orally as a tablet, while GEM is administered intravenously over a period of approximately 30 min (Eli Lilly, 2013). Therefore, it was necessary to determine if OP and GEM would be stable in vitro during the proposed 30 day release period.

5.1.2.1 GEM Stability

GEM was dissolved in 0.1M sodium phosphate buffer pH 7.4 and stored at 37°C for 31 days. Samples were taken periodically and GEM measured using HPLC, as shown

in Figure 10. No significant change in the concentration of GEM was detected, indicating that GEM is stable at pH 7.4 and 37°C for the duration of the release period.

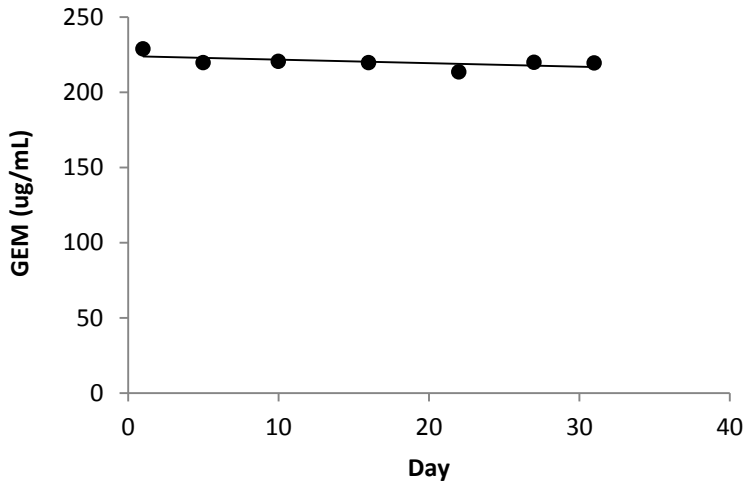

Figure 10. Concentration of GEM in 0.1M sodium phosphate buffered stored at 37°C for 31 days.

5.1.2.2 OP Stability

OP was dissolved in HPLC grade water containing 0.1% (v/v) trifluoroacetic acid (TFA) or 0.1M sodium phosphate buffer pH 7.4 and stored at 37°C for 30 days. No decrease in the amount of OP was observed in water containing 0.1% TFA as seen in Figure 11.

A decrease in the amount of OP was observed when dissolved in sodium phosphate buffer, as seen in Figure 12. The peak representing OP (retention time of 3.0 min) decreased, while a new peak with a retention time of 1.3 min appeared and grew as the experiment progressed. After 30 days, the amount of OP detected was 70% of the initial amount of OP. The emergence of a new peak was thought to represent a change in

the structure of OP, and the increase in the alternate peak area seemed to parallel the decrease in the OP peak area.

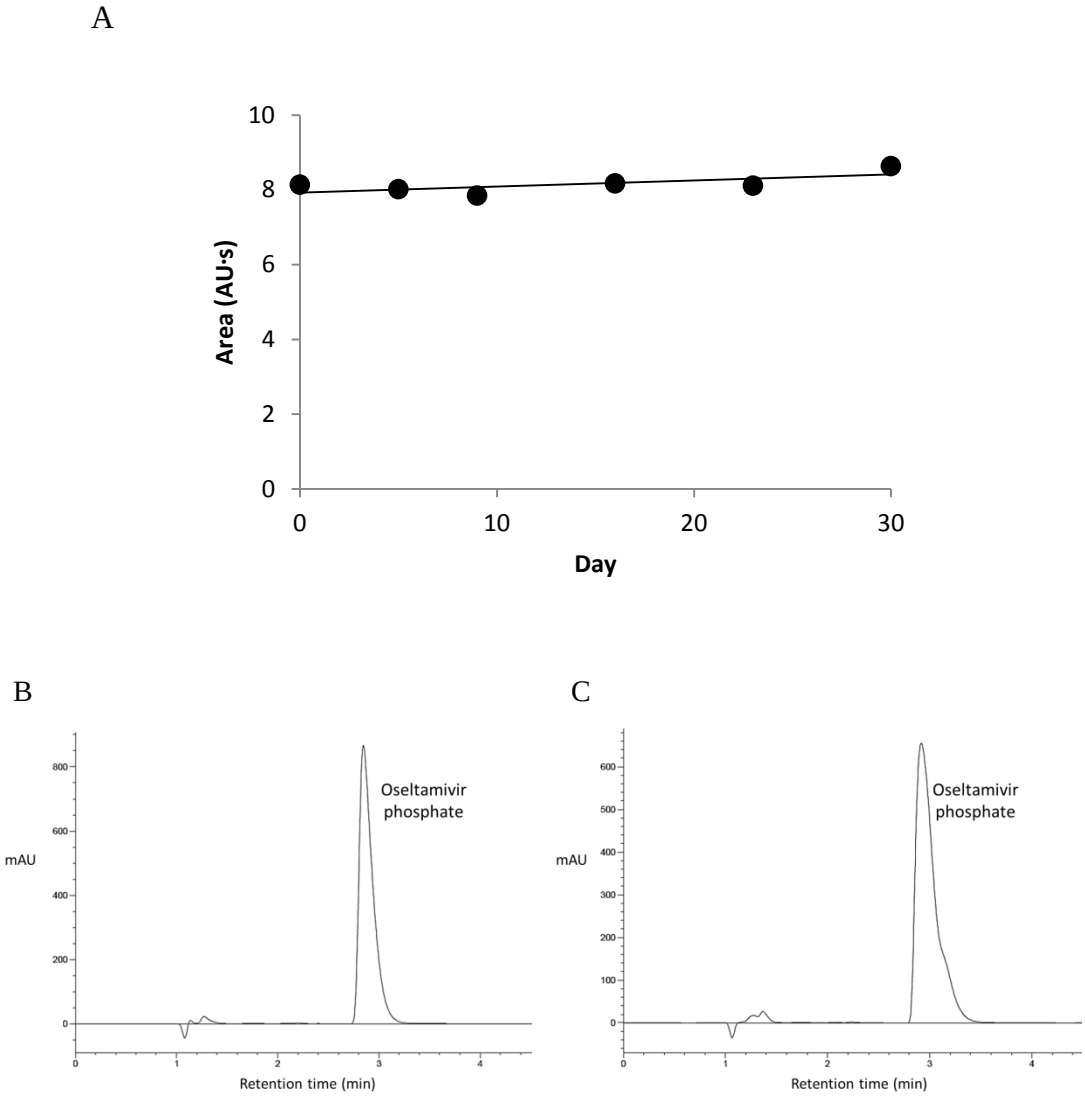

Figure 11. Area under curve of peak representing OP in water with 0.1% TFA at 37°C (A). HPLC chromatograms of OP dissolved in water with 0.1% TFA at 37°C on day 0 (B) and day 30 (C).

A

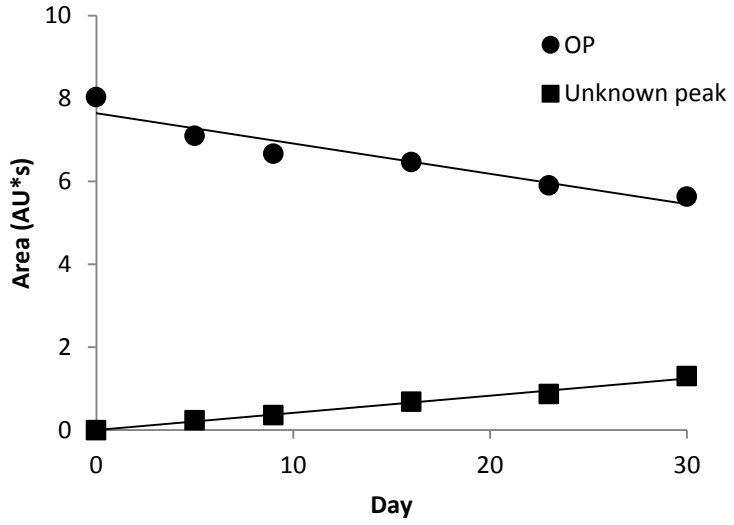

B

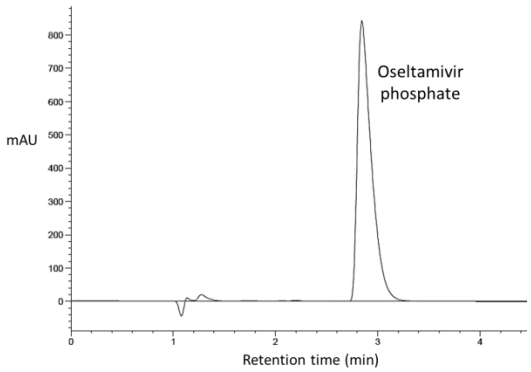

C

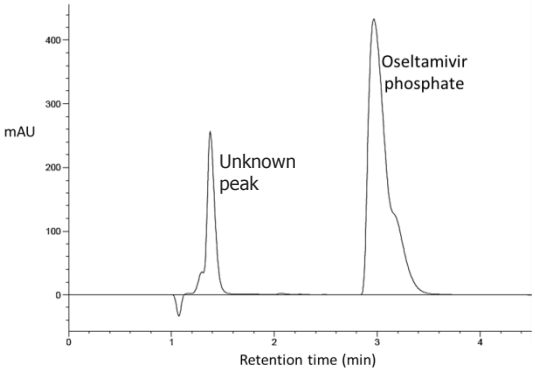

Figure 12. Area under curve of peak representing OP in 0.1M sodium phosphate buffer pH 7.4 at 37°C (A).HPLC chromatograms of OP in sodium phosphate buffer at 37°C on day 0 (B) and day 30 (C).

The change in the structure of OP could be due to ester hydrolysis. Clinically, OP is administered orally as a prodrug and is subsequently converted to oseltamivir carboxylate (OC) through hydrolysis of the ester bond by enzymes in the liver [59]. OC was

analyzed using HPLC and found to have a retention time of 1.3 min, matching that of the emerging peak, as seen in Figure 13. The shorter retention time of OC compared to OP is expected, as OC is a more polar molecule.

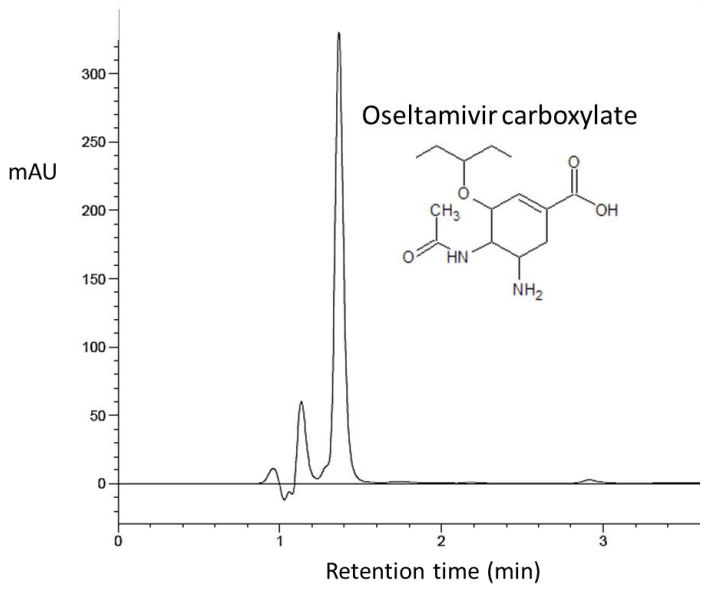

Figure 13. HPLC chromatogram of oseltamivir carboxylate (OC).

Esters, like most carboxylic derivatives, are susceptible to nucleophilic substitution. Hydrolysis of the ester bond in OP produces OC and ethanol. Ester hydrolysis occurs when ester is heated in acid or base. In alkaline conditions, the hydronium ion is a strong nucleophile that attacks the carbonyl carbon, leading to the formation of a resonance-stabilized carboxylic acid salt. Due to the stability of the carboxylic acid, this reaction is more or less irreversible [84]. Therefore, it seems likely that the 30% of OP lost after 30 days is converted to OC at 37°C in a solution with a pH of 7.4.

Under acidic conditions, ester hydrolysis is a reversible reaction. Water acts as a nucleophile and alcohol is the leaving group. In the reverse reaction, esterification, alcohol is the nucleophile while water is the leaving group [84]. The product specification sheet from Sigma-Aldrich states that HPLC grade water containing 0.1% (v/v) TFA has a pH between 1.8 and 2.4. Measurement of the water containing TFA in the laboratory gave a pH of 2.2. Since ester hydrolysis occurs at elevated temperatures in both acidic and alkaline conditions, it is not clear why some OP would be converted to OC in sodium phosphate buffer at pH 7.4, but not in water with 0.1% TFA at pH 2.2. It is possible that OP is converted to OC when in water containing TFA at 37°C, but the reaction is reversed when the sample is exposed to the HPLC mobile phase, which has a pH of 5.2.

These findings are consistent with those of other groups. Oliyai et al [85] investigated the stability of OP at 70°C and found OP could be converted to 3 compounds; OC and 2 other compounds named isomers I and II [85]. Isomers I and II were the result of N,N-acyl migration in the OP and OC compounds respectively, as shown in Figure 14. The first order rate constants of the conversions of OP to OC, isomer I, and isomer II at 70°C and pH 2-8 reached a minimum at pH 4. The rate constant of the conversion of OP to OC, and therefore of ester hydrolysis, was $1.78 \times 10^3\ h^{-1}$ at pH 2; $0.28 \times 10^3\ h^{-1}$ at pH 3; $18.5 \times 10^3\ h^{-1}$ at pH 7; and $78.0 \times 10^3\ h^{-1}$ at pH 8, as shown in Table 3. The rate constant of ester hydrolysis was dramatically higher at pH 7.4 than pH 2.2 [85]. Although the rate constants would be lower at 37°C, the same trend would be expected.

OP and GEM appear stable when dissolved in 0.1M sodium phosphate buffer pH 7.4 and stored at 37°C for 30 days. No loss of GEM was observed and the loss of OP was minimal, with 30% of OP lost over 30 days The decrease in the amount of OP was linear,

indicating the loss of OP was approximately 1% of the initial amount of OP per day. The loss of OP, which corresponded with the appearance and increase of a new peak, is most likely a result of ester hydrolysis of a small portion of the total amount OP to form OC.

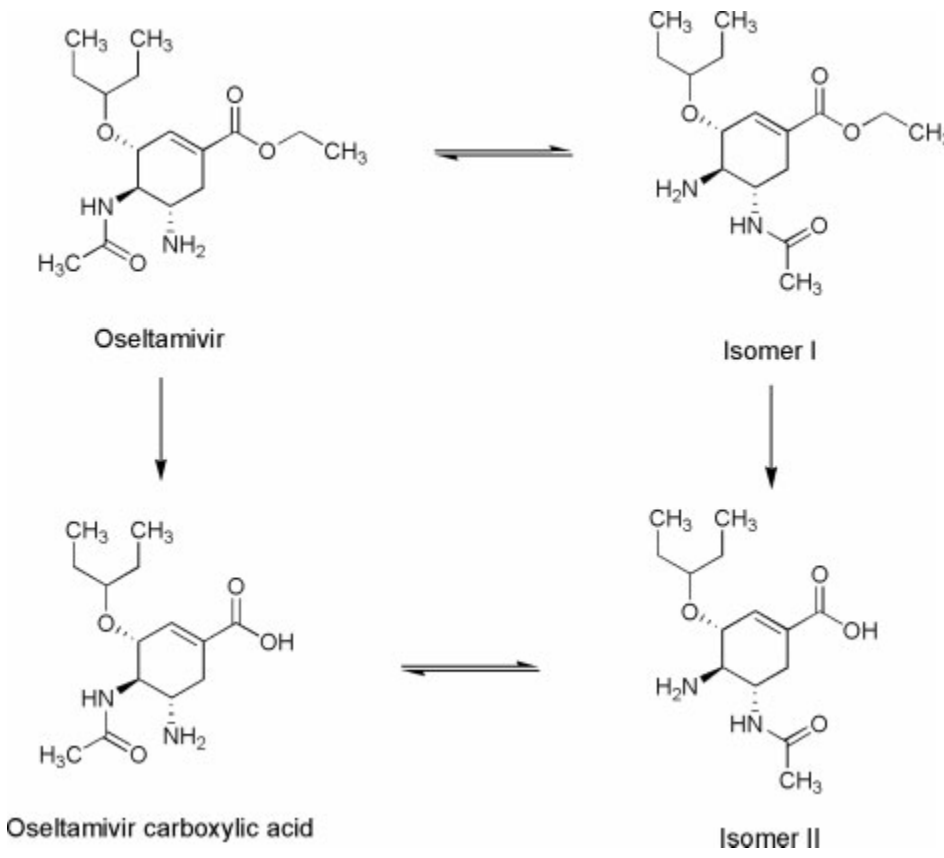

Figure 14. OP and its products formed in aqueous solutions at pH 2-8 [86]**.**

Table 3. First order rate constant in conversion of OP to OC at 70°C, pH 2-8 [85].

pH	First order rate constant (h^{-1}) $x10^3$
2.0	1.78
3.0	0.28
4.0	0.05
5.0	0.43
6.0	3.4
7.0	18.5
8.0	78.0

5.2 Cylinder Production and Controlled Release of OP and GEM from PLGA Cylinder

5.2.1 Cylinder Production

Cylinders were produced by dissolving PLGA and SPAN 80 in acetone. OP or GEM was added and suspended in the PLGA-SPAN 80-acetone solution. SPAN 80 was used to promote a uniform suspension of insoluble particulate drug throughout the polymer solution. The suspension was then ejected dropwise onto a Teflon sheet as illustrated in Figure 15, forming a thin film after evaporation of the acetone. OP and GEM films are made by the addition of one or both of the two drugs and control films were formed without drug. Films were stored at 4°C overnight or at 20°C for 72h. Storing the films at a higher temperature and longer period of time allowed for increased acetone evaporation, and therefore less residual acetone in the film. Films were rolled around a 16 gauge needle lubricated with glycerol to form a cylinder, and lightly moulded by hand to

ensure cylinders were uniform in size and shape. Films stored at 4°C overnight prior to rolling were sticky while those stored at 20°C for 72h were not. Higher amounts of residual acetone were thought to cause the stickiness observed in films stored at 4°C overnight. After rolling, cylinders were stored at -20°C until needed. The schematic demonstrating the production of a single layered cylinder is shown in Figure 15, while a double cylinder was formed by rolling a second film around the first cylinder.

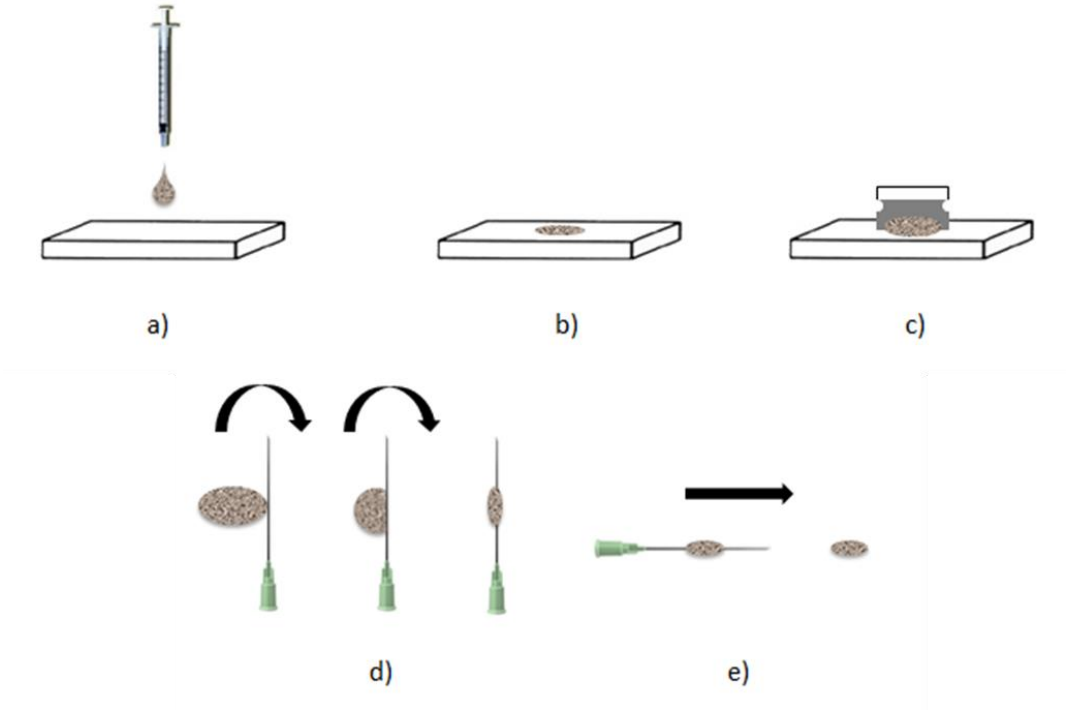

Figure 15. Production of a single layered cylinder. Drug can be suspended in the PLGA, SPAN 80, and acetone solution and ejected dropwise from a syringe or pipette onto a teflon sheet (a). Acetone evaporates from the suspension, resulting in a thin, malleable film (b). The film is scraped off the teflon sheet using a razor blade (c) and is wrapped around a glycerol-lubricated 16G needle (d) to form a cylinder. The cylinder is removed from the needle and shaped by hand, resulting in uniformly sized cylinders (e).

The objective was to encapsulate 16 mg OP and 3 mg GEM in each cylinder. These amounts were selected based on prior studies involving effective dosages administered via intraperitoneal injection to RAG2xCγ double mutant mice with heterotopic xenografts of human pancreatic PANC1 tumors.

Films containing 16 mg OP, 3 mg GEM, or control (no drug) are shown in Figure 16. OP layers are nearly opaque and are white in colour due to OP particles dispersed throughout the film. Few air bubbles are present in the OP film. GEM films have air bubbles and are mostly clear, but some drug crystals are visible. By comparison, the control films have many air bubbles and are transparent. Because the control films are transparent, drug particles are easily identified in the OP and GEM films.

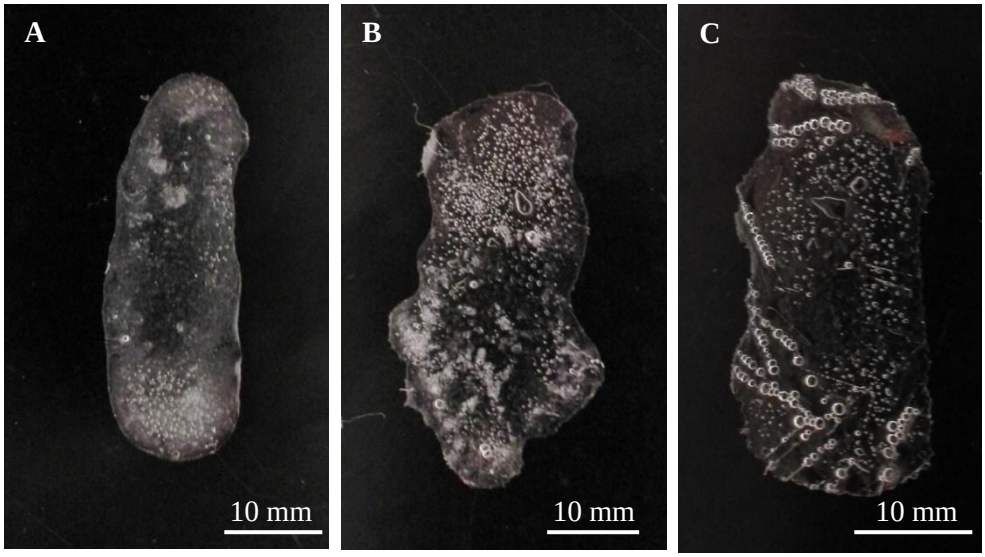

Figure 16. OP films have a white, cloudy appearance due to OP dispersed throughout the film (A). GEM films are mostly clear and some drug particles are visible (B). Control films are clear with visible air bubbles (C).

5.2.2 Cylinder characterization

Single and double layered cylinders were produced. As seen in Figure 17, single layered cylinders measured 9 mm in length and 4 mm in diameter while double layered cylinders measured 10mm in length and 5mm in diameter. The cylinder on the left of Figure 17A is a single layered cylinder containing 16 mg OP, while the cylinder on the right is a single layered control cylinder. The cylinder in Figure 17B is a double layered cylinder, with 16 mg OP in the inner layer and 3 mg GEM in the outer layer.

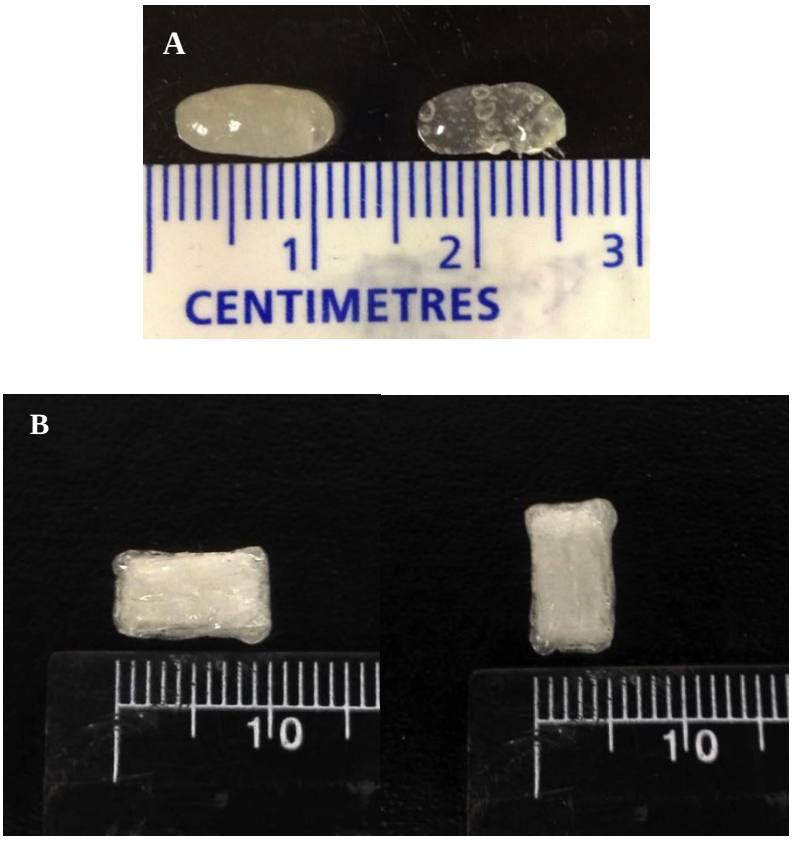

Figure 17. Single layered cylinder containing 16 mg OP (A left), single layered control cylinder containing no drug (A right) and double layered cylinder with 16 mg OP inner layer and 3 mg GEM outer layer (B).

Scanning electron microscopy (SEM) was used to visualize cross sections of double and single layered cylinders. Cylinders had a hollow core and distinct layers of

each film were visible as a result of films being wrapped around a needle, as seen in Figure 18. In Figure 19, the thickness of these layers is seen to vary, ranging from approximately 25 µm to over 200 µm. It is possible that this variation in layer thickness is an artifact caused by the compression of the cylinders when preparing to take cross section images, but is more likely to be a result of the fabrication process. Since the polymer solution is ejected dropwise from a pipette tip onto a flat teflon sheet to form a pool, the centre part of the film is likely thicker than the outer regions.

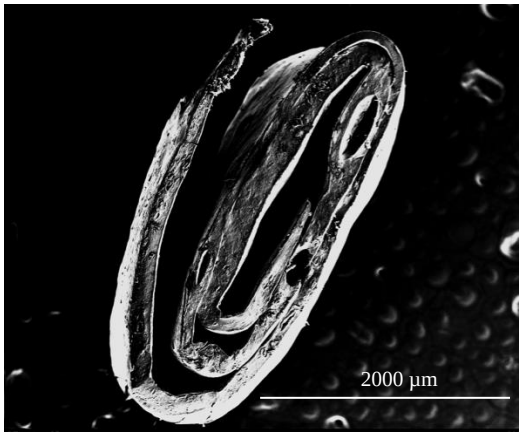

Figure 18. Cross section of a single layered cylinder. A hollow core and distinct layers are visible due to the fabrication process, which involves rolling the film around a needle.

The cylinder cross sections show the drug particles embedded in the PLGA polymer matrix. The control cylinder, containing no drug, appears smooth. In Figure 19B, very fine, small particles of pure OP are visibly embedded in PLGA and are evenly dispersed. The particles are much smaller than those seen in Figure 19C and D, in which GEM and extracted OP are encapsulated, respectively. Aggregates of encapsulated GEM particles are approximately 50 µm, and small air bubbles are also visible in the polymer.

These SEM micrographs are consistent with the appearance of the films, where GEM crystals were visible, as opposed to the OP film, where individual OP particles were not visible. The OP film appeared more opaque and white, indicating OP particles are smaller and were more evenly distributed. Extracted OP particles also appear to be evenly dispersed throughout the polymer but are significantly larger than pure OP particles. Extracted OP particles are approximately 10 μm in size while pure OP particles are between 1 and 5 μm, as seen in Figure 19.

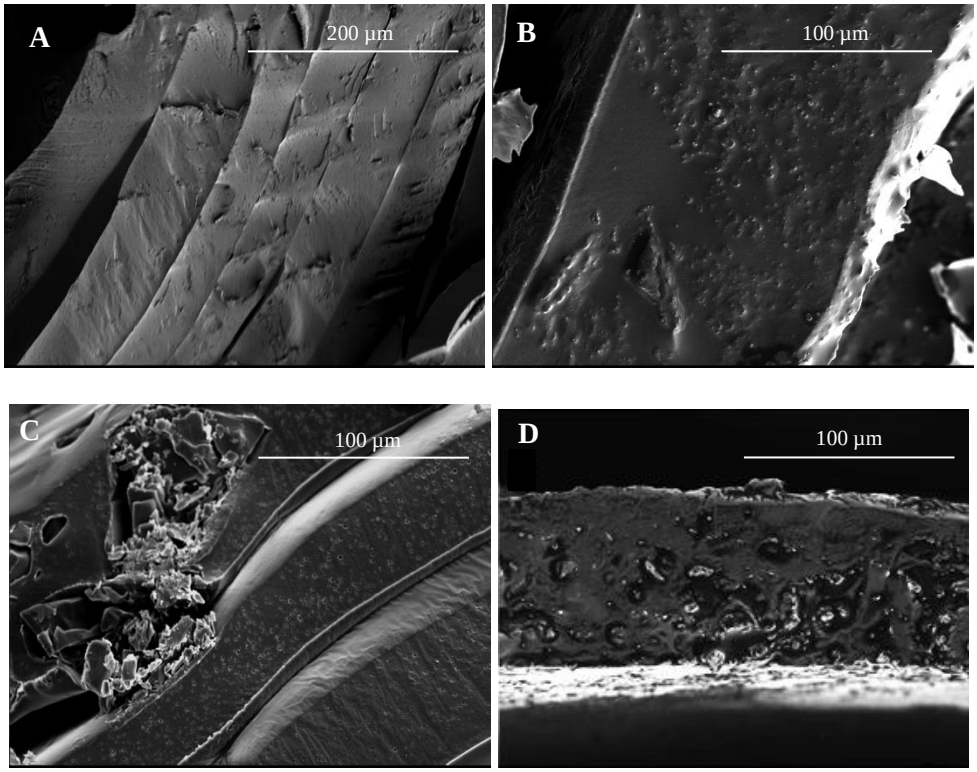

Figure 19. SEM micrographs of a control cylinder (A), and cylinders containing 16 mg pure OP (B), 3 mg GEM (C), and 16 mg extracted OP (D). Image D was taken by Jordan Ellis.

5.2.3 Release of OP and/or GEM from Single Layered PLGA Cylinders

5.2.3.1 Release of Extracted OP from Single Layered Cylinder

Single layered cylinders were initially formulated with OP that had been extracted from Tamiflu® capsules [21]. The fabrication process was replicated, with films stored at 4°C, and the release profile of single layered cylinders containing 16 mg extracted OP is shown in Figure 20. In the initial 24h, 27% of OP was released, increasing by 5% to 32% release after 72h. The majority of OP was released between days 3 and 16, during which time 63% of encapsulated OP was released, leading to a cumulative release of 95% in the first 16 days. The remaining 5% of OP was released steadily and slowly until day 30. Release of extracted OP varied greatly between cylinders during the first 9 days, as shown by the high standard deviations in Figure 20. PLGA was more than 95% degraded after 30 days.

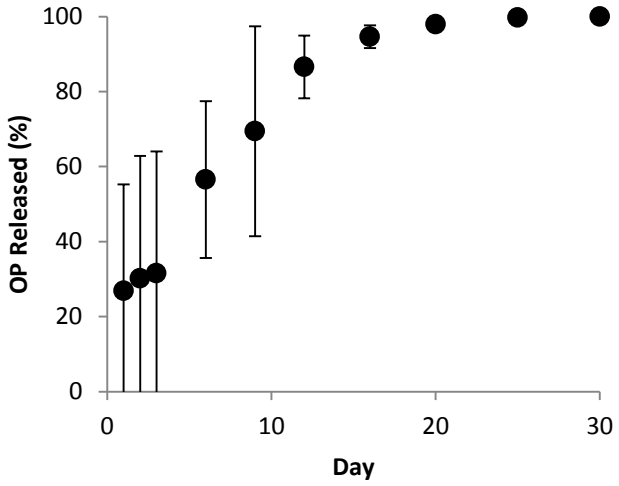

Figure 20. Release of OP from single layered cylinder containing 16 mg extracted OP. Films were stored at 20°C for 2h, then overnight at 4°C. Data points represent the mean ± standard deviation, n=3. OP released is reported as a percentage of the total amount of OP released after 30 days.

5.2.3.2 Release of OP from Single Layered PLGA Cylinders

A source of pure OP was found, so the extraction of OP from Tamiflu® capsules was no longer necessary. Release experiments were performed to determine the release profile of pure OP, as seen in Figure 21. All cylinders contained 16 mg OP and films were stored at 20°C for either 24 or 72h.

Films rolled 24h after fabrication resulted in cylinders with a high initial release of OP, with 31, 74, and 87% release measured after 24, 48, and 72h respectively. OP release slowly increased from 92% on day 4 until day 25, when 100% release was achieved. Films rolled 72h post-fabrication formed cylinders with a very different release profile. The initial release was low, with only 16% of OP released after 24h. The majority of OP was released between days 3 and 21, when OP release increased from 18 to 97%, before plateauing at day 25. Cylinders with a 24h storage time prior to rolling showed high variation in OP release after 24h, especially considering the experiment was performed 10 times, although OP release was more consistent at later time points. Little variation in OP release was observed between replicates of cylinders rolled following 72h at 20°C.

It is noteworthy that cylinders produced from films stored for 72h at 20°C prior to rolling displayed a substantially lower initial release of OP than cylinders made from films stored for 24h. A longer storage period prior to rolling should allow a greater amount of acetone evaporation, thereby reducing the amount of residual acetone in the cylinder. Release profiles of cylinders containing OP produced from films stored for 24 or 72h at 20°C indicate that a larger amount of residual acetone leads to a higher initial rate of OP release.

Cylinders containing pure OP, formed from films stored for 24h at 20°C, had a larger initial release of OP than cylinders containing extracted OP. Cylinders containing pure OP had 87% release of OP after 72h, and 92% release after only 4 days. Meanwhile, cylinders containing extracted OP released 32% of OP in 72h, and 95% release was not reached until day 16. Extracted OP particles were much larger than particles of pure OP, as seen in SEM images of OP embedded in PLGA in Figure 19. These results indicate particle size plays a role in release rate. One possibility is that pure OP is small enough that particles near the surface of the cylinder can diffuse into the supernatant, while larger extracted OP particles are less susceptible to diffusion and are not released until PLGA degradation has begun.

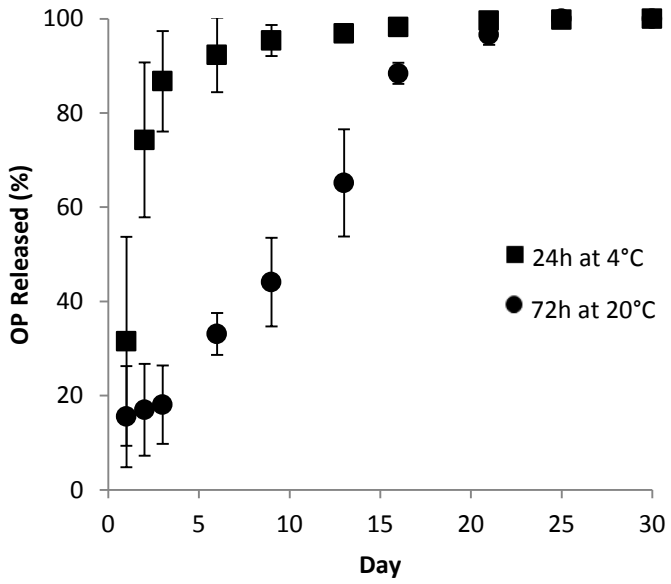

Figure 21. Release of OP from PLGA cylinders containing 16 mg OP. Cylinders were stored for 24h (n=10) or for 72h (n=5) at 20°C prior to rolling. OP released is reported as a percentage of the total amount of OP released after 30 days.

5.2.3.3 Singled Layered Cylinders Containing 16 mg OP and 3 mg GEM

Single layered cylinders containing both OP and GEM were fabricated. All cylinders contained 16mg OP and 3mg GEM, but the amount of PLGA and Span 80 was altered. The ratio of PLGA:SPAN 80 was kept constant at approximately 20:1. All films were stored at 4°C overnight prior to rolling and the release experiment was performed in triplicate for each type of cylinder.

Cylinders containing 80 mg PLGA released high bursts of both OP and GEM within the first 3 days, as seen in Figure 22A. At 24 and 48h, 46 and 79% of OP was released, respectively. During the first 24h, the release of OP varied to a large extent between the three cylinders, compared to later time points. OP release was then linear from day 3 to 20, with the release of OP increasing from 86 to 99%. GEM was released at a slower rate, with 32% released at 24h and 54% released at 48h. GEM release was consistent from day 3, with 61% release, until day 25 when 97% of GEM had been released. With the exception of OP release at 24h, the variation in percent release of both drugs was low for the duration of the experiment.

Cylinders containing 160 mg PLGA were formulated and release experiments were performed. It was hypothesized that increasing the amount of PLGA without changing the amount of OP and GEM in a cylinder would lead to a lower initial release of both drugs. Release of OP and GEM from cylinders containing 160 mg PLGA, as seen in Figure 22B, showed very little variation between triplicates throughout the entire 30 day release period. It was observed that 64% of OP was released within 24h and 83% was released in 48h. OP release was linear from day 2 until day 20, when 98% of OP had been released. The initial release of GEM was slower than that of OP, with 39 and 52%

release at 24 and 48h, respectively. The amount of GEM released was low between days 2 and 12, with only 14% of GEM released in 10 days. The rate of GEM release then increased until day 25, when the amount of GEM released reached 95%. Despite doubling the amount of PLGA in the cylinders, the release of OP and GEM from cylinders containing 160 mg PLGA was similar to that of cylinders containing 80 mg PLGA, as shown in Figures 22B and 22A, respectively.

The cylinders containing 320 mg PLGA had a slower, near linear release of OP and GEM as shown in Figure 22C. OP release was 31 and 55% at 24 and 48h respectively, while 17 and 27% of GEM was released at the same time points. After 48h, the release of both drugs was consistent and nearly linear. However, there was a high degree of variation between replicates in the amount of OP released during the first 9 days of the experiment.

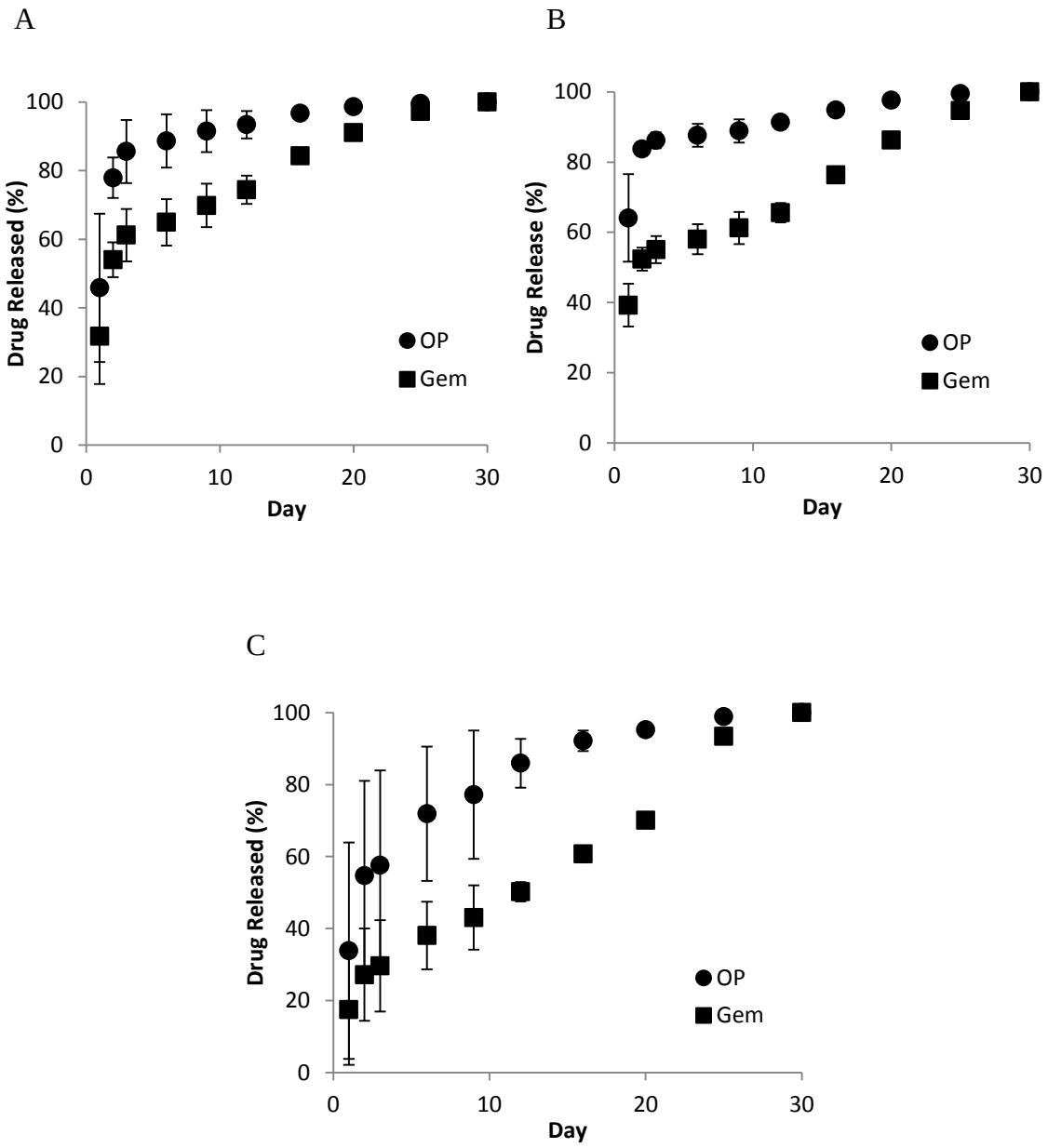

Figure 22. Release profile of single layer cylinders containing 16 mg OP, 3 mg GEM and either 80 (A), 160 (B), or 320 (C) mg of PLGA. Films were stored at 4°C from 24h prior to rolling. Data points represent the mean ± standard deviation, n=3. OP and GEM released are reported as a percentage of the total amount of drug released after 30 days.

5.2.4 Release of OP and GEM from PLGA Double Layered Cylinders

Double layered cylinders were produced with one drug contained in the inner layer, and the other drug in the outer layer. Cylinders with OP in the inner layer and GEM in the outer layer were called OP^{in}/GEM^{out}, while those with GEM in the inner layer and OP in the outer layer were referred to as GEM^{in}/OP^{out}. The objective was to achieve linear, sustained release of both drugs over 30 days. Several variations of the cylinders were fabricated as described in Table 4. All double layered cylinders contained 80 mg PLGA and 4-6 mg SPAN 80 in each layer. After 30 days, PLGA cylinders were more than 95% degraded.

Table 4. Double layered cylinders produced for release experiments. All double layered cylinders contained 80 mg PLGA and 4-6 mg SPAN 80 per film. The amount of drug loaded and conditions of film storage prior to rolling for each type of cylinder are described.

Cylinder Type		OP	GEM	Film storage prior to rolling
A	OP^{in}/GEM^{out}	16 mg	3 mg	4°C overnight
	GEM^{in}/OP^{out}	16 mg	3 mg	4°C overnight
B	OP^{in}/GEM^{out}	8 mg	1.5 mg	4°C overnight
	GEM^{in}/OP^{out}	8 mg	1.5 mg	4°C overnight
C	OP^{in}/GEM^{out}	16 mg	3 mg	20°C for 72h
	GEM^{in}/OP^{out}	16 mg	3 mg	20°C for 72h

5.2.4.1 Double Layered Cylinder Type A

Films were stored at 4°C overnight and rolled the following day. Cylinders were made with OP in the outer layer and GEM in the inner layer (GEM^{in}/OP^{out}), as well as cylinders with GEM in the outer layer and OP in the inner layer (OP^{in}/GEM^{out}). Release

experiments were performed for both cylinder types, as shown in Figure 16. OP^{in}/GEM^{out} and GEM^{in}/OP^{out} cylinders had very similar release profiles. Both cylinders had a high initial release of OP, with 70-90% release in the first three days, and less than 10% of drug still encapsulated after 13 days. GEM release was linear for all cylinders.

It is noteworthy that the single layered cylinder containing 160 mg of PLGA, as seen in Figure 22B, had a very different release profile than the double layered cylinders containing 16mg OP and 3mg GEM, as seen in Figure 23, since these cylinders have the same amount of PLGA and drug. In the first 24 hours, the release of both drugs was greater in the single layered cylinder than either type of double layered cylinder. The initial release of GEM from the double layered cylinders was low, yet the 160 mg PLGA single layered cylinder released nearly 40% of the loaded GEM during the first 24 hours.

5.2.4.2 Double Layered Cylinder Type B

Cylinders were produced using the same amount of PLGA and SPAN 80 as type A double layered cylinders, but the amount of drug loaded was halved. The release profiles for type B OP^{in}/GEM^{out} and GEM^{in}/OP^{out} cylinders are shown in Figure 24. The initial release of OP was dramatically reduced compared to type A double layered cylinders, with less than 40 and 20% of OP released from the OP^{in}/GEM^{out} and GEM^{in}/OP^{out} cylinders in the first 72h.

Both drugs were released more quickly from the OP^{in}/GEM^{out} cylinder than the GEM^{in}/OP^{out} cylinder. At day 13, the OP^{in}/GEM^{out} cylinder had released 77% and 57% of its OP and GEM respectively, while the GEM^{in}/OP^{out} cylinder had released only 55% and 28%. Both cylinder types released 98% of both drugs by day 27.

A

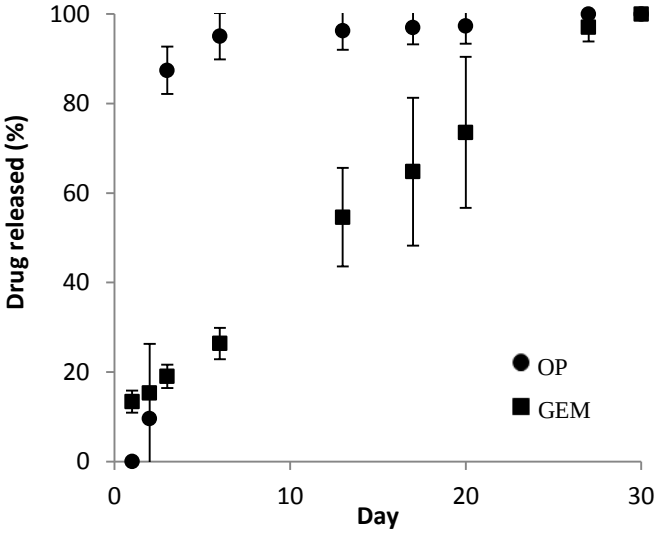

B

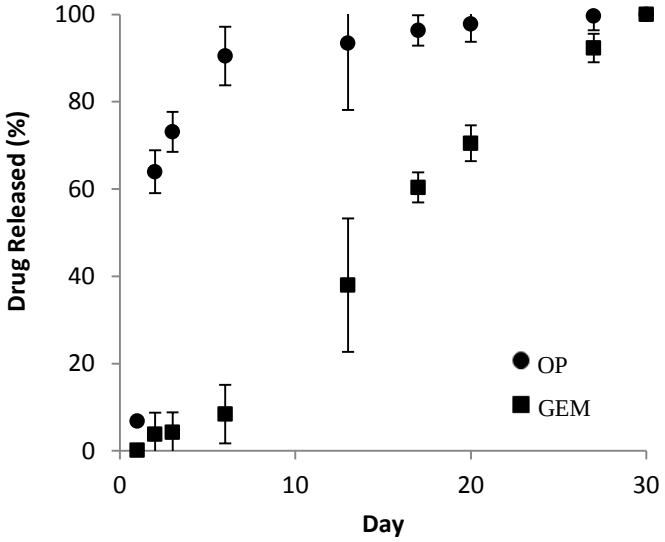

Figure 23. Release profile of type A double layered cylinders. Cylinders contained 16 mg OP inner layer, 3 mg GEM outer layer (A) and 3 mg GEM inner layer, 16 mg OP outer layer (B). Data points represent the mean ± standard deviation, n=3. OP and GEM released are reported as a percentage of the total amount of drug released after 30 days.

A

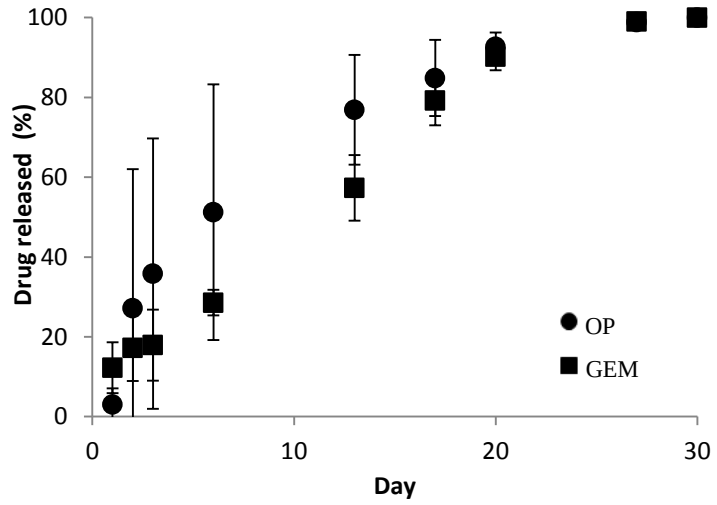

B

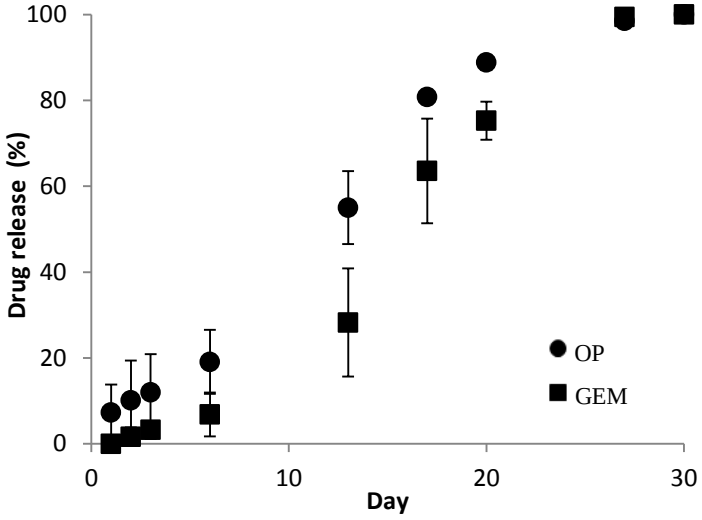

Figure 24. Release profile of type B double layered cylinders. Cylinders contained 8 mg OP inner layer, 1.5 mg GEM outer layer (A) and 1.5 mg GEM inner layer, 8 mg OP outer layer (B). Data points represent the mean ± standard deviation, n=3. OP and GEM released are reported as a percentage of the total amount of drug released after 30 days.

5.2.4.3 Double Layered Cylinder Type C

The films of all cylinders containing OP and GEM presented so far were stored at 4°C overnight and rolled into cylinders the next day. Most also showed a high initial release of OP. The films were sticky, indicating that residual acetone was present in the films. If that were the case, residual acetone remaining in the cylinders may diffuse out of the cylinder when placed in buffer, and leaving pores and channels to allow for the permeation of water and premature diffusion and release of the drugs out of the cylinder. OP may be affected to a greater extent than GEM because OP particles are smaller. To test the hypothesis, cylinders were made from films which had been stored at 20°C for 72h.

The films were no longer sticky after 72h at 20°C and were more rigid than those stored at 4°C overnight. The release profiles of cylinders made from films with 16 mg OP or 3 mg GEM and stored at 20°C for 72h prior to rolling are shown in Figure 25. Release profiles from these cylinders indicate a much lower initial release OP, and the arrangement of the layers did have an impact on the release profile.

Type C OP^{in}/GEM^{out} cylinders had a higher initial release of GEM than OP. After 24h, 39% of GEM and 15.5% of OP had been released. GEM was then released at a constant rate until day 25, at which point 99% of GEM had been released. OP release was sigmoidal, with most OP being released between days 3 and 16, before beginning to plateau, as seen in Figure 25A.

Type C GEM^{in}/OP^{out} cylinders showed a slower release of GEM, as shown in Figure 25B. After 72h, only 2.5% of GEM had been released. GEM release was linear from day 3 until day 25, when the release slowed until day 30. OP was released more

quickly, with 13, 34, and 53% released after 24, 48, and 72h, respectively. OP release was then linear until day 20, when 97% of the OP had been released, with the remaining amount released over the final 10 days.

Release of GEM was linear from type A and type C OP^{in}/GEM^{out} and GEM^{in}/OP^{out} cylinders. As expected, the initial release of GEM was lowest from GEM^{in}/OP^{out} cylinders, and type A and type C GEM^{in}/OP^{out} cylinders demonstrated very similar GEM release profiles. GEM was released more quickly from type A OP^{in}/GEM^{out} cylinders than either type of GEM^{in}/OP^{out} cylinder, and type C OP^{in}/GEM^{out} cylinders had the quickest release of GEM.

The initial release of OP was substantially reduced in type C cylinders when compared to type A cylinders. OP was released quickly and at a similar rate from both type A cylinders, with 87 and 73% of OP released from type A OP^{in}/GEM^{out} and GEM^{in}/OP^{out} cylinders in 72h. Meanwhile, type C OP^{in}/GEM^{out} and GEM^{in}/OP^{out} cylinders released 21 and 53% of OP in the same amount of time. The difference in OP release between type A and type C cylinders is consistent with the hypothesis that storage at a lower temperature for a shorter period of time could lead to a higher amount of residual acetone, and could contribute to a larger initial release of OP. The release of GEM was not affected, but GEM particles were much larger than OP particles, as seen in SEM micrographs in Figure 19, and are therefore less likely to diffuse out of the PLGA matrix.

A

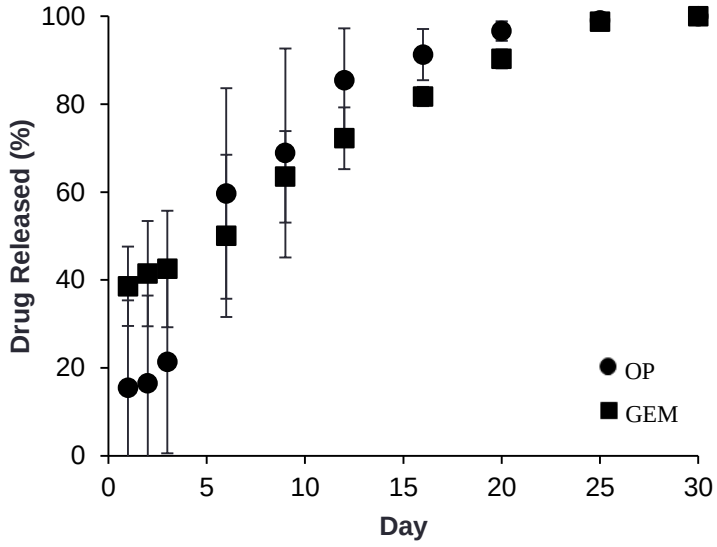

B

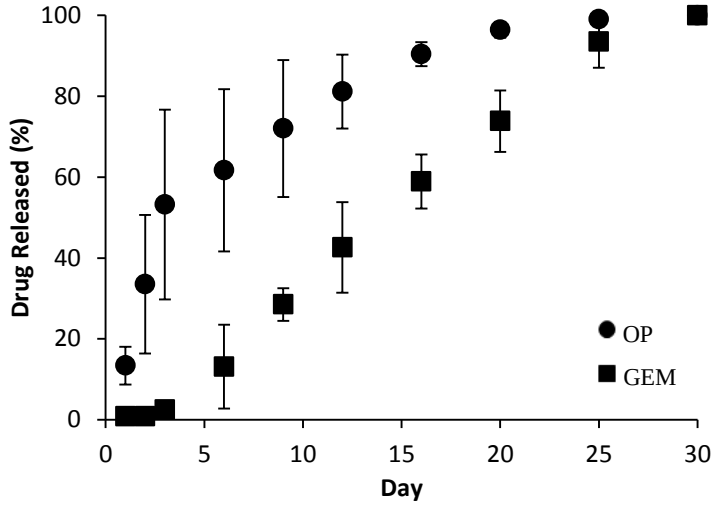

Figure 25. Release profile of type C double layered cylinders. Cylinders contained 16 mg OP inner layer, 3 mg GEM outer layer (A) and 3 mg GEM inner layer, 16 mg OP outer layer (B). Data points represent the mean ± standard deviation, n=3. OP and GEM released are reported as a percentage of the total amount of drug released after 30 days.

5.2.5 Cylinder Selection for Cell Viability Assays

In vivo experiments had previously been performed, during which PANC1 tumor-bearing mice were treated with OP and GEM via intraperitoneal injections (unpublished data). The dosage regimens from these earlier trials in which tumor volume was either reduced or showed no increase, were compared and used to determine the amount of OP and GEM to load in each cylinder for the purpose of the current study. Based on three treatments per week of 50 mg/kg OP and one weekly treatment of 30 mg/kg GEM as determined in vivo, and assuming the average mouse weighs 25 g, the amounts of OP and GEM needed were approximately 16 and 3 mg, respectively. Figure 26 demonstrates the projected release profile of a cylinder containing 16 mg OP and 3 mg GEM, assuming 100% drug encapsulation and a linear rate of release over 30 days. Since the projected release was based on treatment dosages that resulted in either the stagnation or reduction of tumor volume in mice, cylinders prepared in the present study that provided release profiles that most closely matched the projected release were thought most likely to be effective.

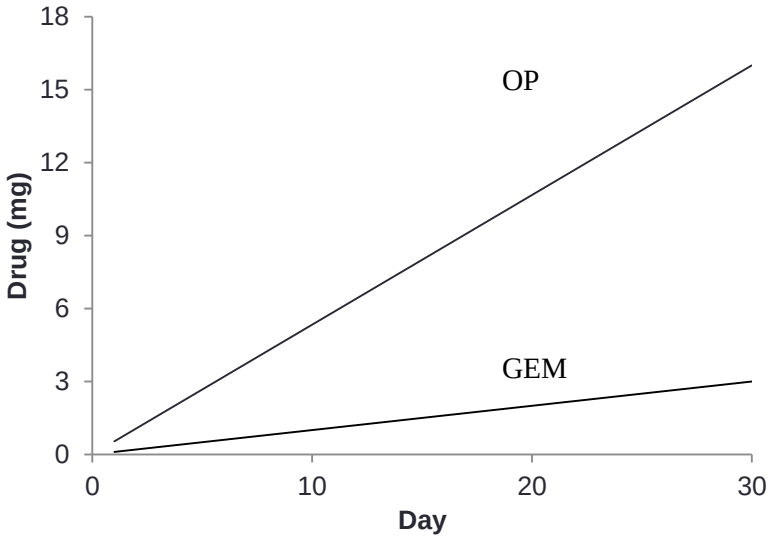

Figure 26. Projected release of OP and GEM from a cylinder containing 16 mg OP and 3 mg GEM, assuming 100% drug encapsulation and linear release rate over 30 days. Cumulative dosages of 16 mg OP and 3 mg GEM were selected based on treating mice with 30 mg/kg GEM weekly and 50 mg/kg OP three times per week, as optimized in vivo, for 30 days.

OP^{in}/GEM^{out} and GEM^{in}/OP^{out} type C double layered cylinders were selected for testing on cell viability using pancreatic cancer cell line PANC1, and GEM resistant PANC1 (PANC1 GEMR). These two cylinders were selected because the release profiles most closely matched the projected release profile as illustrated in Figure 27. The release of GEM from both types of cylinders is a close match to the projected GEM release. The release of OP from both cylinders is similar to the projected release for the first 16-20 days, before the rate of release decreases and plateaus. It is evident that 100% OP loading was not achieved, since the cumulative release of OP was only 8.9 and 10.6 mg from the OP^{in}/GEM^{out} and GEM^{in}/OP^{out} cylinders after 30 days. Overall, both cylinders are similar to the projected release profile, and both were selected for in vitro cell viability assays.

A

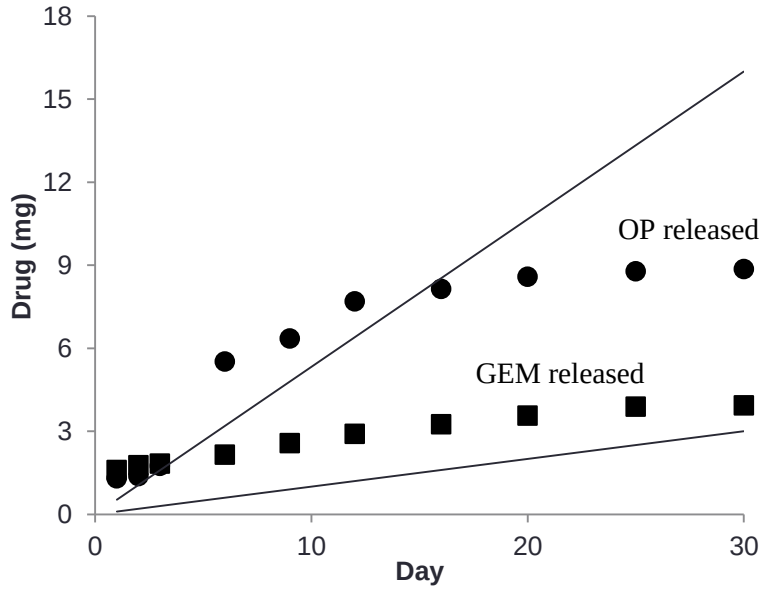

B

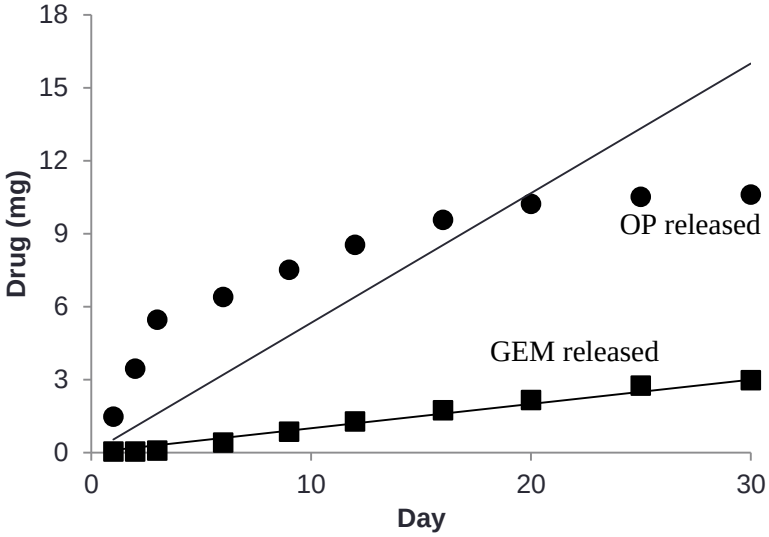

Figure 27. Release profile of double layered type C OP^{in}/GEM^{out} (A) and GEM^{in}/OP^{out} (B) cylinders in comparison to the theoretical release profile, which assumes 100% encapsulation and constant release over 30 days.

5.2.6 Drug Loading

Drug release was calculated as a percentage of the cumulative drug released over 30 days, not as a percentage of the amount of drug added during cylinder production. It was expected that OP encapsulation was reduced since OP could be seen on the sides of the glass vials in which OP is added to the polymer solution, meaning that it was less likely to be encapsulated within the polymer film. The amount of OP and GEM added to the polymer solution during cylinder fabrication and the average of OP and GEM released from the cylinder type C in 30 days (n=3) are shown in Table 5. GEM encapsulation is in the range of 100%, however only 55-66% of OP is being encapsulated. It is possible that some OP is still encapsulated in the cylinder after 30 days because some PLGA is still present, however the plateau in OP release towards the end of 30 days observed in all release profiles suggests that the amount of any OP remaining would be negligible. The loss of OP during cylinder production is likely due to the large amount of OP added (when compared to GEM) and the insolubility of OP in acetone.

Table 5. The amount of OP and GEM loaded and released from type C OP^{in}/GEM^{out} and GEM^{in}/OP^{out} cylinders in 30 days.

Cylinder	OP added during production (mg)	GEM added during production (mg)	OP released in 30 days ±SD (mg)	GEM released in 30 days ±SD (mg)
Type C OP^{in}/GEM^{out} (n=3)	16-16.5	3-3.5	8.9 ± 1.6	3.9± 2.0
Type C GEM^{in}/OP^{out} (n=3)	16-16.5	3-3.5	10.6 ± 1.3	3.0 ± 0.8

5.2.7 Residual Acetone

The US Food and Drug Administration (FDA) has published recommended guidelines for the amount of residual solvent that can be detected in devices implanted or injected into humans. The FDA classifies acetone as a Class III solvent, which "may be regarded as less toxic and of lower risk to human health". Although not binding, current guidelines recommend that 50 mg per day or less of these solvents are considered acceptable [87].

The change in mass of three films containing only PLGA, SPAN 80, and acetone was measured over 72h, and the loss in mass attributed to the loss of acetone, as shown in Table 6. Less than 8 mg of acetone remained in each film after 72h. In a double cylinder, the mass of acetone remaining would be less than 16 mg, well below what is currently considered acceptable.

Table 6. Mass of weigh boats plus films at 0 and 72h, and residual acetone in each film after 72h at 20°C.

Sample Film	Weigh boat plus film at 0h (g)	Weigh boat plus film at 72h (g)	Residual acetone (mg)
1	1.888	1.6223	7.14
2	1.824	1.5542	7.46
3	1.826	1.5750	3.93

5.3 In Vitro Effects of OP, and OP in Combination with GEM Released from PLGA Cylinders

5.3.1 PANC1 and PANC1 GEMR Cell Lines

Human pancreatic cancer cell line PANC1 is widely used in pancreatic cancer research. Dr. Myron Szewczuk developed GEM-resistant PANC1 cells (PANC1 GEMR), by gradually increasing the concentration of GEM present in PANC1 tissue culture medium, to a final concentration of 0.01μM GEM. GEM resistance is a major obstacle during the treatment of pancreatic cancer, making PANC1 GEMR cells an invaluable tool for the study of pancreatic cancer treatment.

PANC1 and PANC1 GEMR cells are shown in Figure 28. PANC1 cells have a polygonal shape and typically grow in clusters. PANC1 GEMR cells have a similar appearance but tend to have more spindles protruding from the cells. Increased spindle-like morphology has been linked to chemoresistance as well as a more metastatic phenotype.

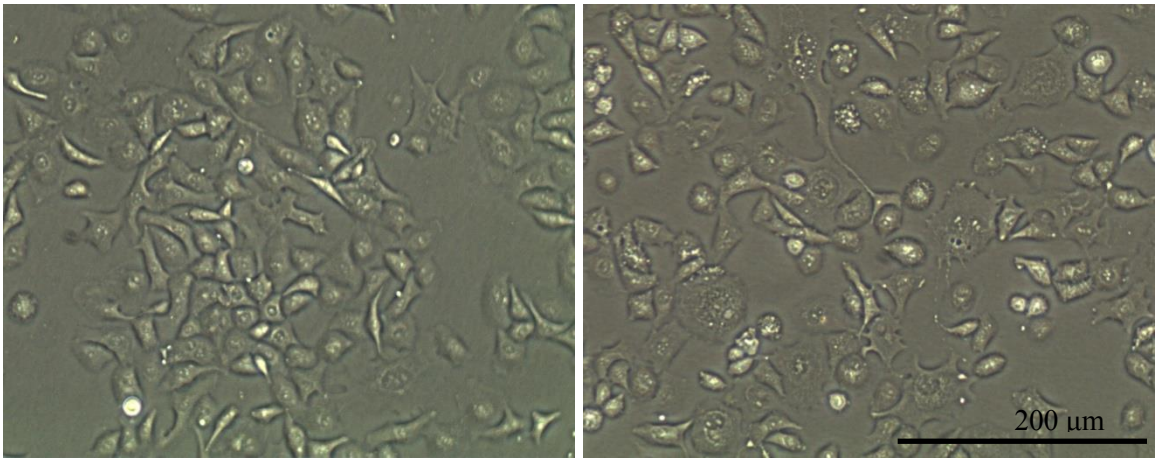

Figure 28. PANC1 (left) and PANC1 GEMR (right) cells in cell culture.

5.3.1.1 Expression of N- and E-cadherin in PANC1 and PANC1 GEMR

Increased expression of N-cadherin and decreased expression of E-cadherin have been linked to epithelial-mesenchymal transition, chemoresistance, and a more metastatic phenotype [41,43]. Therefore, one would expect PANC1 GEMR to have increased N-cadherin expression and decreased E-cadherin expression compared to PANC1. Immunofluorescence was used to visualize and quantify the expression of E- and N-cadherin in PANC1 and PANC1 GEMR, as seen in Figure 29. Background refers to cells stained with secondary antibody only. The secondary antibody should only be able to bind to the primary antibody, however it is possible that non-specific binding could occur. The background is a control to account for non-specific binding of the secondary antibody. Expression of E-cadherin and N-cadherin was significantly greater in PANC1 than PANC1 GEMR, with p-values of 0.0007 and 0.01 respectively. The difference in E-cadherin between cell types was greater than the difference in N-cadherin. Quantification of fluorescence indicates PANC1 are more epithelial than PANC1 GEMR, which is consistent with morphological observations that PANC1 GEMR appear more mesenchymal and metastatic.

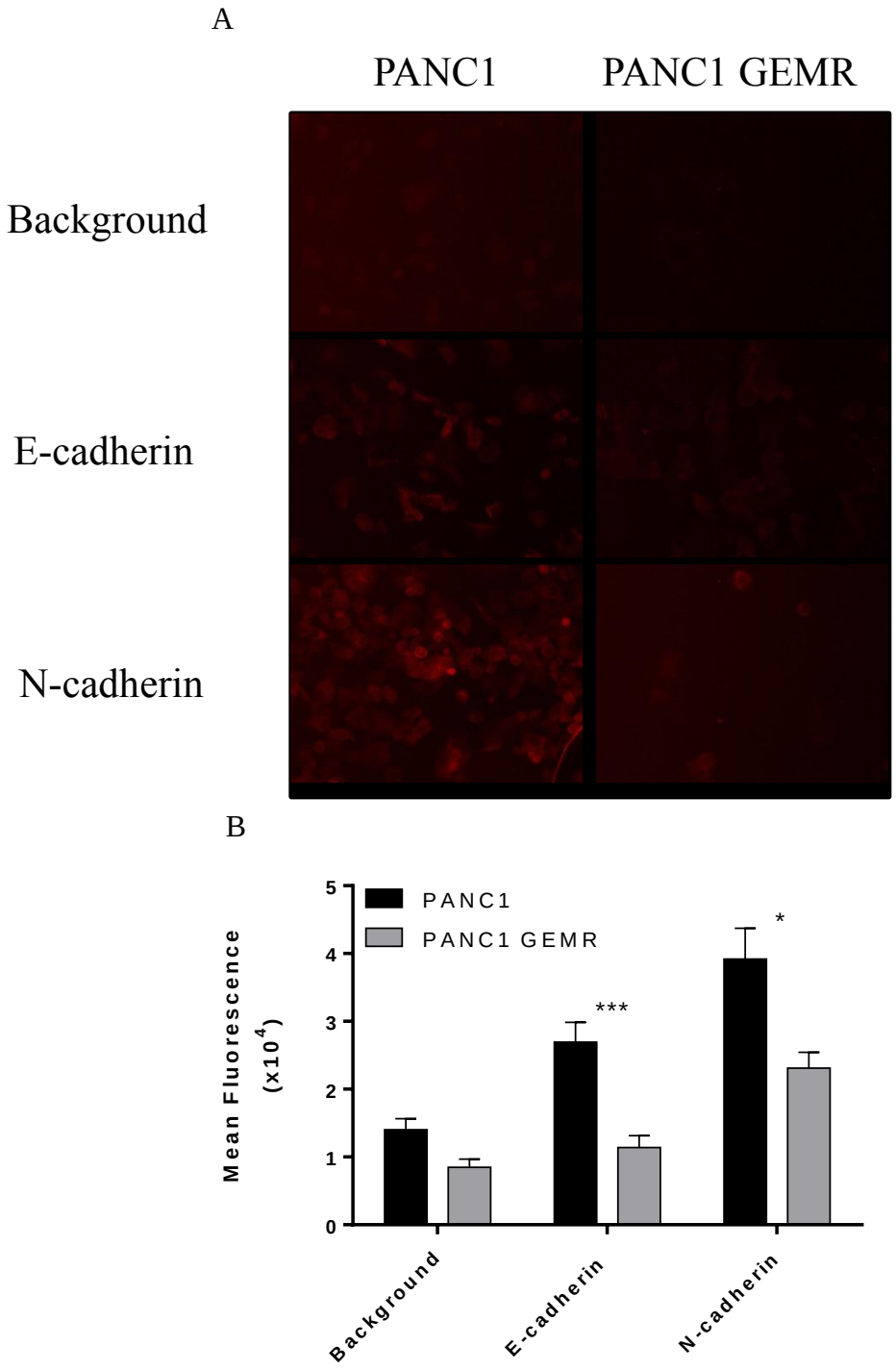

Figure 29. Immunocytochemistry staining of PANC1 and PANC1 GEMR for E- and N-cadherin (A). Mean fluorescence ± standard error of the mean of E-cadherin and N-cadherin expression in individual PANC1 and PANC1 GEMR cells (background n=2, E- and N-cadherin n= 8) (B) (* represent $p < 0.05$, * represents $p < 0.001$).**

5.3.1.2 Cell Growth and Migration of PANC1 and PANC1 GEMR

Scratch wound assays were performed on PANC1 and PANC1 GEMR cells to investigate the migration and growth of both cell types. PANC1 GEMR have characteristics associated with a phenotype that is more metastatic than PANC1, such as resistance to chemotherapy and spindle-like projections. However, experiments had not yet been performed to determine if PANC1 GEMR cells do have an increased ability to metastasize compared to PANC1 cells.

The migratory ability of a cell is indicative of the cell's ability to metastasize. Cancer cells must breach the basement membrane, migrate through neighbouring cells and the stroma to reach the vasculature, then exit the vasculature and begin proliferating at a new site in order to metastasize, making cell migration essential for invasion and metastasis [88]. The decrease in cell-cell adhesion protein E-cadherin and increase in N-cadherin, which facilitates cancer cell binding to the stroma, promote cancer cell migration [89].

Scratch wound assays are used to measure cell migration and normally involve the growth of a confluent cell monolayer, which is then scratched, usually with a pipette tip, to form a cell-free scratch zone. Newer methods involve use of silicone inserts that can be placed in a 24 well plate. These inserts have two square cutouts into which cells are plated, separated by a thin barrier of silicone (eg. 500 μm). After cells have adhered, the insert is removed and the area where the barrier was present forms a cell-free zone. Cell growth was quantified as a percent of the initial scratch width, as shown in Equation 1.

$$Cell\ growth\ (\%\ of\ initial\ cell\ free\ zone) = \frac{Initial\ scratch\ width - Scratch\ width\ at\ time\ t}{Initial\ scratch\ width} \times 100\% \quad (1)$$

Several scratch wound assays were performed on PANC1 and PANC1 GEMR using both scratch methods and cell growth was quantified, as shown in Figure 30. Images from 0, 24, and 48h show the width of the initial scratch as well as cell growth, showing that PANC1 GEMR cells repopulated the wound area faster than PANC1 cells. Quantification shows that PANC1 cell growth was 40 and 73% at 24 and 48h, while PANC1 GEMR cell growth was 53 and 90% at the same time points. Although not statistically significant, PANC1 GEMR cells demonstrated a greater ability to repopulate the cell-free zone and grew more quickly than PANC1 cells, indicating PANC1 GEMR cells do have a more migratory phenotype and are likely more metastatic than PANC1.

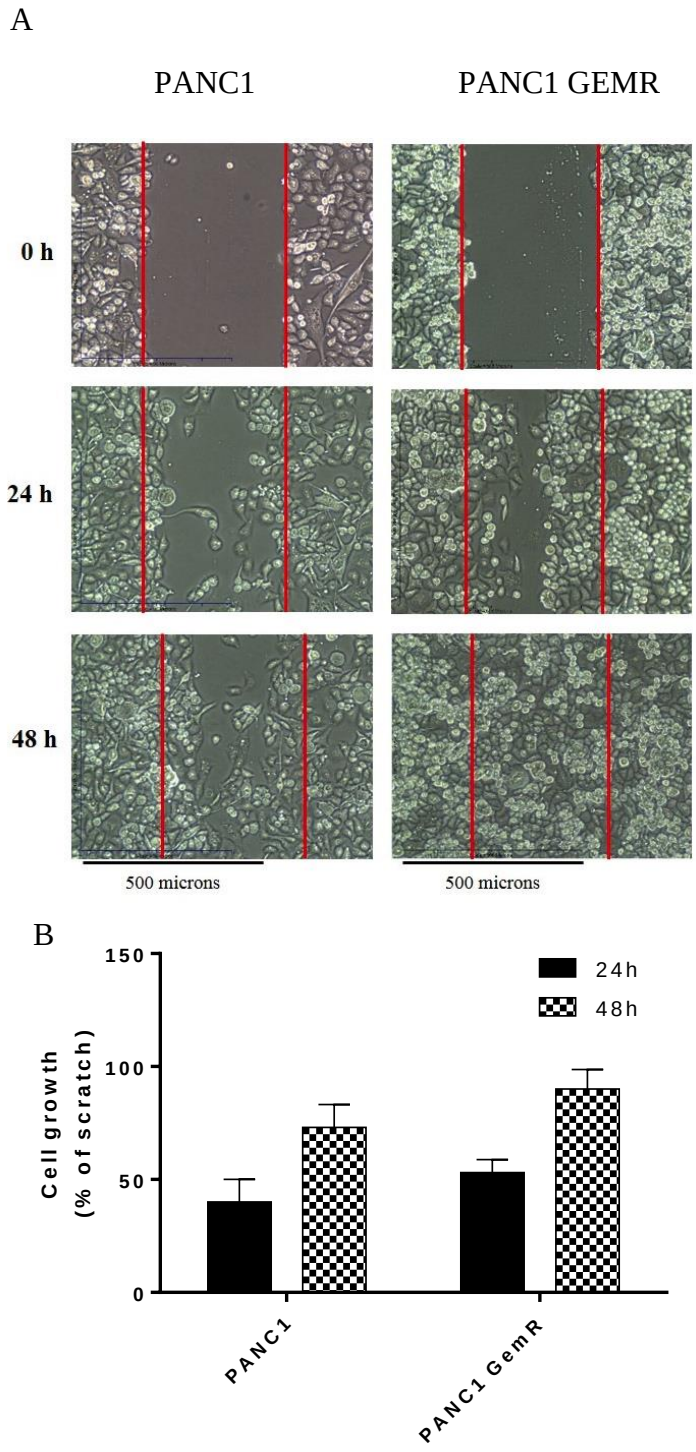

Figure 30. PANC1 and PANC1 GEMR growth over 48 hours. The width of the initial scratch is represented by red vertical lines and cell growth into the cell-free zone is evident (A). Cell growth was quantified as the percent of initial scratch and the mean ± standard error of the mean is shown (PANC1 n=8, PANC1 GEMR n=3) (B).

5.3.2 Effect of OP on PANC1 and PANC1 GEMR Cell Growth and Viability

Previous in vitro and in vivo experiments performed by Dr. Szewczuk's research group have indicated that OP may be a viable drug for the treatment of pancreatic cancer [10,11]. To be an effective form of treatment, is it important that OP be able to inhibit cell migration, growth, and viability.

5.3.2.1 Scratch Wound Assay During Treatment with OP

The scratch wound assay was performed using both methods explained earlier, but PANC1 cells were treated with 0, 400, or 800 μg/mL OP for 48h following the formation of the cell free zone. Images were taken at 0, 24, and 48h and the percentage of cell growth measured, as seen in Figure 31.

Treatment with 400 and 800 μg/mL OP inhibited cell growth and migration. PANC1 treated with 400 μg/mL OP showed cell growth of 36 and 63%, while those treated with 800 μg/mL OP had only 21 and 34% after 24 and 48h. Cell growth of PANC1 treated with 800 μg/mL OP for 48h was significantly lower than that of the control cells at 48h ($p < 0.005$). Cells treated with 0 μg/mL OP served as a control, and had 40 and 73% cell growth at 24 and 48h. Cell growth and migration was inhibited to a greater extent as the concentration of OP increased, and the difference in cell growth between the control and treated cells was larger after 48h than 24h.

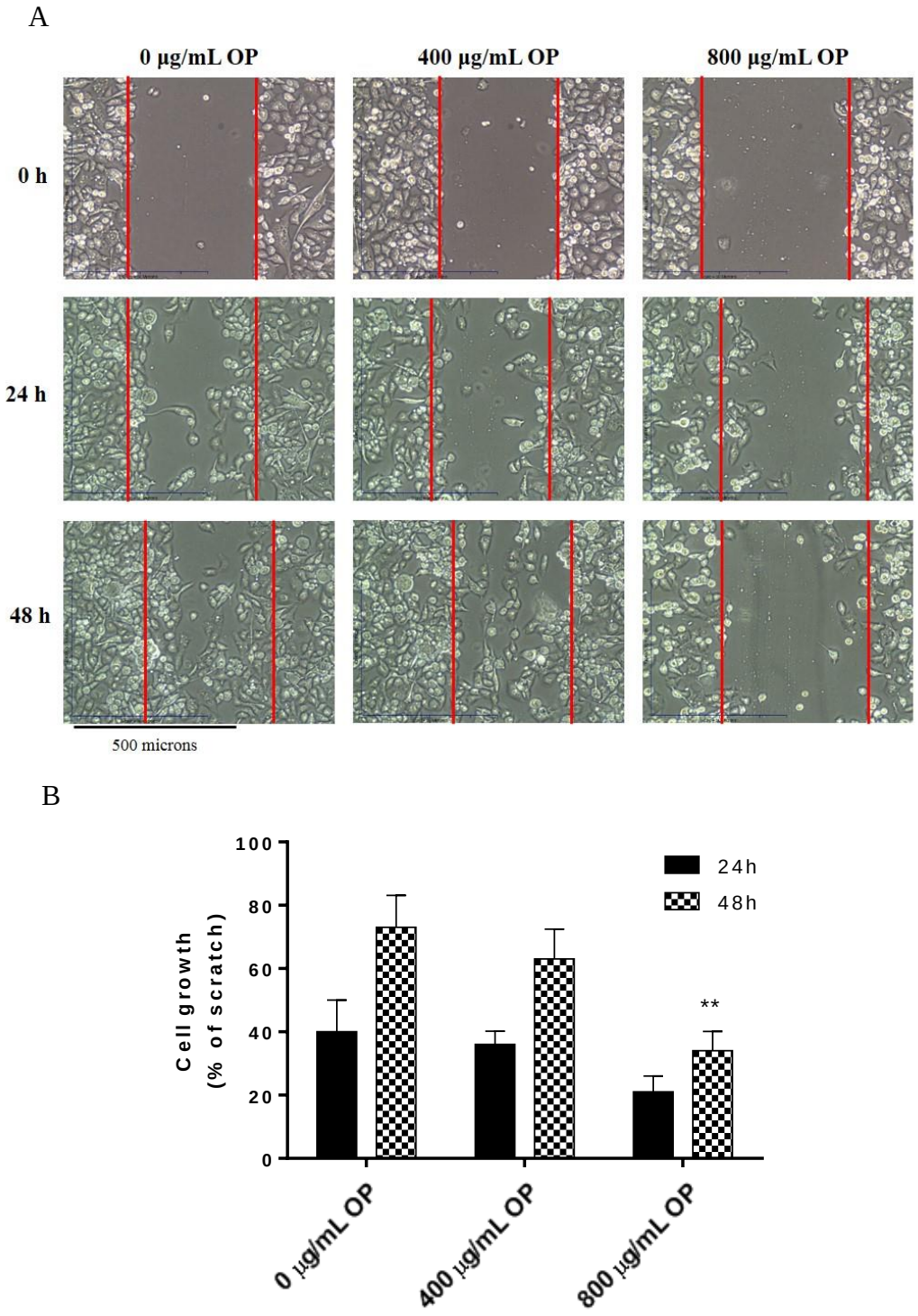

Figure 31. PANC1 cell growth over 48h during treatment with 0, 400, or 800 µg/mL OP (A). PANC1 cell growth as a percentage of the initial scratch width, represented as the mean ± standard error of the mean (n=8 for 0 µg/mL, n=7 for 400 and 800 µg/mL OP treatment concentrations) (B) (indicates $p < 0.005$).**

The scratch wound assay and subsequent treatment with OP was also performed using the PANC1 GEMR cells, as shown in Figure 32. The same trends were observed with the PANC1 GEMR cells, where increasing concentration of OP and longer treatment periods lead to a greater reduction of cell growth into the cell-free zone. PANC1 GEMR treated with 400 μg/mL OP showed 47 and 76% cell growth at 24 and 48h, while those treated with 800 μg/mL OP underwent 29 and 59% cell growth at the same time points. Consistent with previous comparison of the two cell lines, PANC1 GEMR cells showed a higher rate of cell growth than PANC1 cells treated for the same amount of time and with the same concentration of OP. OP effectively inhibited cell migration for both PANC1 and PANC1 GEMR cells in a dose-dependent manner.

The ability of OP to inhibit PANC1 and PANC1 GEMR cell migration is important due to the aggressive nature of pancreatic cancer and limitations of current treatment. In vitro experiments demonstrate OP inhibits cell growth and migration of PANC1 and PANC1 GEMR. If similar inhibition is possible in vivo, OP could inhibit the spread of cancer, even in patients who have already developed resistance to GEM, and potentially increase patient survival time.

A

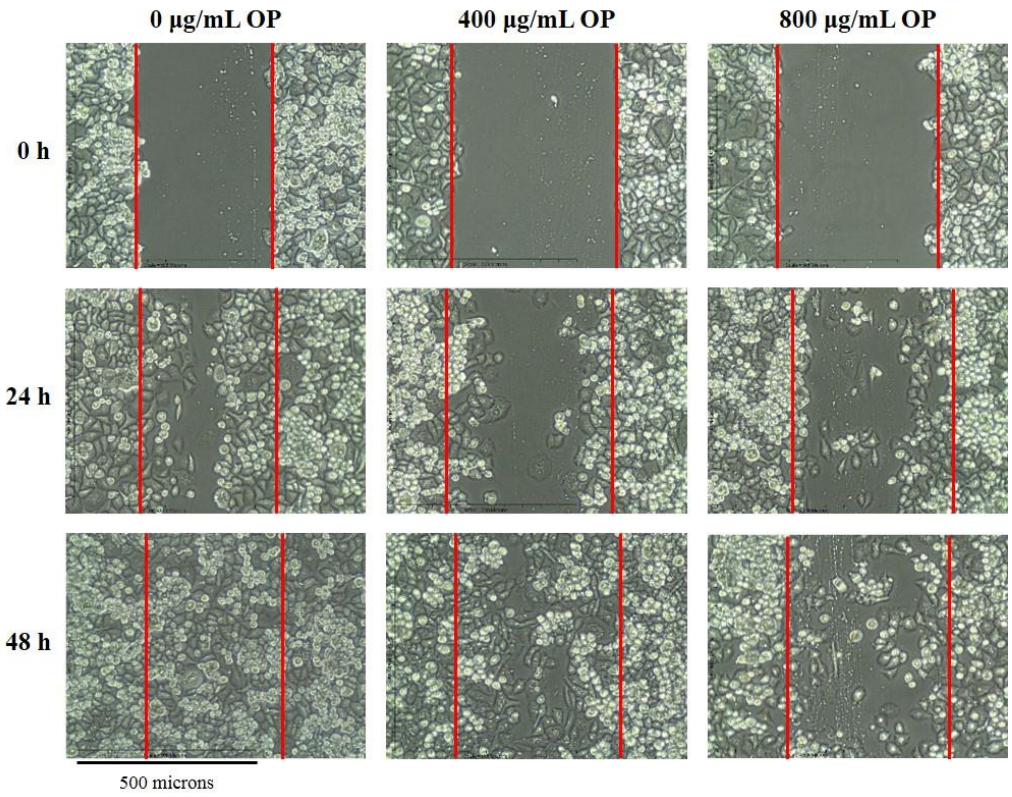

B

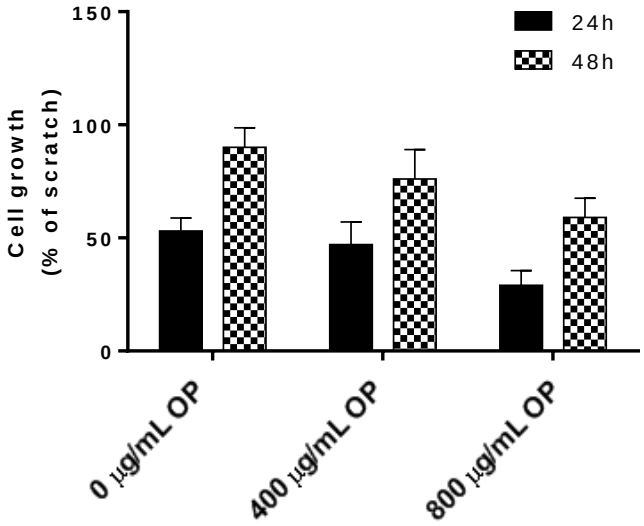

Figure 32. PANC1 GEMR cell growth over 48h during treatment with 0, 400, or 800 µg/mL OP (A). PANC1 cell growth as a percentage of the initial scratch width, represented as the mean ± standard error of the mean (n=3 for 0 µg/mL, n=4 for 400 and 800 µg/mL OP) (B).

5.3.2.2 Cell Viability Following Treatment with OP

WST-1 assays were performed to measure the effect of OP on PANC1 and PANC1 GEMR cell viability. WST-1 is a tetrazolium salt susceptible to cleavage by mitochondrial enzymes to produce a formazan dye. Only metabolically active cells can cleave the WST-1 salt, so cell viability is directly linked to the production of formazan, which is measured with absorbance. Cell viability is determined by comparing the absorbance in wells with treated cells to that of untreated control cells, and measured as a percentage of the control.

PANC1 and PANC1 GEMR cells were treated with 500, 600, 700, and 800 µg/mL of OP for 24, 48, and 72h, as seen in Figure 33A and B respectively. Treatment of PANC1 cells with 500 and 600 µg/mL OP did not differ significantly from the control at any time point. However, treatment with 700 µg/mL for 72h did lead to a significant reduction in cell viability ($p < 0.05$), as did treatment with 800 µg/mL OP for 48 and 72h ($p < 0.005$, $p < 0.0001$ respectively). Treatment with 800 µg/mL OP reduced PANC1 cell viability to 41 and 24% of the control after 48 and 72h. The significant reduction of PANC1 cell viability following treatment with OP indicates that OP is a viable therapeutic for the treatment of pancreatic cancer.

No significant difference was observed in PANC1 GEMR cell viability following treatment with 500, 600, or 700 µg/mL OP. Treatment with 800 µg/mL OP did lead to a significant reduction in cell viability after 48 and 72h ($p < 0.005$, $p < 0.0005$), when cell viability was reduced to 48 and 44% of the control. The ability of OP to reduce PANC1 GEMR cell viability is important given the incidence of GEM-resistance in pancreatic cancer patients. Patients who have developed resistance to GEM should still respond to

treatment with OP, and OP monotherapy or in combination with GEM are both treatment plans worthy of investigation.

Treatment with 800 µg/mL OP is equivalent to 53.3 mg/L in a human, assuming a weight of 75 kg and 5 L of blood. Preclinical toxicity studies with OP have shown minimal adverse effects to intravenous OP at concentrations of 100 and 132 mg/kg/day for 14 days in rats [90]. Using a localized delivery system would ensure that drug concentration would be highest at the implant site and that plasma concentrations could be much lower than 53.3 mg/L. Although the amount of OP released from a cylinder that would be present at the tumor site is unknown, previous success with an implantable PLGA cylinder containing 20 mg OP used in PANC1 tumor-bearing mice suggest a high enough dose can be reached at the zone of the cylinder implant, when using OP-loaded PLGA cylinders [21].

A

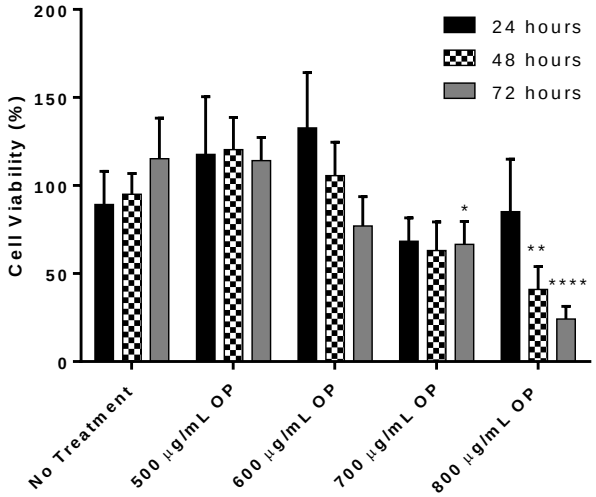

B

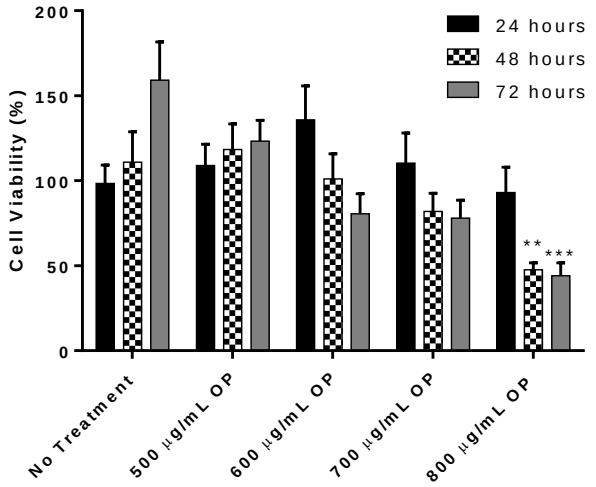

Figure 33. WST-1 cell viability assay performed on A) PANC1 and B) PANC1 GEMR cells with varying concentrations of OP. Cell viability is expressed as a mean percentage of the control, ± standard error of the mean (n=9) (* indicates $p < 0.05$, ** indicates $p < 0.005$, * indicates $p < 0.0005$, **** indicates $p < 0.0001$).**

5.3.2.3 Cell Viability Following Treatment with OP Stored at 37°C

Experiments were conducted as described in section 5.1.2.2 to determine the stability of OP in solution at 37°C over 30 days representing the time frame of release from PLGA cylinders. The activity of OP in solution at 37°C up to 30 days on cell viability was determined using a WST-1 assay on a PANC1 cell line.

WST-1 assays were conducted on samples of OP collected in supernatants and diluted to 1 mg/mL in media. The cell viability of PANC1 treated with OP dissolved in water containing 0.1% TFA is shown in Figure 34. OP in supernatants from days 0, 9, 16, 23, and 30 reduced cell viability to approximately 50% of control or lower after 72h, which is comparable to cells treated with recently dissolved OP, shown in Figure 33A. No loss of OP or change in OP chemical structure was observed following incubation at 37°C in water containing 0.1% TFA for 30 days, as shown in Figure 11. Therefore, it is not unexpected that recently dissolved OP and dissolved OP stored at 37°C in water containing 0.1% TFA demonstrated similar effects on PANC1 cell viability.

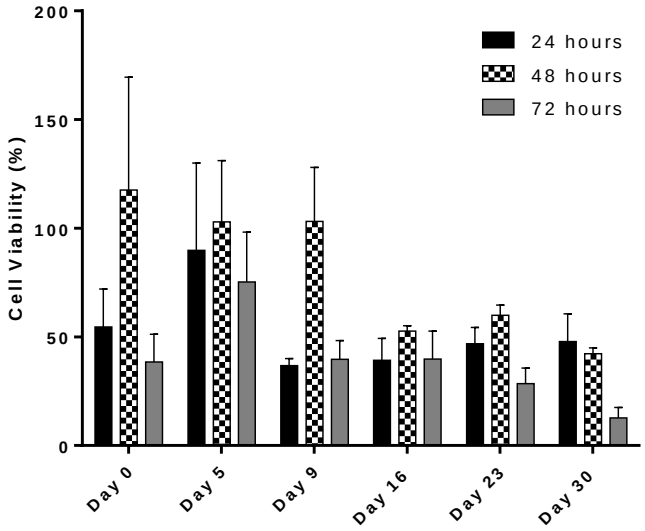

Figure 34. WST-1 cell viability of PANC1 cells treated with 1 mg/mL OP that had been stored in water containing 0.1% TFA for up to 30 days at 37°C. Cell viability is expressed as a mean percentage of untreated control cells, ± standard error of the mean (n=3).

Cell viability as measured by WST-1 assay of PANC1 treated with OP dissolved in sodium phosphate buffer over various periods of time is shown in Figure 35. OP from day 0 reduced cell viability by more than 50% after 72h when compared to untreated control cells. However, the samples taken after day 0 were not effective at reducing cell viability. Although cell viability decreased between 24 and 72 hours, cell viability of PANC1 cells treated with OP in sodium phosphate buffer from days 5, 9, 16, 23, and 30 was comparable to the control. During stability studies of OP incubated at 37°C in sodium phosphate buffer, a decrease in the concentration of OP present was observed with the concurrent increase of another compound, thought to be OC. OC had been previously tested in vitro using a sialidase assay, which measures the activity of Neu1, and OC was found to have little to no inhibitory effect on Neu1 [54]. OC does not inhibit

Neu1 and therefore would not be expected to inhibit cell viability. WST-1 cell viability assays demonstrate that OP incubated at 37°C in sodium phosphate buffer is not stable and loses activity within 5 days.

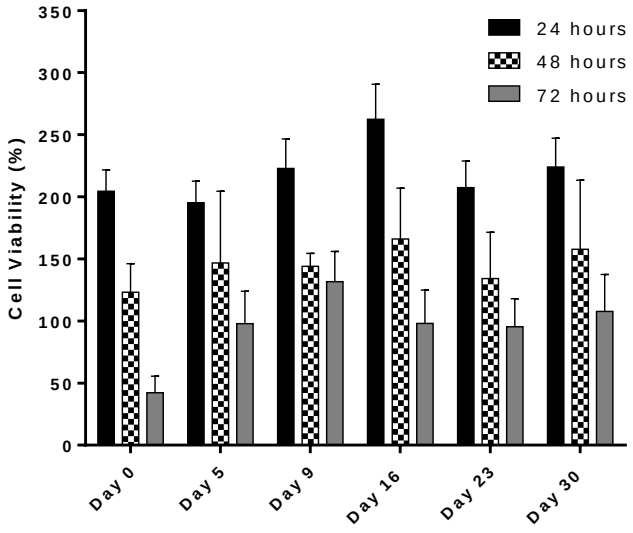

Figure 35. Cell viability of PANC1 cells treated with 1 mg/mL OP that had been stored in 0.1M sodium phosphate buffer pH 7.4 for up to 30 days at 37°C. Cell viability is expressed as a mean percentage of untreated control cells, ± standard error of the mean (n=3).

5.3.3 Cylinders in Cell Culture

Type C double layered cylinders were selected for in vitro cell-based assays because they demonstrated the most linear release. Type C double layered cylinders were produced from films that had been stored at 20°C for 72h prior to rolling and contained 16 mg GEM and 3 mg OP. Cylinders were made with OP in the outer layer and GEM in the inner layer (GEM^{in}/OP^{out}), or with GEM in the outer layer and OP in the inner layer (OP^{in}/GEM^{out}).

5.3.3.1 Cell Viability of PANC1 and PANC1 GEMR Treated with Type C Double Layered Cylinders

The effect of OP and GEM released from type C GEM^{in}/OP^{out} and OP^{in}/GEM^{out} cylinders on cell viability was measured by placing cylinders in tissue culture flasks containing PANC1 or PANC1 GEMR cells. The cylinders flattened and adhered to the tissue culture flask within 24h, losing their cylindrical shape and forming a thin disk. The negative control flask did not contain a cylinder, while the control cylinder flask contained a double layered cylinder with no drug loaded. The media was changed every three days and experiments were 3, 6, 10, or 15 days in duration. On the final day, cells were removed from the flask and counted with a hemocytometer. The dye trypan blue is impermeable to live cells but penetrates the membrane of dead cells. The dye was added immediately before counting cells as a viability assay, defined as the cell count, as a percentage of the negative control.

The images of PANC1 cells on Day 0 and the last day of each experiment are shown in Figure 36. Cells treated with drug released from OP^{in}/GEM^{out} and GEM^{in}/OP^{out} cylinders began to display an altered morphology from day 6 onwards. Cells became elongated and had an increase in spindle-like projections. Cells treated with a control cylinder appeared the same as the negative control cells at all time points, indicating that PLGA does not affect PANC1 morphology.

Cells treated with GEM^{in}/OP^{out} cylinder had the lowest viable cell count for experiments lasting 3 and 6 days at 15.2 and 3.9% of the negative control, compared to 49.0 and 21.5% of the negative control for cells treated with OP^{in}/GEM^{out} cylinders. However, PANC1 treated with OP^{in}/GEM^{out} cylinders had lower viable cell counts after 10 and 15 days. On days 10 and 15, only 10.8 and 1.2% of OP^{in}/GEM^{out} treated cells

remained when compared to the negative control, while 11.7 and 12.2% of cells treated with GEM^{in}/OP^{out} cylinders were viable.

The viable cell count of PANC1 treated with the control cylinder increased at each time point, up to 95% of the negative control on day 15. A cell count of 100% of the negative control would be unexpected due to the physical space the cylinders occupied in the flask, which reduced the surface area available for cell adherence. High cell viability and no visible changes in cell morphology were observed in PANC1 treated with the control cylinder when compared to the negative control. One can conclude that PLGA does not have an effect on PANC1 cells and that any changes in morphology or cell viability following treatment with cylinders containing OP and GEM are due to released OP and GEM.

The results of PANC1 GEMR cells treated with control, OP^{in}/GEM^{out}, or GEM^{in}/OP^{out} cylinders are shown in Figure 37. Images of PANC1 GEMR negative control show that little cell growth occurred after 3 days. At 3 days, cells have covered almost 100% of the flask surface, yet the images from 6, 10, and 15 day experiments show far fewer cells. Very few cells survived treatment with either type of cylinder containing OP and GEM for longer than 3 days, so observations on the morphology of the cells cannot be made. PANC1 GEMR treated with control cylinders have a similar morphology to negative control cells, indicating again that the PLGA cylinders do not affect cells.

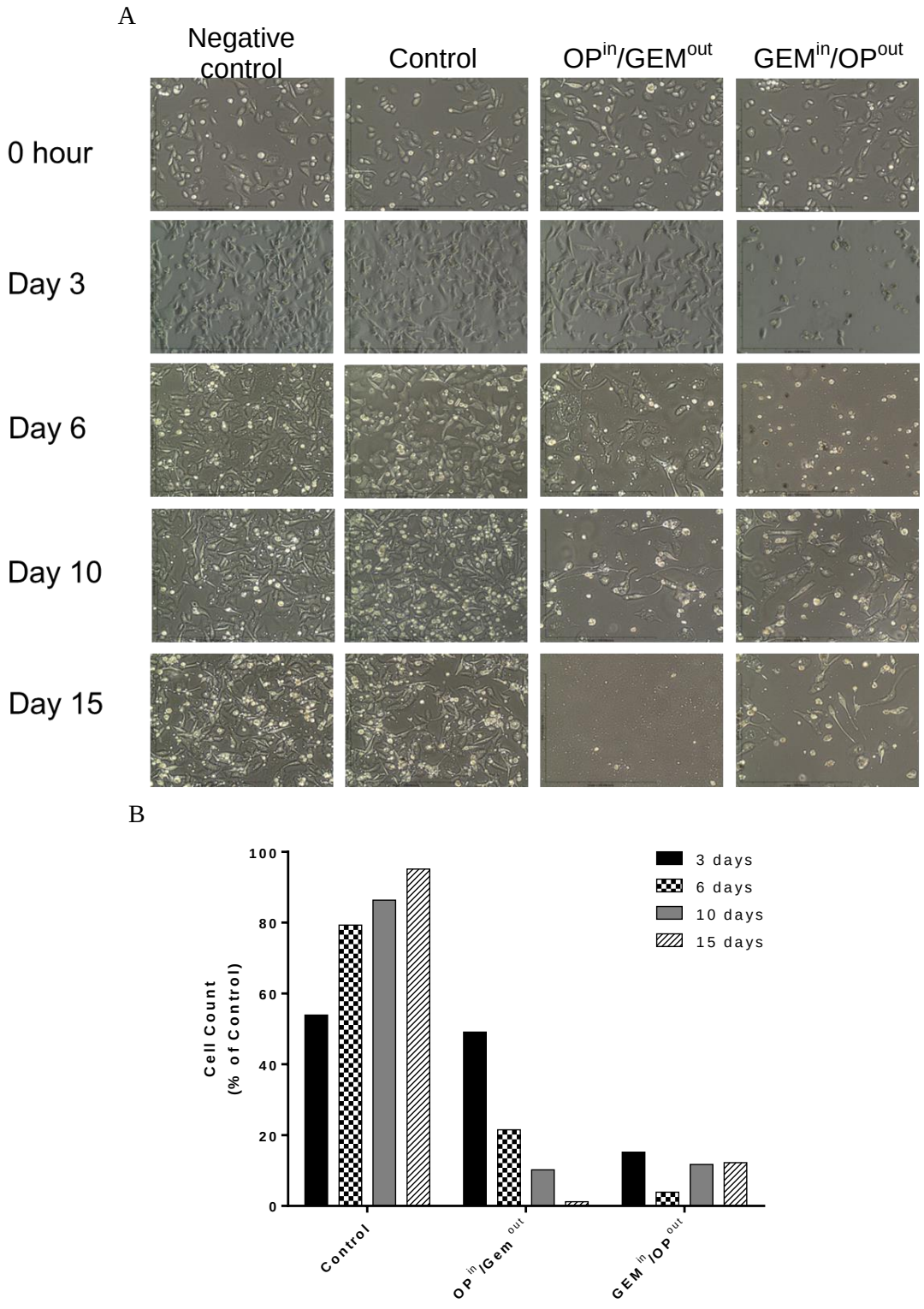

Figure 36. PANC1 cells were treated with control, OP^{in}/GEM^{out}, or GEM^{in}/OP^{out} cylinders, or were untreated (negative control). Images of the cells on days 0, 3, 6, 10, and 15 (A). The cells in each flask were counted when the experiment was terminated, and cell count is expressed as a percentage of the negative control (B). Experiment was performed once.

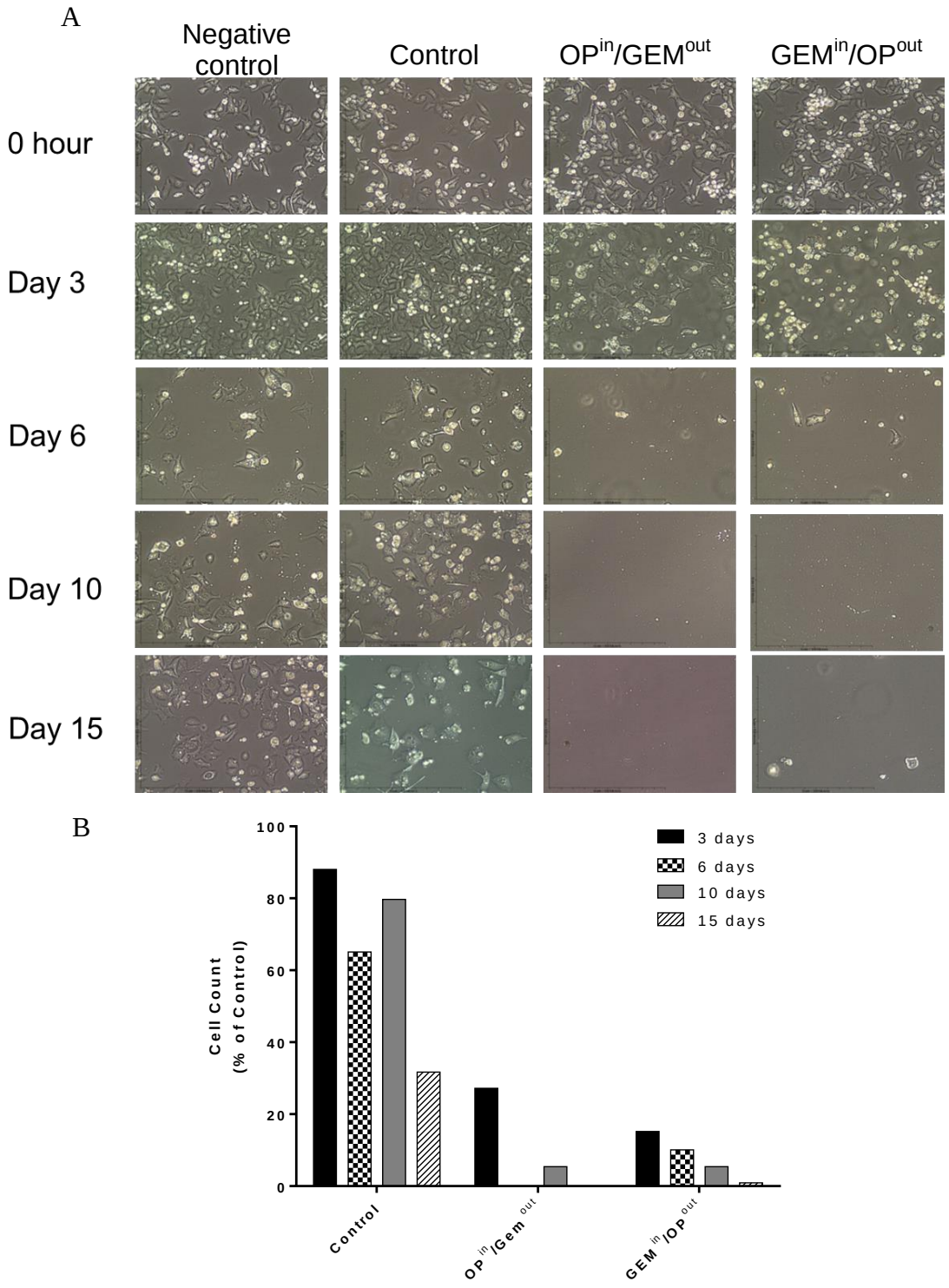

Figure 37. PANC1 GEMR cells were treated with control, OP^{in}/GEM^{out}, or GEM^{in}/OP^{out} cylinders, or were untreated (negative control). Images of the cells on days 0, 3, 6, 10, and 15 (A). The cells in each flask were counted when the experiment was terminated, and cell count is expressed as a percentage of the negative control (B). Absence of a bar indicates no viable cells were present. Experiment was performed once.

OP and GEM released from OP^{in}/GEM^{out} and GEM^{in}/OP^{out} cylinders greatly reduced the number of PANC1 GEMR viable cells at all time points. As seen with PANC1 in Figure 36, cell viability was lower in cells treated with the GEM^{in}/OP^{out} cylinder than the OP^{in}/GEM^{out} cylinder after 3 days. However, treatment with OP^{in}/GEM^{out} cylinders resulted in equal or lower cell counts compared to GEM^{in}/OP^{out} cylinders at all other time points. No viable cells were found in flasks containing OP^{in}/GEM^{out} cylinders for 6 and 15 days, and the cell count was only 5.4% of the negative control in the flask containing an OP^{in}/GEM^{out} cylinder for 10 days.

Viable cell counts indicate that PANC1 GEMR treated with control cylinders were within 65 and 88% of the negative control for experiments lasting 3, 6, and 10 days. However, only 32% of PANC1 GEMR cells treated with a control cylinder were viable at the end of the 15 day experiment, when compared to the negative control. It is unclear why the number of viable cells was reduced to such a high degree, when PANC1 and PANC1 GEMR cells had greater than 65% cell viability when compared to the negative control in every other experiment. One possible explanation for the low cell count is the duration of the experiment. During cell culture, cells would not be cultured for 15 days without having some cells removed to prevent overcrowding. It is possible that the cells covered the entire area of the flask available for cell adhesion, which can lead to cells being covered by other cells and cell death.

Release of OP and GEM from the OP^{in}/GEM^{out} cylinder appeared to be most effective at reducing cell viability in both cell types. The experiment was repeated with the OP^{in}/GEM^{out} cylinder for 3, 6, 10, and 15 days on both PANC1 and PANC1 GEMR

cells, as seen in Figure 38. As before, the OP^{in}/GEM^{out} cylinder dramatically reduced the number of viable cells for both cell types and at every time point.

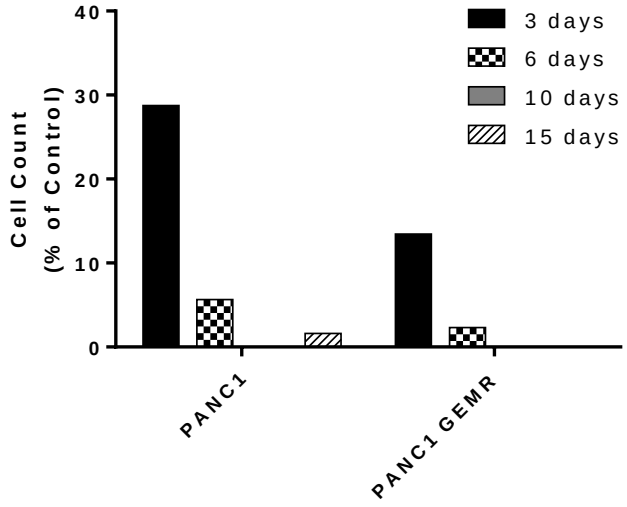

Figure 38. PANC1 and PANC1 GEMR cells were untreated (negative control) or treated with OP^{in}/GEM^{out} cylinders for 3, 6, 10, or 15 days. The cells in each flask were counted when the experiment was terminated, and cell count is expressed as a percentage of the negative control. Absence of a bar indicates no viable cells were present. Experiment was performed once.

5.3.3.2 Morphology and Expression of E- and N-cadherin in PANC1 and PANC1 GEMR Treated with OP and GEM Delivered from PLGA Cylinders

PANC1 and PANC1 GEMR cells were stained with phalloidin after counting, which binds to F-actin and is commonly used for visualizing cell morphology. Cells were also immunostained for E- and N-cadherin to determine if treatment with OP and GEM released from OP^{in}/GEM^{out} or GEM^{in}/OP^{out} cylinders had caused a change in E-cadherin or N-cadherin expression. The fluorescence of individual cells was quantified using Corel Photo Paint 8.0.

Phalloidin staining of PANC1 negative control cells and cells treated with control, OP^{in}/GEM^{out}, and GEM^{in}/OP^{out} cylinders for 3, 6, 10, and 15 days are shown in Figures

39A-42A, and phalloidin staining of PANC1 GEMR treated for 3, 6, and 15 days are shown in Figures 43A, 44 and 45. No differences are visible between cells exposed to different treatments at any time point for either cell type. Cells also appeared more round and less polygonal than typically seen in cell culture, as shown in Figure 28. The atypical appearance of the cells and the lack of difference in morphology between cells exposed to different treatments are likely due to the experimental procedure. Cells were plated on glass coverslips in 24 multiwell plates immediately after cell counting, and phalloidin staining was performed the following day. It seems likely that cells were plated long enough to adhere to cover slips, but not long enough to return to their usual shape. Although our lab has previously used phalloidin to visualize differences in morphology between PANC1 and PANC1 GEMR cells, cells had been plated 2-3 days prior to phalloidin staining which allowed cells time to return to their usual shape before staining[10].

Fluorescent staining and quantification of fluorescence of PANC1 cells treated for 3 days with OP and GEM delivered from OP^{in}/GEM^{out} or GEM^{in}/OP^{out} cylinders was performed. Control cylinders and untreated cells served as controls, as shown in Figure 39. Cells treated with OP and GEM released from a GEM^{in}/OP^{out} cylinder showed higher expression of E-cadherin and a statistically significant lower expression of N-cadherin ($p < 0.005$) when compared to the negative control. Release experiments showed GEM^{in}/OP^{out} cylinders released OP but no GEM during the first 3 days. The increase in E-cadherin expression and the decrease in N-cadherin expression are consistent with previous findings that OP can contribute to the reversal of EMT and chemoresistance. O'Shea et al [10] treated PANC1 and PANC1 GEMR with 600 μg/mL OP for 24h, and

observed a significant increase in E-cadherin expression ($p < 0.05$, $p < 0.0015$) as well as a significant decrease in N-cadherin expression ($p < 0.001$ for both cell types). Cells treated with OP and GEM delivered from an OP^{in}/GEM^{out} cylinder or a control cylinder showed no significant differences in E- or N-cadherin expression when compared to the control.

Fluorescent staining of PANC1 cells following 6 days of treatment with drugs released from an OP^{in}/GEM^{out} cylinder showed no significant difference in E- and N-cadherin expression when compared to the negative control, as seen in Figure 40. Cells treated with OP and GEM released from a GEM^{in}/OP^{out} cylinder could not be seen following fluorescent staining of E- and N-cadherin, so fluorescence could not be quantified. E-cadherin expression was similar between the negative control and cells treated with a control cylinder, however N-cadherin expression was significantly reduced in PANC1 treated with a control cylinder when compared to the negative control ($p < 0.005$).

Fluorescent staining and quantification of fluorescence of PANC1 cells treated for 10 days is shown in Figure 41. Cells treated with OP and GEM released from a GEM^{in}/OP^{out} cylinder showed a significant increase in E-cadherin expressed at the cell surface when compared to the negative control ($p < 0.05$). PANC1 treated with an OP^{in}/GEM^{out} cylinder showed a significant decrease in E-cadherin ($p < 0.05$) and a significant increase in N-cadherin expression ($p < 0.0001$) when compared to the negative control. A decrease in E-cadherin and increase in N-cadherin is consistent with EMT, and indicates a more metastatic phenotype than untreated PANC1 [8,39]

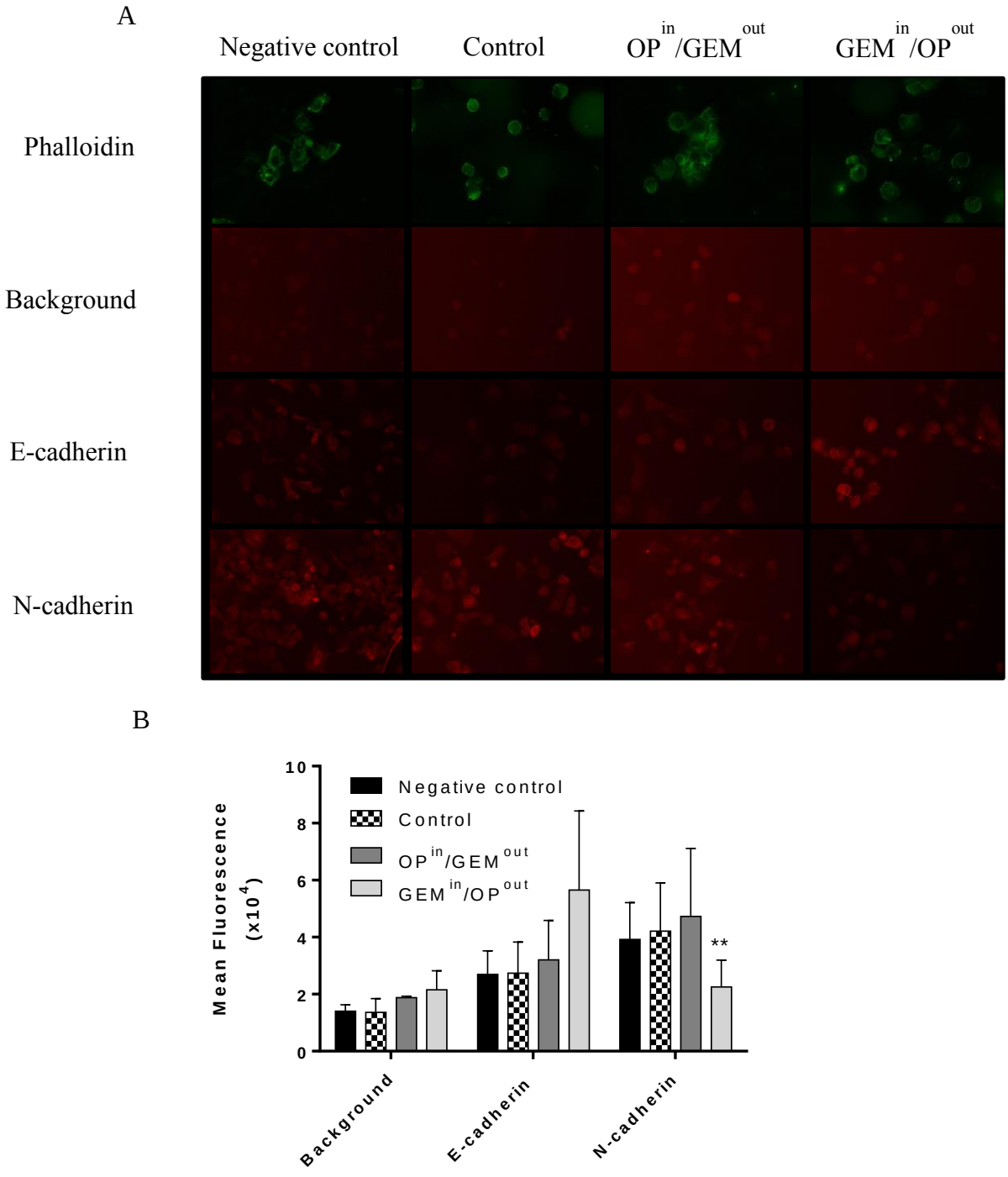

Figure 39. Expression of F-actin and cell surface expression of E- and N-cadherin in PANC1 cells following no treatment (negative control), or treatment with control, OP^{in}/GEM^{out}, or GEM^{in}/OP^{out} cylinders for 3 days (A). Mean fluorescence of E-cadherin and N-cadherin expression in individual PANC1 ± standard deviation (represents $p < 0.005$) (B).**

A

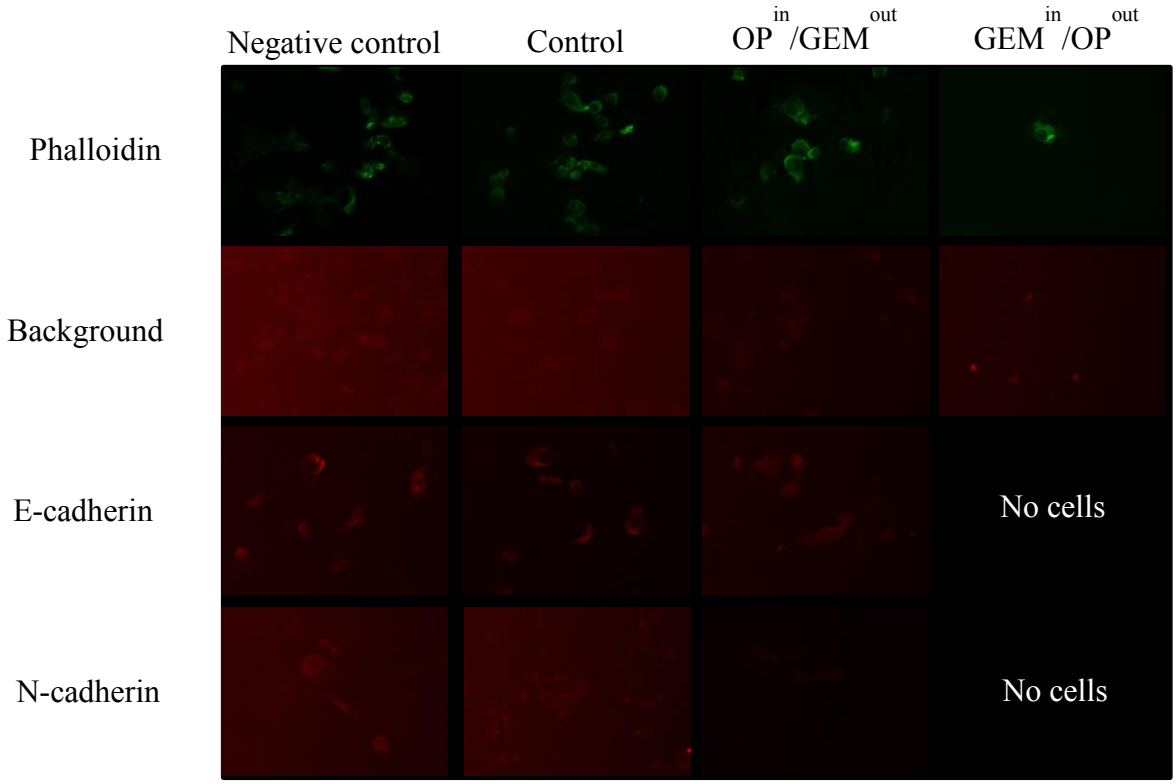

B

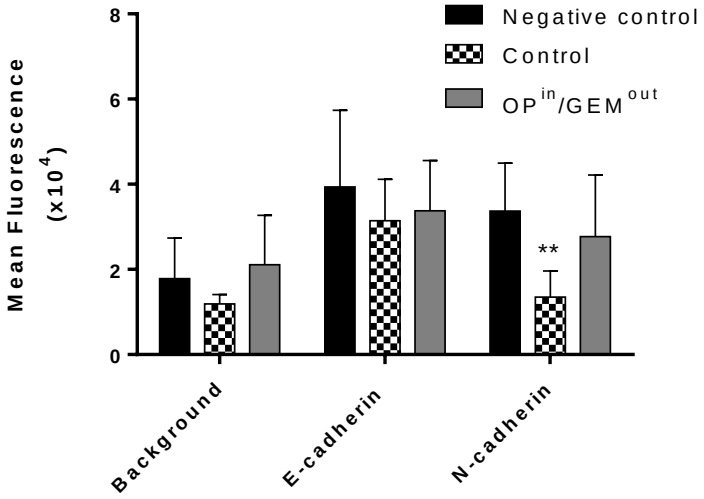

Figure 40. Expression of F-actin and cell surface expression of E- and N-cadherin in PANC1 cells following no treatment (negative control), or treatment with control, OP^{in}/GEM^{out}, or GEM^{in}/OP^{out} cylinders for 6 days (A). Mean fluorescence of E-cadherin and N-cadherin expression in individual PANC1 ± standard deviation (represents $p < 0.005$) (B).**

A

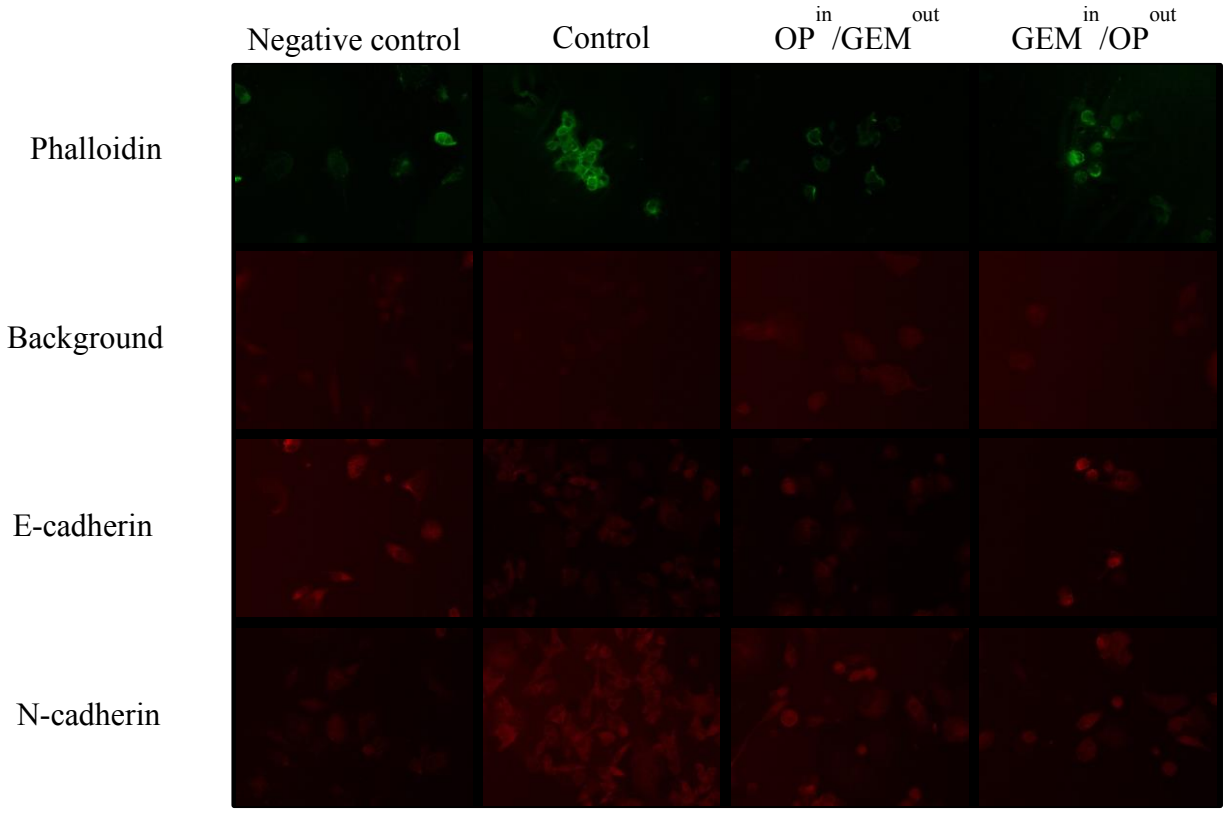

B

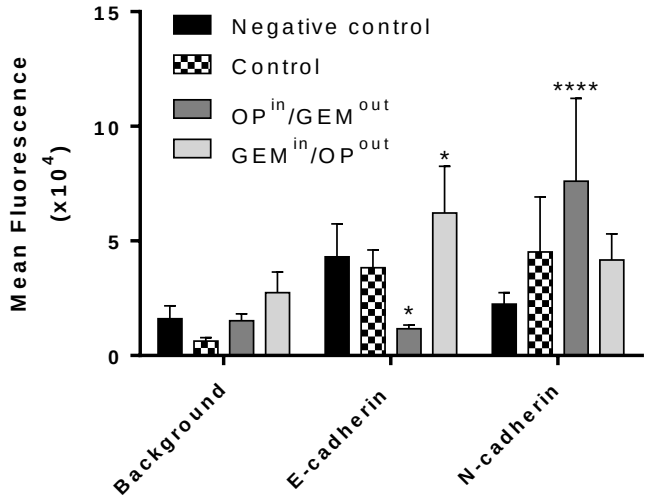

Figure 41. Expression of F-actin and cell surface expression of E- and N-cadherin in PANC1 cells following no treatment (negative control), or treatment with control, OP^{in}/GEM^{out}, or GEM^{in}/OP^{out} cylinders for 10 days (A). Mean fluorescence of E-cadherin and N-cadherin expression in individual PANC1 ± standard deviation (* represents $p < 0.05$, ** represents $p < 0.0001$) (B).**

Through the development of PANC1 GEMR, we have shown that PANC1 can develop resistance to GEM. During release experiments, 39% of GEM was released from type C OP^{in}/GEM^{out} double layered cylinders in the first 24h and a total of 63% of GEM was released after 9 days. Only 10.8% of PANC1 survived treated with OP and GEM released from an OP^{in}/GEM^{out} cylinder for 10 days, and it is possible the few cells that survived treatment were able to develop resistance to GEM, which lead to the increase in N-cadherin and decrease in E-cadherin.

PANC1 negative control cells and cells treated with control, OP^{in}/GEM^{out}, and GEM^{in}/OP^{out} cylinders for 15 days were fluorescently stained for F-actin and E- and N-cadherin and the fluorescence of E- and N-cadherin was quantified, as seen in Figure 42. Only 1.2% of cells survived treatment with an OP^{in}/GEM^{out} cylinder for 15 days when compared to the negative control, and none could be seen following staining for E- and N-cadherin. Cell surface expression of E-cadherin was significantly increased in cells treated with a GEM^{in}/OP^{out} cylinder for 15 days, when compared to the negative control ($p < 0.005$). No significant differences in the expression of N-cadherin were observed between treated cells and the negative control.

Few PANC1 GEMR cells survived treatment with OP and GEM released from OP^{in}/GEM^{out} and GEM^{in}/OP^{out} cylinders for any period time, preventing quantification of fluorescence for all but the 3 day experiment. PANC1 GEMR negative control cells and cells treated with control, OP^{in}/GEM^{out}, and GEM^{in}/OP^{out} cylinders for 3 days were immunostained for E- and N-cadherin and the fluorescence was quantified, as seen in Figure 43. E-cadherin expression was significantly increased in PANC1 GEMR treated with the OP^{in}/GEM^{out} cylinder when compared to the negative control ($p < 0.0005$).

Expression of N-cadherin was significantly reduced in OP^{in}/GEM^{out} and control cylinder treated cells in comparison to the negative control, with p-values less than 0.001 and 0.005, respectively.

Fluorescent staining of untreated PANC GEMR cells and cells treated with control, OP^{in}/GEM^{out}, or GEM^{in}/OP^{out} cylinders for 6 and 15 days are seen in Figures 44 and 45, respectively. Between 0 and 2 cells could be visualized after staining for N- and E-cadherin, which were too few to make any reasonable inferences about the effect of treatment with OP and GEM delivered from OP^{in}/GEM^{out} or GEM^{in}/OP^{out} cylinders on E- and N-cadherin expression. PANC1 GEMR cells treated with drug released from OP^{in}/GEM^{out} or GEM^{in}/OP^{out} cylinders from the 10 day experiment could not be found following cell plating in a 24 well plate, so staining was not performed.

A

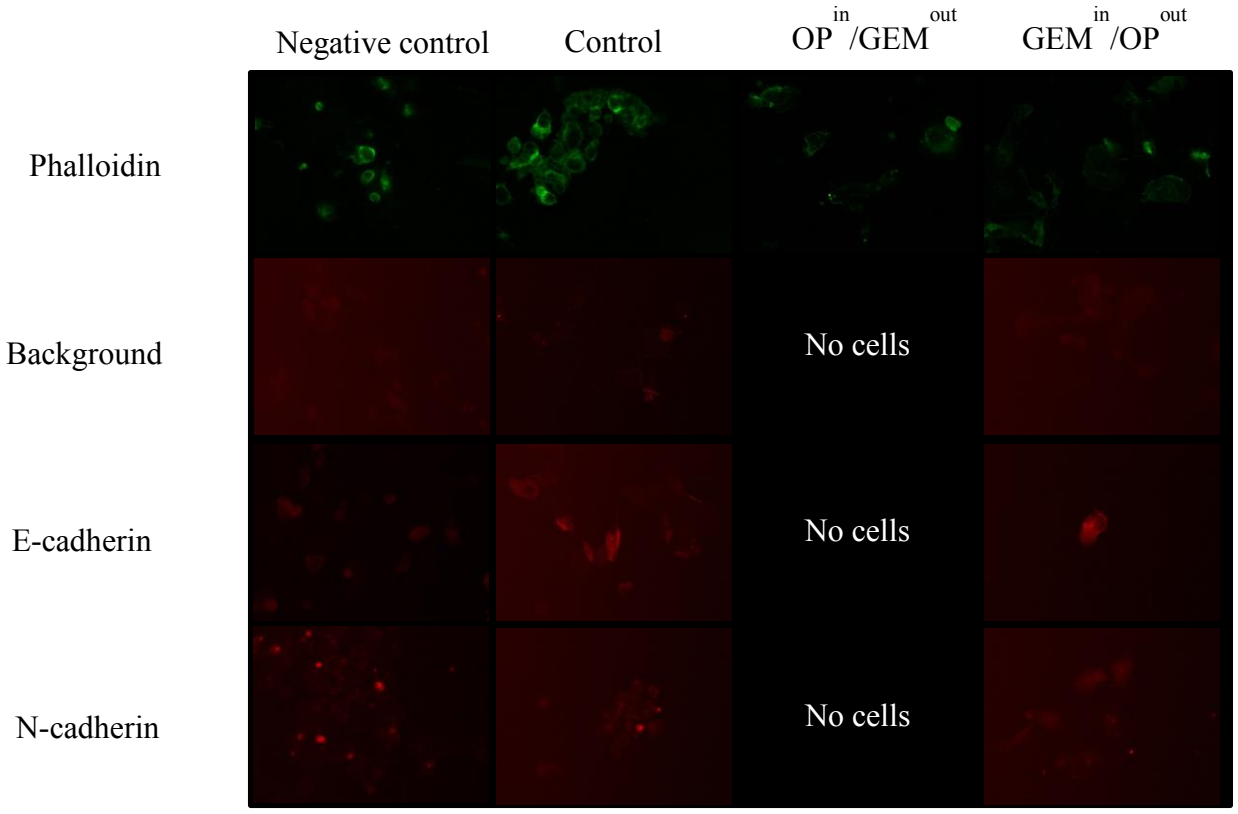

B

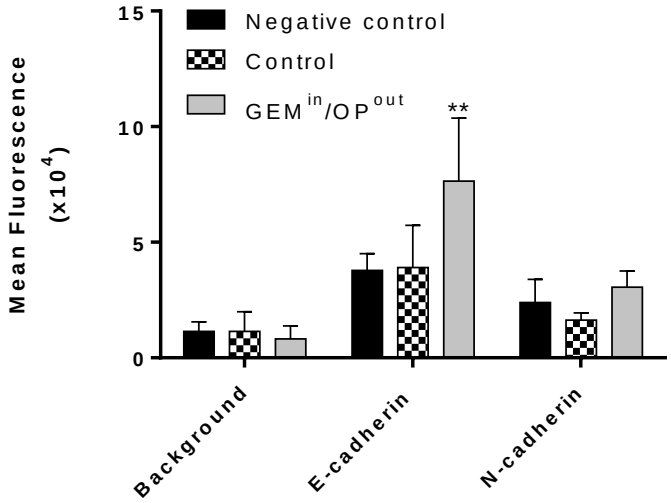

Figure 42. Expression of F-actin and cell surface expression of E- and N-cadherin in PANC1 cells following no treatment (negative control), or treatment with control, OP^{in}/GEM^{out}, or GEM^{in}/OP^{out} cylinders for 15 days (A). Mean fluorescence of E-cadherin and N-cadherin expression in individual PANC1 ± standard deviation (represents $p < 0.005$) (B).**

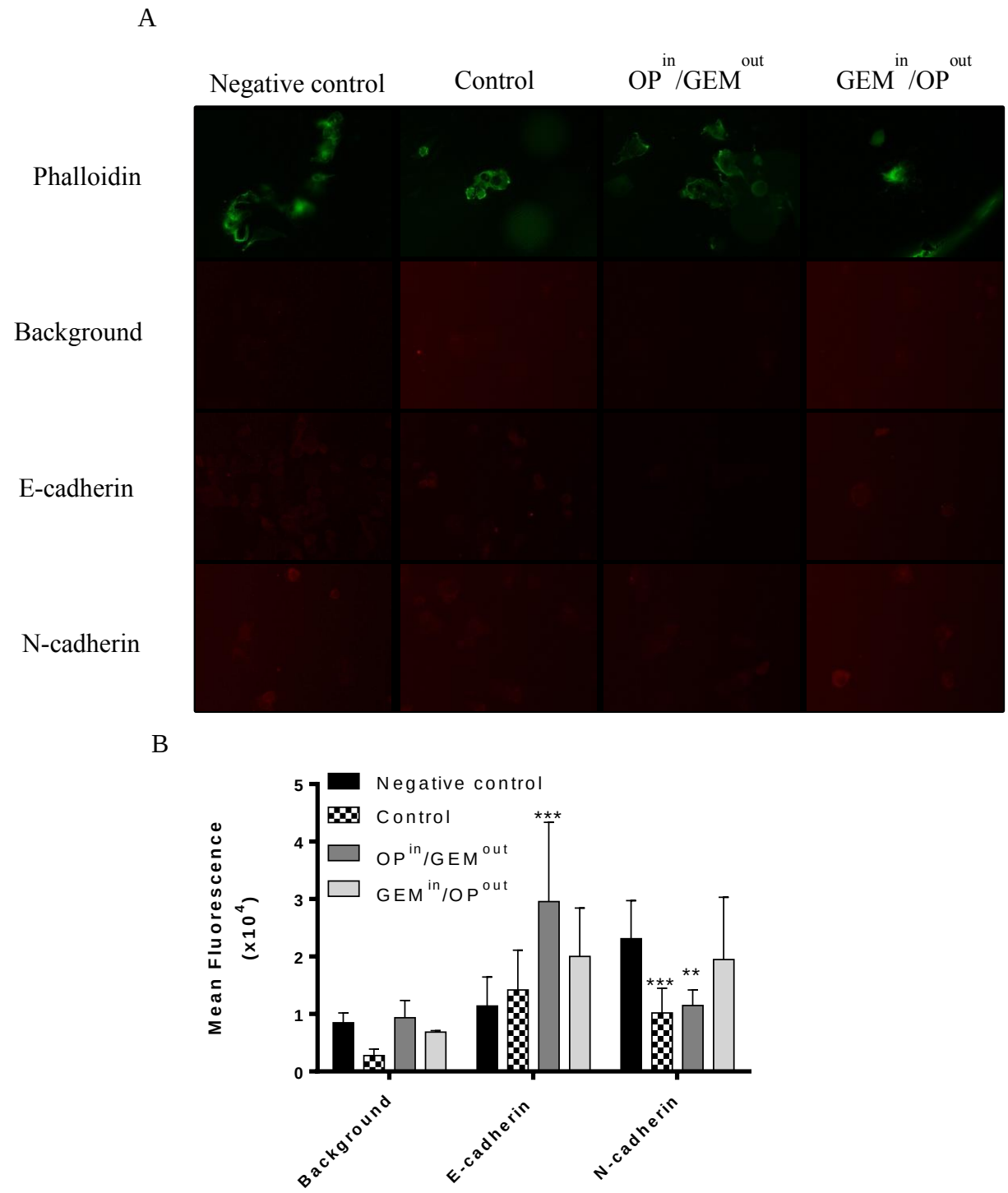

Figure 43. Expression of F-actin and cell surface expression of E- and N-cadherin in PANC1 GEMR cells following no treatment (negative control), or treatment with control, OP^{in}/GEM^{out}, or GEM^{in}/OP^{out} cylinders for 3 days (A). Mean fluorescence of E-cadherin and N-cadherin expression in individual PANC1 ± standard deviation (represents $p < 0.005$, *** represents $p < 0.001$) (B)**

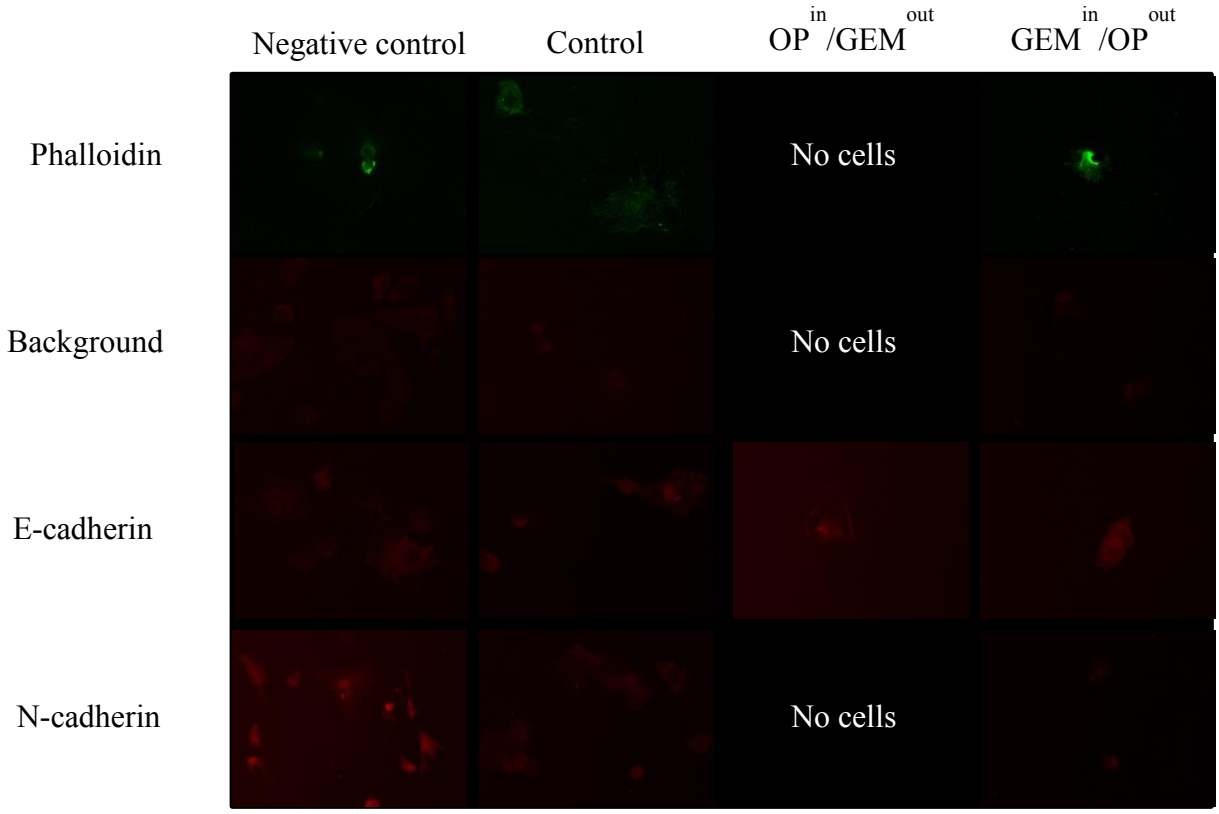

Figure 44. Expression of F-actin and cell surface expression of E- and N-cadherin in PANC1 GEMR cells following no treatment (negative control), or treatment with control, OP^{in}/GEM^{out}, or GEM^{in}/OP^{out} cylinders for 6 days.

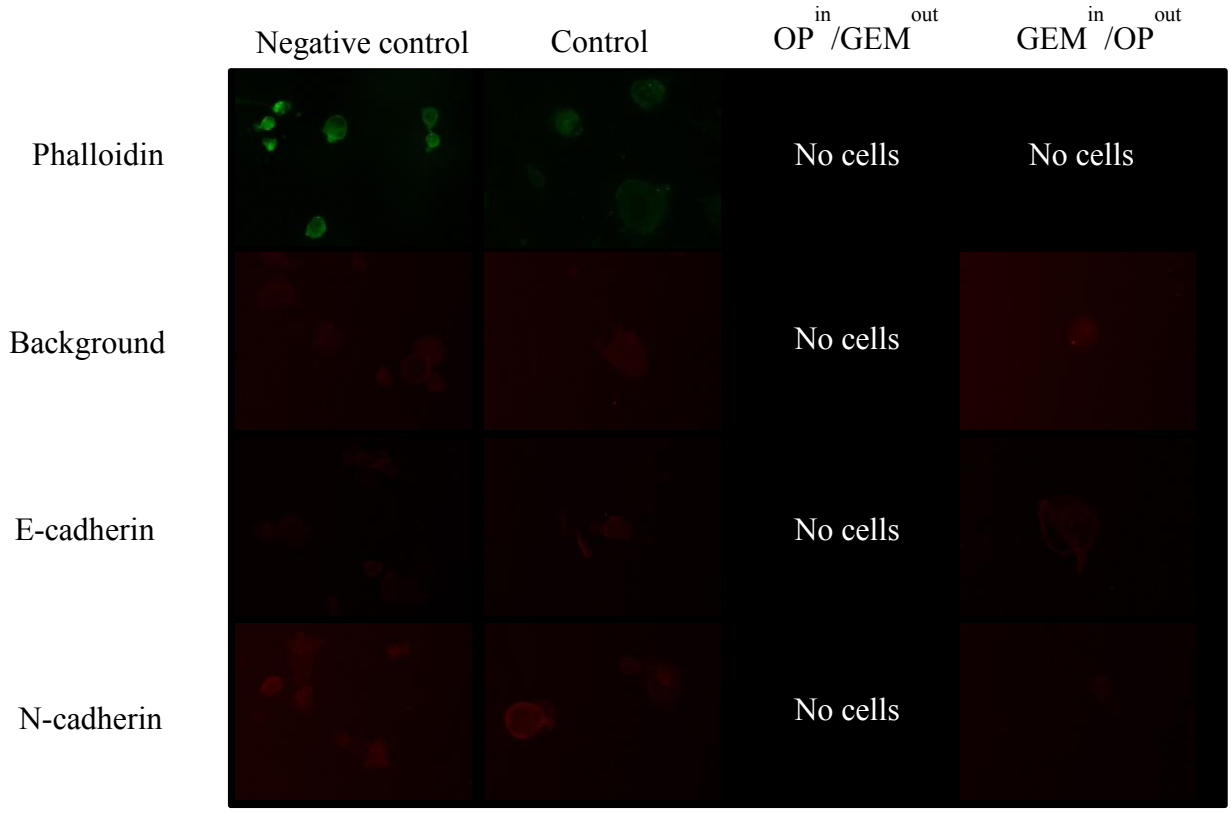

Figure 45. Expression of F-actin and cell surface expression of E- and N-cadherin in PANC1 GEMR cells following no treatment (control), or treatment with empty, OP^{in}/GEM^{out}, or GEM^{in}/OP^{out} cylinders for 15 days.

Cell surface expression of E- and N- cadherin of PANC1 cells following treatment with OP and GEM released from GEM^{in}/OP^{out} cylinders consistently indicated a reversal of EMT. PANC1 treated for 3, 10, and 15 days all showed a significant increase in E-cadherin expression when compared to the negative control, and cells treated for 3 days also displayed a significant decrease in N-cadherin expression, as seen in Figures 39, 41, and 42. No cells from the 6 day experiment were found after fluorescent staining was performed. Of the PANC1 GEMR experiments, only cells treated for 3 days were abundant enough to quantify fluorescence and no significant

difference in N- or E-cadherin expression was observed in comparison to the negative control following treatment with a GEM^{in}/OP^{out} cylinder.

Interestingly, treatment with OP and GEM released from OP^{in}/GEM^{out} cylinders did not lead to a reversal of EMT in PANC1 cells. PANC1 treated for 3 and 6 days showed no significant differences in E- or N-cadherin expression compared to the negative control. In fact, cells immunostained following treatment with an drug released from an OP^{in}/GEM^{out} cylinder for 10 days showed a significant decrease in E-cadherin expression and a significant increase in N-cadherin expression when compared to the negative control, both of which are consistent with EMT. PANC1 GEMR treated with OP and GEM released from an OP^{in}/GEM^{out} cylinder did show a reversal of EMT, with a significant increase in E-cadherin expression and a concomitant decrease in N-cadherin expression.

The difference in response to OP and GEM released from the OP^{in}/GEM^{out} cylinders compared to the GEM^{in}/OP^{out} cylinders are most likely due to the differences in the cylinder release profiles as shown in Figure 25. The GEM^{in}/OP^{out} cylinders have a higher initial release of OP and lower initial release of GEM than the OP^{in}/GEM^{out} cylinders. O'Shea et al [10] demonstrated that treatment of PANC1 and PANC1 GEMR with OP led to an increase in E-cadherin expression and a decrease in N-cadherin expression, consistent with a reversal of EMT. Therefore, it makes sense that the higher initial release of OP from GEM^{in}/OP^{out} cylinders would also lead to a reversal of EMT.

Although the release of OP and GEM from OP^{in}/GEM^{out} cylinders led to a greater reduction in cell viability than GEM^{in}/OP^{out} cylinders, immunofluorescent staining indicates that the drugs did not reverse EMT and that during the 10 day experiment

PANC1 cells actually became more mesenchymal. The development of PANC1 GEMR demonstrates that PANC1 cells can develop resistance to GEM, which have a greater ability to migrate than PANC1 cells, as shown during the scratch wound assays in section 5.3.1.2. One possible explanation is that the high initial release of GEM from OP^{in}/GEM^{out} cylinders, as seen in Figure 25, enabled GEM-resistance in cells that were able to survive. Although release of drug from OP^{in}/GEM^{out} cylinders led to a greater reduction in cell viability, immunofluorescent staining indicates that the release of OP and GEM from GEM^{in}/OP^{out} cylinders is more effective at reversing EMT, and therefore reducing the ability of PANC1 and PANC1 GEMR to metastasize.

5.3.4 Release of OP and GEM from Cylinders in Cell Culture

Cylinders did not retain a cylindrical shape when placed in cell culture, and flattened against the bottom of the cell culture flasks within 24h. The cylinders were in culture medium containing glucose, amino acids, and fetal bovine serum, which are necessary for cell culture, and is quite different from 0.1M sodium phosphate buffer used during release experiments. It is possible that the change in cylinder shape as well as the different solution could lead to a change in the release profile of the cylinders. Following termination of experiment with cylinders in cell culture, several cylinders were dissolved in acetone, centrifuged for 10 min at 3500 rpm, and supernatant was discarded. The drug pellet was resuspended in water prior to being lyophilized. The powdered drug was dissolved in water and OP and GEM were quantified using HPLC. The expected and actual amount of drug remaining in the cylinders is shown in Table 7. Only cylinders

used to treat PANC1 cells were selected, to avoid the addition of any GEM to the samples, due to GEM present in media used for PANC1 GEMR cell culture.

Table 7. Expected and actual amount of drug remaining in cylinders following use in tissue culture. Expected amount of drug was determined using data from release experiments. No samples were taken on days 10 and 15 of release experiments, therefore data from days 9 and 16 were used.

Cylinder	Time in cell culture	Amount of drug expected (mg)	Actual amount of drug	Percent of expected amount
GEM^{in}/OP^{out}	3 days	5.156 mg OP 2.9 mg GEM	5.473 mg OP 1.525 mg GEM	OP: 105.4% GEM: 53.6%
OP^{in}/GEM^{out}	6 days	3.341 mg OP 1.786 mg GEM	4.402 mg OP 0.386 mg GEM	OP: 131.8% GEM: 21.6%
OP^{in}/GEM^{out}	10 days	2.51 mg OP 1.37 mg GEM	3.14 mg OP 1.25 mg GEM	OP: 125.1% GEM: 91.2%
OP^{in}/GEM^{out}	15 days	0.718 mg OP 0.690 mg GEM	3.391 mg OP 0.329 mg GEM	OP: 472.3% GEM: 47.7%
GEM^{in}/OP^{out}	15 days	1.04 mg OP* 1.24 mg GEM	0.98 mg OP 1.81 mg GEM	OP: 94.2% GEM: 146.0%

A greater amount of OP remained in cylinders placed in cell culture for various durations than expected in four of the five dissolved cylinders, with 105.4, 131.8, 125.1, 472.3, and 94.2% of expected OP remaining. The only cylinder that contained less OP than expected was an OP^{in}/GEM^{out} cylinder in culture for 10 days, and the difference in expected and actual amount of OP was within reason. It is however surprising to find that 472.3% of the expected amount of OP remained in an OP^{in}/GEM^{out} cylinder in culture for

15 days. The most likely cause of 472.3% of expected OP remaining is higher drug encapsulation. Although the objective was to load 16 mg OP in each cylinder, release experiments indicated loading was actually lower, and on average only 8.9 mg OP were loaded in OP^{in}/GEM^{out} cylinders, as seen in Table 5.

The dissolved cylinders contained 53.6, 21.6, 91.2, 47.7, and 146.0% of the expected amount of GEM. With the exception of the OP^{in}/GEM^{out} cylinder in culture for 10 days that contained 91.2% of expected GEM, the amount of GEM remaining in the cylinders was substantially different than expected. Two potential causes are the loss of cylindrical shape and lower drug encapsulation than expected. The cylindrical shape of the polymer matrix was lost and resulted in a thin disk, which had a greater surface area and possibly a faster rate of hydrolysis and drug release. However, all cylinders became disk-shaped in cell culture but most cylinders contained a greater amount of OP than expected. Therefore, an increase in surface area and rate of hydrolysis are probably not solely responsible for the low amount of remaining GEM.

5.3.5 Stability of OP Encapsulated in PLGA

A change in the chemical structure of OP was described earlier in section 5.1.2.2, when OP was dissolved in 0.1M sodium phosphate buffer pH 7.4, and stored at 37°C for up to 30 days. It was proposed that a shift in HPLC column retention time was due to ester hydrolysis, leading to OC. The purpose of the following experiment was to determine if OP encapsulated in PLGA would also be susceptible to ester hydrolysis.

Five cylinders containing OP and GEM that had been placed in cell culture for 3-15 days were dissolved, as explained in section 5.3.4, and the remaining amount of OP

and GEM analyzed by HPLC. An HPLC chromatogram of OP and GEM remaining in an OP^{in}/GEM^{out} cylinder that been in cell culture for 15 days is shown in Figure 46. Only peaks corresponding to OP and GEM are present in the chromatograph, indicating that OP which had not been released during the 15 days in cell culture had not been hydrolyzed and appeared stable while encapsulated in PLGA.

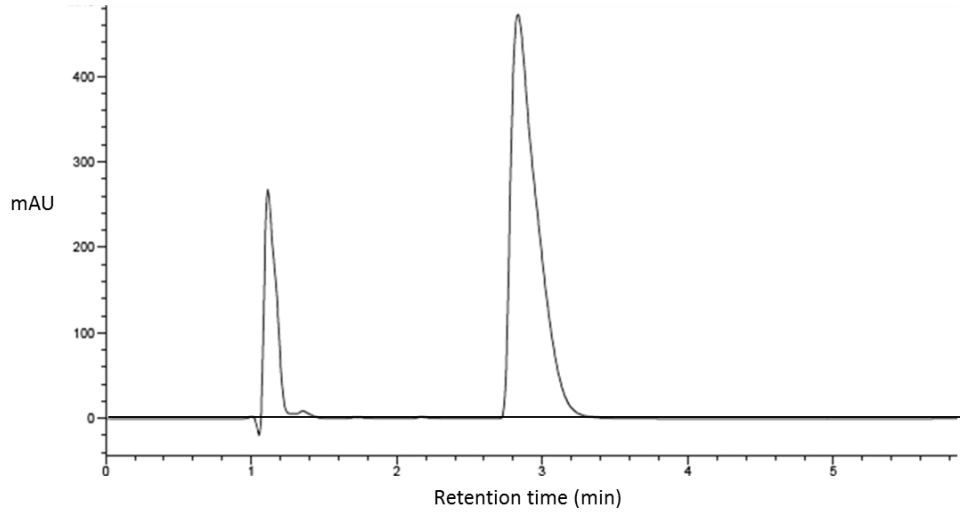

Figure 46. HPLC chromatogram of OP and GEM still encapsulated in an OP^{in}/GEM^{out} cylinder following 15 days in PANC1 cell culture.

OP dissolved in sodium phosphate buffer and stored at 37°C was not as effective at reducing cell viability as OP recently dissolved in sodium phosphate buffer, as shown in the WST-1 assay. However, this instability should not affect the efficacy of the delivery system since OP is not hydrolyzed while encapsulated in PLGA.

Chapter 6

Conclusions and Future Work

6.1 Conclusions

The research had three primary objectives, as stated in Chapter 3. Using HPLC, a method of detecting and quantifying therapeutic levels of OP and GEM was developed. The method was developed by modifying procedures in the literature for detection of OP or GEM alone, as well as building on the findings of previous students. Ultimately, a Poroshell 120 SB-C18 threaded column and a mobile phase of 60% HPLC grade methanol and 40% 0.04 M ammonium acetate buffer (pH 5.2) at a flow rate of 1 mL/min was used. OP and GEM had retention times of 3.0 and 1.1 min, respectively, and were detected at 230 nm. An injection volume of 20 μL and a column temperature of 25°C were used, and each sample was analyzed for 6 min.

Several types of single and double layered cylinders were formulated, containing either OP alone or OP and GEM. Single layered cylinders measured 9 mm in length by 4 mm in diameter, while double layered cylinders were slightly larger at 10 mm in length and 5 mm in diameter. Release experiments with singled layered cylinders containing pure OP and extracted OP demonstrated that greater residual acetone and smaller particle size led to higher initial release of OP. The ratio of drug to polymer also affected drug release. Double layered cylinders containing a total of 160 mg PLGA, 8 mg OP, and 1.5 mg GEM showed a lower initial release of both drugs than cylinders produced under the same conditions that contained 160 mg PLGA, 16 mg OP, and 3 mg GEM.

Variations in cylinder production and the resulting differences in drug release led to the production of type C OP^{in}/GEM^{out} or GEM^{in}/OP^{out} cylinders. Such cylinders showed sustained release over 30 days and most closely matched the projected release profile developed based on treatment dosages that resulted in either the stagnation or reduction of tumor volume during studies in tumor-bearing mice, and were selected for cell viability testing.

OP and GEM released from type C OP^{in}/GEM^{out} or GEM^{in}/OP^{out} cylinders greatly reduced PANC1 and PANC1 GEMR cell viability. OP^{in}/GEM^{out} cylinders reduced PANC1 cell viability by 49.1, 21.5, 10.2, and 1.2% of the untreated negative control after 3, 6, 10, and 15 days respectively while treatment with GEM^{in}/OP^{out} cylinders reduced cell viability by 15.2, 3.9, 11.7, and 12.2% of the untreated control at the same time periods. Treatment with OP and GEM released from OP^{in}/GEM^{out} or GEM^{in}/OP^{out} cylinders was even more effective at reducing the cell viability of PANC1 GEMR cells.

OP and GEM released from type C OP^{in}/GEM^{out} cylinders was more effective at reducing cell viability than drug released from type C GEM^{in}/OP^{out} cylinders. However, immunofluorescent staining of cells for N- and E-cadherin following cell viability experiments indicate that treatment with OP and GEM released from GEM^{in}/OP^{out} cylinders led at a reversal of EMT, while treatment of OP and GEM released from OP^{in}/GEM^{out} cylinders did not. Although fewer cells survived treatment with OP^{in}/GEM^{out} cylinders, E- and N-cadherin expression indicates the cells that did survive may have a more metastatic phenotype than those treated with the GEM^{in}/OP^{out} cylinders.

6.2 Future Work

The next step in this work is to test type C OP^{in}/GEM^{out} or GEM^{in}/OP^{out} cylinders in an animal model of pancreatic cancer. Release of OP and GEM from both cylinders dramatically reduced PANC1 and PANC1 GEMR cell viability for up to 15 days in vitro. Although release of OP and GEM from OP^{in}/GEM^{out} cylinders lead to a greater reduction in cell viability, N- and E-cadherin expression demonstrated the surviving cells shared characteristics with chemoresistant cells and a mesenchymal phenotype, indicating these cells may more be metastatic. Cells surviving treatment with OP and GEM released from GEM^{in}/OP^{out} cylinders appeared to have undergone a reversal of EMT when compared to the untreated control, which means cells should be less metastatic. Therefore, it is important to test both cylinder types in vivo to determine whether the reduction in cell viability or reversal of EMT will lead to a better outcome.

The cylinders developed provide proof of concept of long-term delivery of OP and GEM for the treatment of pancreatic cancer. Cylinders were an excellent starting point for the sustained delivery of OP and GEM due to straightforward fabrication, high loading of small hydrophilic drugs, stability of OP and GEM while encapsulated, localized drug delivery, and ease of use for in vitro experiments. However, injectable delivery systems would be preferable to an implantable cylinder. The cylinders require an incision and must be surgically inserted into the abdomen. Meanwhile, an injectable formulation could be quickly administered at a hospital or doctor's office.

While cylinders were useful for laying the groundwork for sustained delivery of OP and GEM, future research should include alternate possibilities for long-term delivery that are injectable. Currently, our lab is investigating injectable formulations such as

nanoparticles, pickering emulsions, and polymer based micelles for the targeting and delivery of OP and/or GEM. The added focus on targeted drug delivery has the potential to further reduce systemic drug concentrations and adverse side effects.

References

(1) Folkman, J. Tumor angiogenesis: therapeutic implications. *N. Engl. J. Med.* 1971, *285* (21), 1182–1186 DOI: 10.1056/NEJM197111182852108.

(2) What Is Cancer? - National Cancer Institute http://www.cancer.gov/about-cancer/what-is-cancer#types-of-cancer (accessed Jun 3, 2015).

(3) Mini, E.; Nobili, S.; Caciagli, B.; Landini, I.; Mazzei, T. Cellular pharmacology of gemcitabine. *Ann. Oncol.* 2006, *17* (SUPPL. 5), 7–12 DOI: 10.1093/annonc/mdj941.

(4) Shah, A. N.; Summy, J. M.; Zhang, J.; Park, S. I.; Parikh, N. U.; Gallick, G. E. Development and characterization of gemcitabine-resistant pancreatic tumor cells. *Ann. Surg. Oncol.* 2007, *14* (12), 3629–3637 DOI: 10.1245/s10434-007-9583-5.

(5) Li, X.; Lewis, M. T.; Huang, J.; Gutierrez, C.; Osborne, C. K.; Wu, M. F.; Hilsenbeck, S. G.; Pavlick, A.; Zhang, X.; Chamness, G. C.; et al. Intrinsic resistance of tumorigenic breast cancer cells to chemotherapy. *J. Natl. Cancer Inst.* 2008, *100* (9), 672–679 DOI: 10.1093/jnci/djn123.

(6) Bast, R. C.; Hennessy, B.; Mills, G. B. The biology of ovarian cancer: new opportunities for translation. *Nat. Rev. Cancer* 2009, *9* (6), 415–428 DOI: 10.1038/nrc2644.

(7) Dallas, N. A.; Xia, L.; Fan, F.; Gray, M. J.; Gaur, P.; Van Buren, G.; Samuel, S.; Kim, M. P.; Lim, S. J.; Ellis, L. M. Chemoresistant colorectal cancer cells, the cancer stem cell phenotype, and increased sensitivity to insulin-like growth factor-I receptor inhibition. *Cancer Res.* 2009, *69* (5), 1951–1957 DOI: 10.1158/0008-5472.CAN-08-2023.

(8) Thiery, J. P. Epithelial-mesenchymal transitions in tumour progression. *Nat. Rev. Cancer* 2002, *2* (6), 442–454 DOI: 10.1038/nrc822.

(9) Abdulkhalek, S.; Szewczuk, M. R. Neu1 sialidase and matrix metalloproteinase-9 cross-talk regulates nucleic acid-induced endosomal TOLL-like receptor-7 and -9 activation, cellular signaling and pro-inflammatory responses. *Cell. Signal.* 2013, *25* (11), 2093–20105 DOI: 10.1016/j.cellsig.2013.06.010.

(10) O'Shea, L. K.; Abdulkhalek, S.; Allison, S.; Neufeld, R. J.; Szewczuk, M. R. Therapeutic targeting of Neu1 sialidase with oseltamivir phosphate (Tamiflu®) disables cancer cell survival in human pancreatic cancer with acquired chemoresistance. *Onco. Targets. Ther.* 2014, *7*, 117–134 DOI: 10.2147/OTT.S55344.

(11) Gilmour, A. M.; Abdulkhalek, S.; Cheng, T. S. W.; Alghamdi, F.; Jayanth, P.; O'Shea, L. K.; Geen, O.; Arvizu, L. A.; Szewczuk, M. R. A novel epidermal growth factor receptor-signaling platform and its targeted translation in pancreatic cancer. *Cell. Signal.* 2013, *25* (12), 2587–2603 DOI: 10.1016/j.cellsig.2013.08.008.

(12) Eli Lilly. *GEMZAR: Gemcitabine for Injection Information Sheet*; 2013.

(13) Nair, L. S.; Laurencin, C. T. Biodegradable polymers as biomaterials. *Progress in Polymer Science (Oxford)*. 2007, pp 762–798.

(14) Sanofi-Aventis. Eligard Prescribing Information http://www.accessdata.fda.gov/drugsatfda_docs/label/2007/021731s005,021488s010,021379s010,021343s015lbl.pdf.

(15) Takeda Pharmaceuticals. Lupron Depot Prescribing Information http://www.rxabbvie.com/pdf/lupronuro_pi.pdf.

(16) Debiopharm Group. Decapeptyl®, Neo Decapeptyl®, Trelstar®, Pamorelin® https://www.debiopharm.com/products/decapeptyl-trelstar-pamorelin.html (accessed Jul 22, 2015).

(17) AstraZeneca. Zoladex 3.6 Prescribing Information http://www.azpicentral.com/zoladex-36/zoladex3_6.pdf#page=1.

(18) AstraZeneca. Bydureon (exenatide extended-release) for injectable suspension http://www.azpicentral.com/bydureon/pi_bydureon.pdf#page=1.

(19) AstraZeneca. Zoladex 10.8 Prescribing Information http://www.azpicentral.com/zoladex/zoladex10_8.pdf#page=1.

(20) Novartis. Sandostatin LAR (octreotide acetate) Core Data Sheet http://www.sandostatin.com/globalassets/resources/acromegaly/sandostatin_lar_cds.pdf.

(21) Hrynyk, M.; Ellis, J. P. J. P.; Haxho, F.; Allison, S.; Steele, J. A. M. J. A. M.; Abdulkhalek, S.; Neufeld, R. J. R. J.; Szewczuk, M. R. Therapeutic designed poly (lactic-co-glycolic acid) cylindrical oseltamivir phosphate loaded implants impede tumor neovascularization, growth and metastasis in mouse model of human pancreatic carcinoma. *Drug Des. Devel. Ther.* 2015, *9*, 4573–4586.

(22) Pancreatic Cancer Canada http://www.pancreaticcancercanada.ca/site/PageServer (accessed Jun 3, 2015).

(23) Hurton, S.; MacDonald, F.; Porter, G.; Walsh, M.; Molinari, M. The current state of pancreatic cancer in Canada: incidence, mortality, and surgical therapy. *Pancreas* 2014, *43* (6), 879–885 DOI: 10.1097/MPA.0000000000000147.

(24) Know the Facts - Pancreatic Cancer Canada http://www.pancreaticcancercanada.ca/site/PageServer?pagename=facingpancreaticcancer_facts (accessed Jun 3, 2015).

(25) Huang, P.; Chubb, S.; Hertel, L.; Grindey, G.; Plunkett, W. Action of 2′, 2′-difluorodeoxycytidine on DNA synthesis. *Cancer Res.* 1991, *51*, 6110–6117.

(26) Moore, M. J.; Hamm, J.; Dancey, J.; Eisenberg, P. D.; Dagenais, M.; Fields, a; Hagan, K.; Greenberg, B.; Colwell, B.; Zee, B.; et al. Comparison of gemcitabine versus the matrix metalloproteinase inhibitor BAY 12-9566 in patients with advanced or metastatic adenocarcinoma of the pancreas: a phase III trial of the National Cancer Institute of Canada Clinical Trials Group. *J. Clin. Oncol.* 2003, *21* (17), 3296–3302 DOI: 10.1200/JCO.2003.02.098.

(27) Burris, H. A.; Moore, M. J.; Andersen, J.; Green, M. R.; Rothenberg, M. L.; Modiano, M. R.; Cripps, M. C.; Portenoy, R. K.; Storniolo, A. M.; Tarassoff, P.; et al. Improvements in survival and clinical benefit with gemcitabine as first-line therapy for patients with advanced pancreas cancer: a randomized trial. *J. Clin. Oncol.* 1997, *15* (6), 2403–2413.

(28) Gemcitabine Hydrochloride - National Cancer Institute http://www.cancer.gov/about-cancer/treatment/drugs/gemcitabinehydrochloride (accessed Jun 4, 2015).

(29) Heinemann, V.; Hertel, L. W.; Grindey, G. B.; Plunkett, W. Comparison of the cellular pharmacokinetics and toxicity of 2’,2'-difluorodeoxycytidine and 1-??-D-arabinofuranosylcytosine. *Cancer Res.* 1988, *48* (14), 4024–4031.

(30) Heinemann, V.; Xu, Y. Z.; Chubb, S.; Sen, A.; Hertel, L. W.; Grindey, G. B.; Plunkett, W. Inhibition of ribonucleotide reduction in CCRF-CEM cells by 2’,2'-difluorodeoxycytidine. *Mol. Pharmacol.* 1990, *38* (4), 567–572.

(31) Gandhi, V.; Huang, P.; Xu, Y. Z.; Heinemann, V.; Plunkett, W. Metabolism and action of 2’,2'-difluorodeoxycytidine: self-potentiation of cytotoxicity. *Adv. Exp. Med. Biol.* 1991, *309A*, 125–130.

(32) Bergman, A. M.; Pinedo, H. M.; Peters, G. J. Determinants of resistance to 2′,2′-difluorodeoxycytidine (gemcitabine). *Drug Resist. Updat.* 2002, *5* (1), 19–33 DOI: 10.1016/S1368-7646(02)00002-X.

(33) Hiscox, S.; Jiang, W. G.; Obermeier, K.; Taylor, K.; Morgan, L.; Burmi, R.; Barrow, D.; Nicholson, R. I. Tamoxifen resistance in MCF7 cells promotes EMT-

like behaviour and involves modulation of β-catenin phosphorylation. *Int. J. Cancer* 2006, *118* (2), 290–301 DOI: 10.1002/ijc.21355.

(34) Pan, J.-J.; Yang, M.-H. The role of epithelial-mesenchymal transition in pancreatic cancer. *Journal of gastrointestinal oncology*. 2011, pp 151–156.

(35) Yang, A. D.; Fan, F.; Camp, E. R.; van Buren, G.; Liu, W.; Somcio, R.; Gray, M. J.; Cheng, H.; Hoff, P. M.; Ellis, L. M. Chronic oxaliplatin resistance induces epithelial-to-mesenchymal transition in colorectal cancer cell lines. *Clin. Cancer Res.* 2006, *12* (14 Pt 1), 4147–4153 DOI: 10.1158/1078-0432.CCR-06-0038.

(36) Lu, Y.; Lu, J.; Li, X.; Zhu, H.; Fan, X.; Zhu, S.; Wang, Y.; Guo, Q.; Wang, L.; Huang, Y.; et al. MiR-200a inhibits epithelial-mesenchymal transition of pancreatic cancer stem cell. *BMC Cancer* 2014, *14* (1), 85 DOI: 10.1186/1471-2407-14-85.

(37) Boyer, B.; Vallés, A. M.; Edme, N. Induction and regulation of epithelial-mesenchymal transitions. *Biochem. Pharmacol.* 2000, *60* (8), 1091–1099.

(38) Savagner, P. Leaving the neighborhood: molecular mechanisms involved during epithelial-mesenchymal transition. *Bioessays* 2001, *23* (10), 912–923 DOI: 10.1002/bies.1132.

(39) Creighton, C. J.; Gibbons, D. L.; Kurie, J. M. The role of epithelial-mesenchymal transition programming in invasion and metastasis: a clinical perspective. *Cancer Manag. Res.* 2013, *5*, 187–195 DOI: 10.2147/CMAR.S35171.

(40) Weber, C. E.; Li, N. Y.; Wai, P. Y.; Kuo, P. C. Epithelial-Mesenchymal Transition, TGF-β, and Osteopontin in Wound Healing and Tissue Remodeling After Injury. *J. Burn Care Res.* 2012, *33* (3), 311–318 DOI: 10.1097/BCR.0b013e318240541e.

(41) Bhowmick, N. a; Ghiassi, M.; Bakin, a; Aakre, M.; Lundquist, C. a; Engel, M. E.; Arteaga, C. L.; Moses, H. L. Transforming growth factor-beta1 mediates epithelial to mesenchymal transdifferentiation through a RhoA-dependent mechanism. *Mol. Biol. Cell* 2001, *12* (1), 27–36 DOI: 10.1091/mbc.12.1.27.

(42) Nieman, M. T.; Prudoff, R. S.; Johnson, K. R.; Wheelock, M. J. N-Cadherin Promotes Motility in Human Breast Cancer Cells Regardless of their E-Cadherin Expression. 1999, *147* (3), 631–643.

(43) Arumugam, T.; Ramachandran, V.; Fournier, K. F.; Wang, H.; Marquis, L.; Abbruzzese, J. L.; Gallick, G. E.; Logsdon, C. D.; McConkey, D. J.; Choi, W. Epithelial to mesenchymal transition contributes to drug resistance in pancreatic cancer. *Cancer Res.* 2009, *69* (14), 5820–5828 DOI: 10.1158/0008-5472.CAN-08-2819.

(44) Hotz, B.; Arndt, M.; Dullat, S.; Bhargava, S.; Buhr, H. J.; Hotz, H. G. Epithelial to mesenchymal transition: Expression of the regulators snail, slug, and twist in pancreatic cancer. *Clin. Cancer Res.* 2007, *13* (16), 4769–4776 DOI: 10.1158/1078-0432.CCR-06-2926.

(45) Martin, T. A.; Goyal, A.; Watkins, G.; Jiang, W. G. Expression of the transcription factors snail, slug, and twist and their clinical significance in human breast cancer. *Ann Surg Oncol* 2005, *12* (6), 488–496.

(46) Cano, A.; Pérez-Moreno, M. A.; Rodrigo, I.; Locascio, A.; Blanco, M. J.; del Barrio, M. G.; Portillo, F.; Nieto, M. A. The transcription factor snail controls epithelial-mesenchymal transitions by repressing E-cadherin expression. *Nat. Cell Biol.* 2000, *2* (2), 76–83 DOI: 10.1038/35000025.

(47) Nakajima, S.; Doi, R.; Toyoda, E. N-Cadherin Expression and Epithelial-Mesenchymal Transition in Pancreatic Carcinoma N-Cadherin Expression and Epithelial-Mesenchymal Transition in Pancreatic Carcinoma. 2004, *10*, 4125–4133 DOI: 10.1158/1078-0432.CCR-0578-03.

(48) Li, Y.; Vandenboom, T. G.; Kong, D.; Wang, Z.; Ali, S.; Philip, P. a.; Sarkar, F. H. Up-regulation of miR-200 and let-7 by natural agents leads to the reversal of epithelial-to-mesenchymal transition in gemcitabine-resistant pancreatic cancer cells. *Cancer Res.* 2009, *69* (16), 6704–6712 DOI: 10.1158/0008-5472.CAN-09-1298.

(49) Liu, J.; Valencia-Sanchez, M. A.; Hannon, G. J.; Parker, R. MicroRNA-dependent localization of targeted mRNAs to mammalian P-bodies. *Nat. Cell Biol.* 2005, *7* (7), 719–723 DOI: 10.1038/ncb1274.

(50) Saxena, S.; Jónsson, Z. O.; Dutta, A. Small RNAs with imperfect match to endogenous mRNA repress translation. Implications for off-target activity of small inhibitory RNA in mammalian cells. *J. Biol. Chem.* 2003, *278* (45), 44312–44319 DOI: 10.1074/jbc.M307089200.

(51) Gschwind, A.; Fischer, O. M.; Ullrich, A. The discovery of receptor tyrosine kinases: targets for cancer therapy. *Nat. Rev. Cancer* 2004, *4* (5), 361–370 DOI: 10.1038/nrc1360.

(52) Ullrich, a; Schlessinger, J. Signal transduction by receptors with tyrosine kinase activity. *Cell* 1990, *61* (2), 203–212 DOI: 10.1007/s00497-011-0177-9.

(53) Zwick, E.; Bange, J.; Ullrich, A. Receptor tyrosine kinases as targets for anticancer drugs. *Trends Mol. Med.* 2002, *8* (1), 17–23 DOI: 10.1016/S1471-4914(01)02217-1.

(54) Jayanth, P.; Amith, S. R.; Gee, K.; Szewczuk, M. R. Neu1 sialidase and matrix metalloproteinase-9 cross-talk is essential for neurotrophin activation of Trk receptors and cellular signaling. *Cell. Signal.* 2010, *22* (8), 1193–1205 DOI: 10.1016/j.cellsig.2010.03.011.

(55) Alghamdi, F.; Guo, M.; Abdulkhalek, S.; Crawford, N.; Amith, S. R.; Szewczuk, M. R. A novel insulin receptor-signaling platform and its link to insulin resistance and type 2 diabetes. *Cell. Signal.* 2014, *26* (6), 1355–1368 DOI: 10.1016/j.cellsig.2014.02.015.

(56) Amith, S. R.; Jayanth, P.; Franchuk, S.; Siddiqui, S.; Seyrantepe, V.; Gee, K.; Basta, S.; Beyaert, R.; Pshezhetsky, A. V.; Szewczuk, M. R. Dependence of pathogen molecule-induced Toll-like receptor activation and cell function on Neu1 sialidase. *Glycoconj. J.* 2009, *26* (9), 1197–1212 DOI: 10.1007/s10719-009-9239-8.

(57) Amith, S. R.; Jayanth, P.; Finlay, T.; Franchuk, S.; Gilmour, A.; Abdulkhalek, S.; Szewczuk, M. R. Detection of Neu1 sialidase activity in regulating Toll-like receptor activation. *Journal of visualized experiments : JoVE*. 2010.

(58) Centers for Disease Control and Prevention. Types of Influenza Viruses | Seasonal Influenza (Flu) | CDC http://www.cdc.gov/flu/about/viruses/types.htm (accessed Jul 20, 2015).

(59) Genentech Inc. *Tamiflu Prescribing Information*; San Francisco, 2013.

(60) Abdulkhalek, S.; Hrynyk, M.; Szewczuk, M. R. A novel G-protein-coupled receptor-signaling platform and its targeted translation in human disease. *Res. Reports Biochem.* 2013, *3*, 17–30 DOI: 10.2147/RRBC.S28430.

(61) Canadian Cancer Society. Treatment - Canadian Cancer Society http://www.cancer.ca/en/cancer-information/diagnosis-and-treatment/treatment/?region=on (accessed Jul 22, 2015).

(62) Jain, R. K. Delivery of molecular and cellular medicine to solid tumors. *Advanced Drug Delivery Reviews*. 2012, pp 353–365.

(63) Obara, K.; Ishihara, M.; Ozeki, Y.; Ishizuka, T.; Hayashi, T.; Nakamura, S.; Saito, Y.; Yura, H.; Matsui, T.; Hattori, H.; et al. Controlled release of paclitaxel from photocrosslinked chitosan hydrogels and its subsequent effect on subcutaneous tumor growth in mice. *J. Control. Release* 2005, *110* (1), 79–89 DOI: 10.1016/j.jconrel.2005.09.026.

(64) Dhanikula, A. B.; Panchagnula, R. Localized paclitaxel delivery. *International Journal of Pharmaceutics*. 1999, pp 85–100.

(65) Dash, A. K.; Cudworth, G. C. Therapeutic applications of implantable drug delivery systems. *J. Pharmacol. Toxicol. Methods* 1998, *40* (1), 1–12 DOI: 10.1016/S1056-8719(98)00027-6.

(66) Williams, D. F. *The Williams Dictionary of Biomaterials*; Liverpool University Press: Liverpool, 1999.

(67) Hatefi, A.; Amsden, B. Biodegradable injectable in situ forming drug delivery systems. *Journal of Controlled Release*. 2002, pp 9–28.

(68) Gilding, D. K.; Reed, A. M. Biodegradable polymers for use in surgery—polyglycolic/poly(actic acid) homo- and copolymers: 1. *Polymer*. 1979, pp 1459–1464.

(69) Middleton, J. C.; Tipton, A. J. Synthetic biodegradable polymers as orthopedic devices. *Biomaterials* 2000, *21* (23), 2335–2346 DOI: 10.1016/S0142-9612(00)00101-0.

(70) Mooney, D. J.; Breuer, C.; McNamara, K.; Vacanti, J. P.; Langer, R. Fabricating tubular devices from polymers of lactic and glycolic Acid for tissue engineering. *Tissue Eng.* 1995, *1* (2), 107–118 DOI: 10.1089/ten.1995.1.107.

(71) Wu, X. S.; Wang, N. Synthesis, characterization, biodegradation, and drug delivery application of biodegradable lactic/glycolic acid polymers. Part II: Biodegradation. *J. Biomater. Sci. Polym. Ed.* 2001, *12* (1), 21–34.

(72) Maurus, P. B.; Kaeding, C. C. Bioabsorbable implant material review. *Operative Techniques in Sports Medicine*. 2004, pp 158–160.

(73) Remesh, A. Tackling the problems of tumour Chemotherapy by optimal drug scheduling. *J. Clin. Diagnostic Res.* 2013, *7* (7), 1404–1407 DOI: 10.7860/JCDR/2013/6223.3144.

(74) Lü, J.-M.; Wang, X.; Marin-Muller, C.; Wang, H.; Lin, P. H.; Yao, Q.; Chen, C. Current advances in research and clinical applications of PLGA-based nanotechnology. *Expert Rev. Mol. Diagn.* 2009, *9* (4), 325–341 DOI: 10.1586/erm.09.15.

(75) Danhier, F.; Ansorena, E.; Silva, J. M.; Coco, R.; Le Breton, A.; Préat, V. PLGA-based nanoparticles: An overview of biomedical applications. *Journal of Controlled Release*. 2012, pp 505–522.

(76) Health Canada; Government of Canada. Health Canada - Home Page http://www.hc-sc.gc.ca/index-eng.php (accessed Jul 29, 2015).

(77) De Rosa, G.; Maiuri, M. C.; Ungaro, F.; De Stefano, D.; Quaglia, F.; La Rotonda, M. I.; Carnuccio, R. Enhanced intracellular uptake and inhibition of NF-??B activation by decoy oligonucleotide released from PLGA microspheres. *J. Gene Med.* 2005, *7* (6), 771–781 DOI: 10.1002/jgm.724.

(78) Feng, T.; Tian, H.; Xu, C.; Lin, L.; Xie, Z.; Lam, M. H.-W.; Liang, H.; Chen, X. Synergistic co-delivery of doxorubicin and paclitaxel by porous PLGA microspheres for pulmonary inhalation treatment. *Eur. J. Pharm. Biopharm.* 2014, *88* (3), 1086–1093 DOI: 10.1016/j.ejpb.2014.09.012.

(79) Danhier, F.; Lecouturier, N.; Vroman, B.; Jérôme, C.; Marchand-Brynaert, J.; Feron, O.; Préat, V. Paclitaxel-loaded PEGylated PLGA-based nanoparticles: In vitro and in vivo evaluation. *J. Control. Release* 2009, *133* (1), 11–17 DOI: 10.1016/j.jconrel.2008.09.086.

(80) Lee, J. S.; An, T. K.; Chae, G. S.; Jeong, J. K.; Cho, S. H.; Lee, H. B.; Khang, G. Evaluation of in vitro and in vivo antitumor activity of BCNU-loaded PLGA wafer against 9L gliosarcoma. *Eur. J. Pharm. Biopharm.* 2005, *59* (1), 169–175 DOI: 10.1016/j.ejpb.2004.06.006.

(81) Arshad, A.; Yang, B.; Bienemann, A. S.; Barua, N. U.; Wyatt, M. J.; Woolley, M.; Johnson, D. E.; Edler, K. J.; Gill, S. S. Convection-Enhanced Delivery of Carboplatin PLGA Nanoparticles for the Treatment of Glioblastoma. *PLoS One* 2015, *10* (7), e0132266 DOI: 10.1371/journal.pone.0132266.

(82) Schwendeman, S. Importance of Regulatory Research Funding for Long Acting Release (LAR) Drug Products. In *FY 2014 Regulatory Science Initiatives Part 15 Public Meeting*; Silver Spring, MD, 2014.

(83) Janssen Pharmaceuticals. Risperdal Consta - Important Product Information http://www.risperdalconsta.com/important-product-information (accessed Jul 22, 2015).

(84) Morrison, R. T.; Boyd, R. N. *Organic Chemistry*, Fifth.; Allyn and Bacon, Inc.: Newton, Massachussets, 1987.

(85) Oliyai, R.; Yuan, L.-C.; Dahl, T. C.; Swaminathan, S.; Wang, K.-Y.; Lee, W. A. Biexponential decomposition of a neuraminidase inhibitor prodrug (GS-4104) in aqueous solution. *Pharm. Res.* 1998, *15* (8), 1300–1304.

(86) Albert, K.; Bockshorn, J. Chemical stability of oseltamivir in oral solutions. *Pharmazie* 2007, *62* (9), 678–682 DOI: 10.1691/ph.2007.9.7106.

(87) US Food and Drug Administration. Guidance for Industry. Q3C — Tables and List. 2012, No. February, 10.

(88) Entschladen, F.; Drell VI, T. L.; Lang, K.; Joseph, J.; Zaenker, K. S. Tumour-cell migration, invasion, and metastasis: Navigation by neurotransmitters. *Lancet Oncol.* 2004, *5* (4), 254–258 DOI: 10.1016/S1470-2045(04)01431-7.

(89) Steeg, P. S. Tumor metastasis: mechanistic insights and clinical challenges. *Nat. Med.* 2006, *12* (8), 895–904 DOI: 10.1038/nm1469.

(90) European Medicines Agency. *Summary on Compassionate Use for Tamiflu IV*; London, UK, 2011.